Development of LC-MS Based Metabolomics and Lipidomics Techniques

By

Jaspaul Tatlay

A thesis submitted in partial fulfillment of the requirements for the degree of

Master of Science

Department of Chemistry

University of Alberta

Abstract

The analysis of thousands of metabolites and lipids for discovery of metabolite biomarkers for disease monitoring and diagnosis requires the highest sensitivity and robust methods. Metabolomics is the study of metabolites found in the body, which can be used to discover biomarkers of disease or monitor interactions in our body. In my thesis, I developed liquid chromatography mass spectrometry (LC-MS) methods that analyze small volumes of samples for metabolomics and profile the changes in lipids in serum samples collected from Parkinson's disease (PD) patients and healthy controls to find PD biomarkers.

Separation techniques have improved the field of metabolomics and lipidomics by increasing sensitivity, throughput, and resolution. In particular, the use of nanoliter flow liquid chromatography (nLC) and ultra-high performance liquid chromatography (UHPLC) have shown great promise. nLC takes the regular flow of the LC and reduces it to micro- or nano liter flow. With the decreased flow, the column size and connections need to be reduced as well. The advancements of these technologies have increased the coverage of the metabolome and lipidome.

I used nLC-MS to improve the overall analytical performance of metabolomic profiling for handling of samples with small volumes. I first optimized nLC-MS for high performance chemical isotope labeling (CIL) metabolomics. CIL is a method used to chemically label metabolites to increase their retention on reversed phase (RP) separation, to improve ionization efficiency, and to allow for relative quantification. CIL is a sensitive technique, although when sample volumes are limited or the concentration of samples is low, the use of nLC is needed. nLC is used to increase coverage of the CIL metabolome and reduce sample consumption through the use of analyte trapping.

Recent advancements in mass spectrometry, specifically in quadrupole time-of-flight (QTOF) instruments, have allowed for higher resolution, faster collection rates and improved sensitivity. This new generation of instrumentation allows us to examine the metabolome and lipidome further.

In lipidomics, LC-MS is used to analyze thousands of lipids to get a better understanding of the lipidome and their roles in diseases. We used an ultra-high resolution quadrupole time of flight (UHR-QTOF) instrument connected to UHPLC to profile PD samples to identify potential biomarkers. Ultra-high resolution allows for higher mass precision and increased confidence in identification. Using statistical analyses we determined five lipids to distinguish the diseased samples from the controls. In receiver operating characteristic (ROC) analysis, these potential biomarkers had an area under the curve (AUC) of 0.976 with sensitivity of 92% and specificity of 90%. The same panel of five lipids plus another compound were used to distinguish PDD from PD. ROC analysis of the 6 compounds gave an AUC of 0.958 with sensitivity of 87% and specificity of 94%. We also observed an increasing trend of the 5 common lipids in concentration, suggesting the potential of using these biomarkers for not only diagnosis of PD, but also tracking PD progression into PDD.

Preface

Chapter 2 has been published as "Nanoflow LC-MS for High-Performance Chemical Isotope Labeling Quantitative Metabolomics" Li, Z.; Tatlay, J.; Li, L. Anal. Chem. 87, 11468-11474. Zhendong Li and I helped with experimental design, data collection and data processing. I prepared the samples, collected the samples, processed data and wrote and edited the manuscript. Professor Liang Li was involved in the concept discussion, experimental design and editing the manuscript.

Chapter 3 was a collaboration between our group and Dr. Richard Camicolli from the Neuroscience and Mental Health Institute and the Department of Medicine at the University of Alberta, to profile the lipidome of Parkinson's disease samples. Dorothea Mung and I prepared samples, collected data, wrote and edited the manuscript. In addition, I processed the data and used software and manual interpretation for identification. Professor Liang Li was involved in the concept discussion, experimental design and manuscript editing. The University of Alberta health ethics review board approved this study and all participants provided informed consent.

Acknowledgements

I would like to thank my supervisor Dr. Liang Li for his patience and guidance throughout the years. His mentorship has allowed me to grow as an analytical chemist. The experience and education that I received from working in Dr. Li's lab is invaluable.

I am grateful to my supervisory committee, Dr. Charles A. Lucy and Dr. Robert E. Campbell for their advice and guidance. I would like to especially thank Dr. Charles A. Lucy for being a great teacher and mentor over the years. I would like to thank Dr. Derrick Clive for reviewing my thesis and participating in my oral examination.

I would like to thank my group members for their support and friendship over the years. I would like to thank: Dr. Zhendong Li for teaching me instrumentation and his mentorship, Dorothea Mung, Kevin Hooton, Yunong Li, Xian Luo, Shuang Zhao, Wei Han, Dr. Tao Huan, Dr. Yiman Wu, Dr. Chiao-Li Tseng, Dr. Ruokun Zhou, and Dr. Nan Wang.

Also I am grateful for the help provided by Dr. Randy Whittal and everyone else in the mass spectrometry lab, Jing Zheng and Bela Reiz. Also Al Chilton and Kim Do in the electronic shop, for letting me use their workspace and their advice on electronics. Thanks to the machine shop Dirk Kelm, Vince Bizon, Dieter Starke, and Paul Crothers for their help on projects and installations. I am also grateful for the help provided by Ryan Lewis in shipping. Also the entire support staff for all there help over the years.

Finally I would like to thank my family and friends for their support and understanding. My parents Major and Surjit Tatlay and my girlfriend, Tia MacLachlan for their unwavering support over the years.

Table of Contents

List of Tables

List of Figures

List of Abbreviations

%RSD	Percent Relative standard deviation
AC	Alternating current
AD	Alzheimer's disease
API	Atmospheric pressure ionization
AUC	Area under the curve
CE	Collision energy
CE	Cholesterol esters
Cer	Ceramide
CID	Collision induced dissociation
CIL	Chemical isotope labeling
DC	Direct current
DDA	Data dependent acquisition
DG	Diacylglycerols
DIA	Data independent acquisition
DmPA	p-dimethylaminophenacyl
ESI	Electrospray Ionization
FC	Fold change
fmol	Femtomole
GBA	Glucocerebrosidase
GC	Gas chromatography
H	Control group
HILIC	Hydrophilic interaction chromatography
HMDB	Human Metabolome Database
HPLC	High performance liquid chromatography

IEM	Ion evaporation model
LC	Liquid chromatography
LC-MS	Liquid chromatography mass spectrometry
LOD	Limit of detection
LysoPC	Lysophosphatidylcholine
LysoPE	Lysophosphatidylethanolamine
MCID	MyCompoundID
mL	Milliliter
mLC-MS	Microbore LC-MS
MS	Mass spectrometry
MS/MS	Tandem MS
nL	Nanoliter
nLC	Nanoflow liquid chromatography
nLC-MS	Nanoflow-LC MS
NMR	Nuclear magnetic resonance spectroscopy
OPLS-DA	Orthogonal partial least square discriminant analysis
PC	Phosphatidylcholines
PCA	Principal component analysis
PD	Parkinson's Disease
PDD	Parkinson's Disease with Dementia
PE	Phosphatidylethanolamine
PG	Phosphtatidylglycerols
PI-Cer	Ceramide phosphoinositol
PLS-DA	Partial least squares discriminant analysis
pmol	Picomole
QTOF	Quadrupole time of flight
ROC	Receiver operator characteristic
RP	Reversed phase

SM	Sphingomyelin
Sph	Sphingoid bases
TG	Triacylglycerols
TIC	Total ion count
UHPLC	Ultra-high performance liquid chromatography
UHR	Ultra-high resolution
UHR-QTOF	Ultra-high resolution quadrupole time of flight
UPLC	Ultra-performance liquid chromatography
UV	Ultra violet
WE	Wax ester

List of Symbols

A	Aqueous mobile phase
Da	Daltons
kV	Kilovolts
m/z	Mass to charge ratio
min	Minutes
B	Organic mobile phase
ppm	Parts per million
S/N	Signal to noise
σ	Standard deviation of sample
µL	Microliter
µm	Micron
v/v	Volume per volume

Chapter 1 Introduction

1.1 History of Mass Spectrometry

Mass spectrometry (MS) has been developed over the years to be one of the most valuable analytical tools available to chemists. The concept of mass spectrometry was developed by J.J. Thomson in the year 1913. However the modern mass spectrometer was developed by Arthur Jeffrey Dempster in 1918, portions of which are still used to this day.[1] Throughout the years, breakthroughs in the MS field have taken MS from simple mass analysis to a tool for sensitive quantification and detection of complicated biological compounds. Furthermore, MS can be combined with separation techniques such as gas chromatography[2] (GC) and liquid chromatography[3] (LC) to analyze biological samples. Advancements in mass spectrometry has allowed the field of metabolomics and lipidomics to grow exponentially.

1.2 Metabolomics

Metabolomics has grown rapidly due to advancements in MS technologies. Metabolomics is the study of metabolites, which are endogenous and exogenous to human bodies.[4] Metabolomics is used to learn about the many interactions and roles metabolites play in the human body. Metabolites are small molecules of less than 1000 Daltons (Da) in mass that are constantly being used and produced by our bodies. Many of these small molecules take part in metabolic pathways such as the Krebs cycle, and play integral roles in our daily lives. When these metabolic pathways break down or malfunction, diseases can occur. These diseases can be monitored and diagnosed using the many metabolites found in our body, leading to treatments and drug targets.

When metabolomics was first developed, it was done using simple techniques and chemical reactions where one metabolite was analyzed at a time. With the development of nuclear magnetic

resonance (NMR) spectroscopy, came the ability to analyze 10's to 100's of metabolites at once, due to its capacity to respond equally to all chemical moieties in a sample.[5] Despite these advancements, biological matrices are complicated, and thus the spectra are hard to interpret. NMR also requires a large volume of sample. The development of LC-MS has allowed for the analysis of 1000's of metabolites at a time with less sample.[6] LC-MS metabolomics has quickly replaced older techniques and provides complimentary data to NMR due to its high sensitivity and high throughput.

The general metabolomics LC-MS[7] workflow is simple compared to other techniques used to profile the metabolome. First, the metabolites are extracted from the biological matrix. Following extraction, the samples need to be normalized due to the concentration differences in the metabolites from sample to sample. This is especially important for urine, as water content varies across samples. Normalization can be done in multiple ways: the total sample concentration can be measured using ultraviolet (UV) absorption area,[8] adjusted in comparison to an endogenous marker such as creatinine,[9] or adjusted after sample injection using total ion count (TIC).[10] Metabolites are then injected onto the LC instrument. Where the sample is then separated to reduce biological complexity, in which specific metabolites can be targeted using different separation phases.[11] The sample then flows into an ionization source and is introduced into the mass spectrometer. After the LC-MS portion, the data is processed and aligned using software, which is then ready for statistical analysis. The statistical analysis provides metabolite targets that can be screened for biomarkers and drug targets.

1.2.1 Chemical Isotope Labeling Metabolomics

Chemical isotope labeling (CIL) improves on general metabolomics by increasing the sensitivity and improving quantification of labeled metabolites. CIL metabolomics is done using

a chemical reagent. The chemical reagent can contain deuterium isotopes (^{2}H) or enriched carbon thirteen isotopes (^{13}C). These are both classified as the heavy labels, whereas the labels without enrichment are called the light labels. The individual samples are reacted with the light label. The pooled sample, which is a collection of all the samples, are reacted with the heavy label. The light and heavy labels are then mixed together after determining the total sample concentration using UHPLC-UV.[8] Once the sample is injected into the MS, two peaks are detected for each metabolite: the light and heavy peak. Each heavy peak acts as an internal standard for each individual labeled metabolite.

In our group we use dansyl chloride[12] and ρ-dimethylaminophenacyl[13] (DmPA) bromide to target the various sub metabolomes. Amine and phenol groups are targeted by dansyl chloride and organic acids are targeted using DmPA. The use of CIL allows for UV normalization and changes the retention properties of the polar metabolites, allowing them to be separated on a reversed phase column. The addition of the chemical tag also increases the ionizability of the labelled molecule in the electrospray. The comparison of the heavy label against the light label allows for relative quantification. We have also developed software to extract this data and identify these labeled metabolites.[14,15] The combination of these properties improve the detectability of thousands of metabolites and provide a more comprehensive profile of the metabolome.

1.3 Lipidomics

Similar to metabolomics, the field of lipidomics has advanced rapidly due to developments in mass spectrometry. Lipids are a diverse group of molecules that play many important biological roles including energy storage, structural components and cell signaling.[16] Lipids are generally described as hydrophobic or amphiphilic small molecules. Lipids can further interact with sugars, proteins and other biological components to create large complexes. Even though there are many

classes of lipids, they all arise from two main building blocks: the ketoacyl and isoprene groups.[17] With the discovery that lipids play a large role in certain diseases, lipids have become an ever increasing class of biological molecules that need to be probed.[18,19,20]

Lipidomics is generally done using high performance liquid chromatography (HPLC), which is used to separate the lipids prior to MS analysis. Separation can be performed by either reversed phase or hydrophilic interaction chromatography (HILIC). Reversed phase allows for separation based on hydrophobicity, chain length, degrees of saturation or modifications.[21,22] Alternatively, HILIC can be used to separate the lipids based on their polarity, such as the head group of the lipid.[23,24] The separation can be further improved using UHPLC. With UHPLC, columns with particle sizes smaller than 2 μm can be used. The use of UHPLC columns allows for better resolution of complex lipid samples, allowing for increased sensitivity. After separation, the lipids are eluted into a mass spectrometer for detection. Mass spectrometry is used to analyze lipid composition and for quantification.

A lipidomics LC-MS workflow is similar to a metabolomics workflow, as samples are extracted, injected onto HPLC, and then analyzed using mass spectrometry. Where lipidomics differs is that in order to extract lipids from the complex biological matrices, special extraction methods were developed, such as the Folch[25] method or the Bligh and Dyer[26] method. These involve the use of nonpolar organic solvents such as chloroform or dichloromethane to extract the relatively non polar lipids, leaving behind the other biological species.

The data is then normalized using the total ion counts (TIC), and features are extracted and analyzed using various statistical tools. Univariate and multivariate analyses are used to examine large changes in the sample groups and individual features. The most common multivariate

methods are principal component analysis (PCA) and partial least squares discriminant analysis (PLS-DA).[27,28]

After statistical analysis, important lipid features are identified and screened as potential biomarkers. Identification is done by matching experimental tandem MS (MS/MS) spectra to library MS/MS spectra.[29,30] High resolution MS is needed to increase confidence in the library matches, especially when lipids have similar chemical compositions and can differ in the parts per million (ppm) mass precision. The need for ultra high resolution QTOF coupled to UHPLC is shown in chapter 3.

1.4 Instrumentation

1.4.1 Electrospray Ionization

Electrospray ionization (ESI) is an atmospheric pressure ionization (API) technique developed by Masamichi Yamashita and John Fenn in 1984.[31] An API source does not require a complete vacuum to function, unlike other sources. ESI revolutionized the world of mass spectrometry by allowing the ionization of intact molecules (metabolites and lipids) at atmospheric pressures. Its ability to couple with liquid chromatography has allowed metabolomics and lipidomics to flourish.

ESI is done by infusing liquid mobile phase into a thin metal capillary, housed within a larger metal tube through which nitrogen gas flows to aid solvent evaporation.[32] The inner tube has a high voltage (3-5 kV) applied to it, which causes the liquid within to form a "Taylor cone". A filament of ions forms at the tip of the cone, and as the filament gets further away from the cone it destabilizes due to columbic repulsion between the ions.[33] As the filament destabilizes it breaks into small micrometer droplets.[34] The ions within the droplets are introduced into the mass spectrometer after they enter the gas phase. The exact mechanism of how the ions enter the gas

phase from the droplets is not known but there are several theories. The one that applies to small molecules such as metabolites and lipids is the ion evaporation model (IEM).[35,36] In the IEM, as the droplets evaporate and decrease in size, the ions within the droplet get closer to each other. As they get closer, the repulsive forces between them get stronger and the droplets break apart, and the ions are pushed into the gas phase and into the mass spectrometer.

1.4.2 Nano-ESI

With the development of nLC, ESI sources had to be scaled down to accommodate nanoliter flow. The metal capillaries used by ESI sources were too large and caused large post column delays and peak broadening. In a nano-ESI source, these metal capillaries are replaced by glass capillaries less than 20 μm inner diameter. The reduction in size not only reduced peak broadening but further enhanced ESI sensitivity. The sensitivity increase was caused by the reduced dilution at the tip of the sprayer, producing smaller droplets that evaporate quicker, releasing more ions into the mass spectrometer.

1.4.3 Quadrupole Time of Flight Mass Spectrometer

QTOF mass spectrometers are readily used in the fields of metabolomics and lipidomics.[37,38,39,40] QTOF is a combination of a quadrupole and a time of flight instrument.[41] A quadrupole is made up of four symmetrical metal cylinders to which both an alternating current (AC) and direct current (DC) are applied. By manipulating the AC and DC potential, we focus the ions to the center of the quadrupole and can select a specific mass to charge ratio (m/z).[42] A QTOF usually has two main quadrupoles: the first quadrupole controls the entry of ions and can be seen as a filter, and the second is the collision cell positioned between two acceleration plates. The collision cell is kept at high gas pressure, containing either nitrogen gas or argon gas. At low acceleration voltages the ions pass through unmolested. However at higher acceleration voltages,

the ions collide with the gas molecules. This causes the ions to fragment into smaller ions, making the fragments useful for identification. As the ions enter the TOF portion of the instrument, they are ejected orthogonally, to ensure all ions entering the TOF start from the same position. The amount of time spent in the flight tube is proportional to the mass of the individual ion, thus giving an accurate m/z. The detector records the time it takes for the ions to reach it from the ejection and transfers the data to the computer through a digitizer, which converts the analog signal to a digital signal.

To increase the resolution of the TOF, a section of closely spaced metal plates are put at the other end of the tube called a reflectron.[43] The reflectron increases the flight path and reduces the spreading of the ions with similar m/z, which reduces resolution. The reflectron works by applying an increasing potential to a series of metal plates. Ions with higher kinetic energy penetrate deeper than ions with lower kinetic energy. As the ions are slowed, the ions with the same m/z are collapsed together and pushed out towards the detector at the same energy. The combination of high mass resolution, accuracy and fast scan speeds, which are needed for the ever improving separation methods being developed, the QTOF is becoming more popular in the fields of metabolomics and lipidomics.

1.5 Tandem Mass Spectrometry

Tandem mass spectrometry is mostly used for identification of ions that are introduced into the mass spectrometer. Generally there are two modes of tandem mass spectrometry: in time and in space. In time tandem mass spectrometry involves the ion remaining in one chamber. A small amount of collision gas is then released into the chamber, causing the ions and gas to collide, creating fragments.

QTOF instruments use in space tandem mass spectrometry. The ions are physically pushed through a gas filled chamber to create collisions, which lead to fragmentation. The fragments created are characteristic of the molecule and can be used to identify it. Furthermore, in space MS/MS can be divided into the amount of energy used to fragment the molecule. The mode used to fragment molecules for QTOF is collision induced dissociation (CID).[44]

1.5.1 MS/MS in Lipidomics

In lipidomics, MS/MS is acquired using both data dependent acquisition (DDA) and data independent acquisition (DIA). DDA is used when a specific molecule needs to be fragmented. This one molecule is isolated and fragmented. This is useful for targeted lipidomics or to achieve higher confidence quantification.[45] DIA is used to identify as many lipids as possible. This allows for every molecule entering the quadrupole to be fragmented, and the data is then deconvoluted using software. The resultant MS/MS spectra are matched against libraries that have either simulated or real spectra from standards.[29,30] This matching is done using the accurate precursor mass and the pattern of fragmentation of the experimental spectra is matched against that of the library. The matching is given a score determining the goodness of fit. Not all spectra are matched as there is no global library for every lipid or metabolite.

1.6 nLC

Where high performance liquid chromatography (HPLC) uses flow rates of microliter (μL) to milliliter (mL), nLC uses nanoliter (nL) flow rates. This decrease in flow rate allows for increased sensitivity due to decreased dilution of sample and reduced sample consumption.[46] To accommodate nL flowrates, column sizes are typically shrunk to around 75 μm in diameter.[47] The use of HPLC in metabolomics and lipidomics is commonplace, but in special cases the sensitivity of HPLC is not enough. Therefore the use of nLC is needed.

To use nLC, the delays from the sample loop and gradient mixing need to be reduced. To desalt and concentrate the sample, there is a small trapping step prior to the sample being introduced to the analytical column. During trapping, samples are pushed onto a small trapping column using higher flow rates of µL. For trapping to work, the analytes must be retained on the trap column or be washed out to waste. Most metabolites however, are polar and would be washed into the waste, losing most, if not the entire sample. Without trapping, µL samples would take longer than twenty minutes to be loaded onto the analytical column at nanoliter flow rates. Unlike general metabolomics, CIL metabolomics are well suited for trapping. Chapter 2 leverages the advantages of nLC to develop a sensitive method for CIL metabolomics.

1.7 Scope of Thesis

The objective of this thesis research is to develop new LC-MS techniques for metabolomics and lipidomics, ranging from nLC CIL metabolomics to profiling the lipidome of Parkinson's disease samples for potential biomarkers.

In Chapter 2, I use nLC combined with mass spectrometry to reduce sample consumption and increase the coverage of the amine and phenol labeled metabolites.

In Chapter 3, I use UHPLC-UHR-QTOF to profile the lipidome of Parkinson's disease patients in order to find potential lipid biomarkers. Using UHR I increase confidence in the identification of biomarkers.

1.8 Literature Cited

(1) Dempster, A. J. *Physical Review* **1918**, *11*, 316-325.

(2) Zerbinati, C.; Galli, F.; Regolanti, R.; Poli, G.; Iuliano, L. *Clin. Chim. Acta* **2015**, *446*, 156-162.

(3) Lu, Z.; Peart, T. E.; Cook, C. J.; De Silva, A. O. *J. Chromatogr. A* **2016**.

(4) Turkoglu, O.; Zeb, A.; Graham, S.; Szyperski, T.; Szender, J. B.; Odunsi, K.; Bahado-Singh, R. *Metabolomics* **2016**, *12*.

(5) Fan, T. W. M.; Lane, A. N. *Prog. Nucl. Magn. Reson. Spectrosc.* **2016**, *92-93*, 18-53.

(6) Mohamed, R.; Varesio, E.; Ivosev, G.; Burton, L.; Bonner, R.; Hopfgartner, G. *Anal. Chem.* **2009**, *81*, 7677-7694.

(7) Otter, D.; Cao, M.; Lin, H. M.; Fraser, K.; Edmunds, S.; Lane, G.; Rowan, D. *J. Biomed. Biotechnol.* **2011**, *2011*, 974701.

(8) Wu, Y. M.; Li, L. *Anal. Chem.* **2012**, *84*, 10723-10731.

(9) Waikar, S. S.; Sabbisetti, V. S.; Bonventre, J. V. *Kidney Int.* **2010**, *78*, 486-494.

(10) Deininger, S. O.; Cornett, D. S.; Paape, R.; Becker, M.; Pineau, C.; Rauser, S.; Walch, A.; Wolski, E. *Anal. Bioanal. Chem.* **2011**, *401*, 167-181.

(11) Yan, Z.; Yan, R. *Anal. Chim. Acta* **2015**, *894*, 65-75.

(12) Guo, K.; Li, L. *Anal. Chem.* **2009**, *81*, 3919-3932.

(13) Guo, K.; Li, L. *Anal. Chem.* **2010**, *82*, 8789-8793.

(14) Zhou, R.; Tseng, C. L.; Huan, T.; Li, L. *Anal. Chem.* **2014**, *86*, 4675-4679.

(15) Huan, T.; Wu, Y.; Tang, C.; Lin, G.; Li, L. *Anal. Chem.* **2015**, *87*, 9838-9845.

(16) Tenenboim, H.; Burgos, A.; Willmitzer, L.; Brotman, Y. *Biochimie* **2016**.

(17) Fahy, E.; Subramaniam, S.; Brown, H. A.; Glass, C. K.; Merrill, A. H., Jr.; Murphy, R. C.; Raetz, C. R.; Russell, D. W.; Seyama, Y.; Shaw, W.; Shimizu, T.; Spener, F.; van Meer, G.; VanNieuwenhze, M. S.; White, S. H.; Witztum, J. L.; Dennis, E. A. *J. Lipid Res.* **2005**, *46*, 839-861.

(18) Adibhatla, R. M.; Hatcher, J. F.; Dempsey, R. J. *AAPS J.* **2006**, *8*, E314-321.

(19) Goldenberg, N. A.; Everett, A. D.; Graham, D.; Bernard, T. J.; Nowak-Gottl, U. *Proteomics Clin. Appl.* **2014**, *8*, 828-836.

(20) Sas, K. M.; Nair, V.; Byun, J.; Kayampilly, P.; Zhang, H.; Saha, J.; Brosius, F. C., 3rd; Kretzler, M.; Pennathur, S. *J. Proteomics Bioinform.* **2015**, *Suppl 14*.

(21) Narvaez-Rivas, M.; Zhang, Q. *J. Chromatogr. A* **2016**, *1440*, 123-134.

(22) Ovcacikova, M.; Lisa, M.; Cifkova, E.; Holcapek, M. *J. Chromatogr. A* **2016**, *1450*, 76-85.

(23) Shen, Q.; Dai, Z.; Huang, Y. W.; Cheung, H. Y. *Food Chem.* **2016**, *205*, 89-96.

(24) Cifkova, E.; Holcapek, M.; Lisa, M.; Vrana, D.; Melichar, B.; Student, V. *J. Chromatogr. B Analyt. Technol. Biomed. Life. Sci.* **2015**, *1000*, 14-21.

(25) Caprioli, G.; Giusti, F.; Ballini, R.; Sagratini, G.; Vila-Donat, P.; Vittori, S.; Fiorini, D. *Food Chem.* **2016**, *192*, 965-971.

(26) Hussain, J.; Liu, Y.; Lopes, W. A.; Druzian, J. I.; Souza, C. O.; Carvalho, G. C.; Nascimento, I. A.; Liao, W. *Appl. Biochem. Biotechnol.* **2015**, *175*, 3048-3057.

(27) Robotti, E.; Marengo, E. *Methods Mol. Biol.* **2016**, *1384*, 237-267.

(28) Saccenti, E.; Timmerman, M. E. *J. Proteome Res.* **2016**.

(29) Kind, T.; Liu, K. H.; Lee do, Y.; DeFelice, B.; Meissen, J. K.; Fiehn, O. *Nat. Methods* **2013**, *10*, 755-758.

(30) Tsugawa, H.; Cajka, T.; Kind, T.; Ma, Y.; Higgins, B.; Ikeda, K.; Kanazawa, M.; VanderGheynst, J.; Fiehn, O.; Arita, M. *Nat. Methods* **2015**, *12*, 523-+.

(31) Yamashita, M.; Fenn, J. B. *J. Phys. Chem.* **1984**, *88*, 4451-4459.

(32) de la Mora, J. F. *Annu. Rev. Fluid Mech.* **2007**, *39*, 217-243.

(33) Grimm, R. L.; Beauchamp, J. L. *J. Phys. Chem. A* **2010**, *114*, 1411-1419.

(34) Chen, X. J.; Bichoutskaia, E.; Stace, A. J. *J. Phys. Chem. A* **2013**, *117*, 3877-3886.

(35) Awad, H.; Khamis, M. M.; El-Aneed, A. *Appl. Spectrosc. Rev.* **2015**, *50*, 158-175.

(36) Iribarne, J. V.; Thomson, B. A. *J. Chem. Phys.* **1976**, *64*, 2287-2294.

(37) Xu, X.; Gao, B.; Guan, Q.; Zhang, D.; Ye, X.; Zhou, L.; Tong, G.; Li, H.; Zhang, L.; Tian, J.; Huang, J. *J. Pharm. Biomed. Anal.* **2016**, *129*, 34-42.

(38) Millan, L.; Sampedro, M. C.; Sanchez, A.; Delporte, C.; Van Antwerpen, P.; Goicolea, M. A.; Barrio, R. J. *J. Chromatogr. A* **2016**, *1454*, 67-77.

(39) Godzien, J.; Ciborowski, M.; Martinez-Alcazar, M. P.; Samczuk, P.; Kretowski, A.; Barbas, C. *J. Proteome Res.* **2015**, *14*, 3204-3216.

(40) Kang, Y. P.; Lee, W. J.; Hong, J. Y.; Lee, S. B.; Park, J. H.; Kim, D.; Park, S.; Park, C. S.; Park, S. W.; Kwon, S. W. *J. Proteome Res.* **2014**, *13*, 3919-3929.

(41) Shevchenko, A.; Chernushevich, I.; Ens, W.; Standing, K. G.; Thomson, B.; Wilm, M.; Mann, M. *Rapid Commun. Mass Spectrom.* **1997**, *11*, 1015-1024.

(42) Chernushevich, I. V.; Loboda, A. V.; Thomson, B. A. *J. Mass Spectrom.* **2001**, *36*, 849-865.

(43) Bimurzaev, S. B. *Tech. Phys. Lett.* **2014**, *40*, 108-111.

(44) Wells, J. M.; McLuckey, S. A. *Methods Enzymol.* **2005**, *402*, 148-185.

(45) Wu, Y.; Jiang, X.; Zhang, S.; Dai, X.; Liu, Y.; Tan, H.; Gao, L.; Xia, T. *J. Chromatogr. B Analyt. Technol. Biomed. Life. Sci.* **2016**, *1017-1018*, 10-17.

(46) Vissers, J. P. C.; Claessens, H. A.; Cramers, C. A. *J. Chromatogr. A* **1997**, *779*, 1-28.

(47) Vissers, J. P. *J. Chromatogr. A* **1999**, *856*, 117-143.

Chapter 2 Nanoflow LC-MS for High-Performance Chemical Isotope Labeling Quantitative Metabolomics

2.1 Introduction

The growth of metabolomics in the past decade has been directly linked to the development of modern analytical techniques that are able to quantitatively profile a wide range of metabolites in a sample. LC-MS has become a powerful tool for metabolomic profiling.[1,2] To increase the sensitivity of the LC-MS platform, researchers are continually developing more sensitive mass spectrometers, new LC techniques, and improving ionization efficiency of metabolites. The latter can be done using chemical labeling such as isotope encoded chemical derivatization or chemical isotope labeling (CIL).[3-10] In CIL, one isotopic form of a reagent is used to target a broad submetabolome (e.g., all amines and phenols when using dansyl chloride,[4] or all carboxylic acids using DmPA[5]). In parallel, a reference sample of very similar composition but distinct from the sample, which is most commonly made by pooling all available samples, is labeled with another isotopic form of the reagent.[11,12] The derivatized sample and reference are then mixed together and injected into LC-MS for analysis. Peak pairs detected from differentially labeled metabolites are used for metabolite quantification and identification. By using a proper labeling reagent,[3-5] CIL LC-MS allows concomitant improvement in LC separation and MS detection. Accurate relative and absolute quantification of thousands of metabolites can be obtained from a single experiment.[12]

Further sensitivity increase in LC-MS is still highly desirable in handling samples of limited amounts, particularly those requiring multiple analyses. For example, in CIL LC-MS, each labeling reagent covers a selected submetabolome. Therefore, multiple labeling of the same sample

*A version of this has been published as "Nanoflow LC-MS for High-Performance Chemical Isotope Labeling Quantitative Metabolomics" Li, Z.; Tatlay, J.; Li, L. Anal. Chem. 87, 11468-11474. I prepared the samples, ran the samples, data processed, and wrote and edited the manuscript.

using different aliquots needs to be carried out in order to increase the coverage of the overall metabolome. If multidimensional separation of a metabolome or submetabolome is used, the amount of metabolites in individual pre-fractionated aliquots for LC-MS analysis may be very limited,[13-15] requiring a sensitive detection technique. In this regard, there exists a high sensitivity platform that is already widely used in proteomics,[16] but less common in metabolomics: the nanoflow-LC MS. Only a few studies have been reported using nLC-MS for metabolomic analysis.[17-22] This can be attributed to several reasons including technical challenges. In untargeted metabolomic profiling, four modes of LC-MS experiments using two different stationary columns (e.g., reversed phase (RP) and hydrophilic interaction (HILIC) columns) with each operated at positive and negative ion MS detection are often performed on a sample to detect both polar and nonpolar metabolites.[23-27] In nLC-MS, it is a relatively time-consuming process to switch different capillary columns and then optimize their performances thereafter. In addition, injecting a large volume of sample to increase sample loading to nLC is a major challenge.[18] nLC-MS systems used for shotgun proteome analysis is often equipped with a trap column to capture peptides in several microliters of volume prior to nLC separation. However, high efficiency trapping of all metabolites that possess wide variations in chemical and physical properties is very difficult in metabolome analysis.

CIL metabolomic profiling using a rationally designed labeling reagent can overcome these technical challenges, because chemical labeling such as dansylation increases the hydrophobicity of a labeled metabolite to a great extent so that polar or even ionic metabolites can be retained on RP columns after labeling.[4,5] Both a RP trap column and a RP analytical column can be used. There is no need to switch columns to handle different classes of metabolites. CIL also reduces the impact of large retention time shifts in nLC than conventional LC, because quantification is

not reliant on accurate chromatographic alignment between different samples and each metabolite is quantified with its own isotopic counterpart as a peak pair in a mass spectrum.[11,12] We note that there were reports of using nLC-MS for quantifying a limited number of metabolites using chemical isotope labeling.[9,21,22] However, no trapping was used and the labeling reagents used in these reported studies are expected not to alter the metabolite hydrophobicity to such an extent that would allow efficient trapping using an RP column.

In this chapter, I report a workflow based on nLC-MS equipped with a RP trapping column for routine analysis of chemical isotope labeled metabolomic samples with coverage of a few thousand metabolites and describe its performance, particularly in comparison with microbore LC-MS (mLC-MS) commonly used in metabolomics. Dansylation labeling was used for analyzing metabolite standards and the amine/phenol submetabolome of human urine and sweat to demonstrate the improvement of detection sensitivity and metabolome coverage by using nLC-MS.

2.2 Experimental

2.2.1 Chemicals and Reagents

All chemicals and reagents were from Sigma-Aldrich Canada (Markham, ON, Canada) except those otherwise noted. The synthesis of $^{13}C_2$-dansyl chloride has been reported.[4] LC-MS grade water and acetonitrile were from Thermo Fisher Scientific (Edmonton, AB, Canada).

2.2.2 Dansyl Labeling

The labeling protocol has been reported.[4] Briefly, 25 µL of sample was diluted with 25 µL of water and 25 µL of sodium bicarbonate buffer (250 mM) was added, and the solution vortexed. 75 µL of 13 mg/mL $^{12}C_2$ or $^{13}C_2$-dansyl chloride was added and vortexed. Sample was incubated for 40 min at 45°C and then quenched with 10 µL of 250 mM sodium hydroxide. Sample was

heated for 10 min at 45°C for complete quenching. Finally, the sample was acidified with 50 μL of 425 mM formic acid.

2.2.3 LC-UV Quantification.

The method for LC-UV quantification of total labeled metabolites was reported previously.[23] Briefly, a dansyl labeled sample was injected into Waters LC-UV instrument with a Waters Acquity C18 (2.1 mm x 50 mm, 1.7 μm), and eluted with a step gradient. The peak area of the UV absorbance at 338 nm was used to quantify the total labeled metabolites in the sample.

2.2.4 nLC-MS

All nLC-MS experiments were performed on a Waters nanoACQUITY UPLC (Milford, MA, USA) connected to a Waters Q-TOF Premier quadrupole time-of-flight (QTOF) mass spectrometer (Milford, MA, USA) equipped with a nano-ESI source. Mass spectrometer settings were: capillary voltage 3.5 kV, sampling cone 30 V, extraction cone 3.0 V, source temperature 110°C, and collision gas 0.45 mL/min. A 5 μm I.D. PicoTip by New Objective (Woburn, MA, USA) was used with the nano-ESI source. Chromatographic separations were performed on an Acclaim PepMap RSLC C18 (75 μm x 150 mm, 2 μm) and Acclaim PepMap 100 trap column (75 μm x 20 mm, 3 μm). A Waters nanoACQUITY C18 (75 μm x 200 mm, 1.7 μm) column and nanoAcquity Atlantis trap column (180 μm x 20 mm, 5.0 μm) was also evaluated. Mobile phase A was 0.1 % LC-MS formic acid in LC-MS water, and mobile phase B was 0.1 % LC-MS formic acid in LC-MS acetonitrile. The 45 minute gradient conditions were: 0 min (15% B), 0-2.0 min (15% B), 2.0-4.0 min (15-25% B), 4.0-24 min (25-60% B), 24-28 min (60-90% B), and 28-45 min (90% B). A wash and equilibration injection was run between samples; the gradient was: 0-10 min (90% B), 10-25 min (15% B). The flow rate was 350 nL/min and the injection volume was 5 μL

(the maximum volume of the sample loop used) in most cases except that of studying the trapping efficiency.

2.2.5 LC-MS

All LC-MS experiments were performed on an Agilent 1100 Series Binary LC System (Santa Clara, CA, USA) connected to the same Q-TOF Premier mass spectrometer used in the nLC-MS experiment, with the nESI source swapped out for an ESI source. Mass spectrometer settings were: capillary voltage 3.5 kV, sampling cone 30 V, extraction cone 3.0 V, source temperature 110°C, desolvation temperature 220°C, desolvation gas 800 L/hr, and collision gas 0.45 mL/min. Chromatographic separations were performed on a Waters Acquity BEH C18 column (2.1 mm x 100 mm, 1.7 μm) with the same mobile phases as the nano-LC. The 45 min gradient conditions were; 0 min (20% B), 0-3.5 min (20-35% B), 3.5-18 min (35-65% B), 18-24 min (65-99% B), 24-37 min (99% B), and 37.1-45 min (20% B). The flow rate was 180 μL/min.

2.2.6 nLC-MS Trapping Efficiency

A mixture of amino acids at a concentration of 1 mM each was dansylated.[4] The dansylation efficiencies for these amino acids have been determined previously by comparing the signal intensities of labeled product and any remaining unlabeled metabolite using LC-MS.[4] $^{12}C_2$ and $^{13}C_2$-dansyl labeled amino acids were mixed 1:1 by volume and diluted to 1000, 2000, 4000, 6000, 8000, and 10000 fold using serial dilution. Injection volume was varied for each diluted sample to ensure 120 fmol of dansylated amino acids was loaded onto the column for each injection. Data was de-noised, smoothed, centered and peak areas extracted using Waters QuanLynx software.

2.2.7 Dynamic Range of Peak Pair Detection

$^{12}C_2$-dansylated amino acids were diluted by half and mixed with undiluted $^{13}C_2$-dansylated amino acids in a 1:1 volume ratio. The theoretical peak ratio of $^{12}C_2$- to $^{13}C_2$-labeled amino acid should be 1:2. The sample was then diluted using serial dilution and increasing sample amounts were injected into the nLC-MS and mLC-MS. Ratios were calculated by dividing the $^{12}C_2$-labeled amino acid peak area by the $^{13}C_2$-labeled amino acid peak area.

2.2.8 Urine and Sweat Analysis

A human urine sample was split into two vials; one was $^{12}C_2$-dansyl labeled and the other was $^{13}C_2$-dansyl labeled. The $^{12}C_2$-dansyl urine was quantified to be 48.2 mM using the LC-UV method.[28] The $^{12}C_2$-dansyl urine and $^{13}C_2$-dansyl urine were mixed 1:1 by volume then diluted using serial dilution. These diluted samples were injected at increasing concentrations into the nLC-MS and LC-MS. Peak pairs were then extracted from the processed data using IsoMS.[11]

A human sweat sample was treated in the same way as the urine sample. The concentration of the sweat was determined to be 8.4 mM using the LC-UV method. The $^{12}C_2$-dansyl sweat and $^{13}C_2$-dansyl sweat were mixed 1:1 (v/v) for injection into nLC-MS and mLC-MS for analysis.

2.3 Results and Discussion

2.3.1 Column Selection

Some users may re-purpose an existing nLC-MS system used for shotgun proteomic analysis to analyze metabolomic samples for metabolomics. Various factors need to be considered to make such a switch including column selection. We initially used a set of Waters trap column and analytical column used for proteomic analysis to analyze the dansyl labeled urine samples. The resulting chromatogram showed wide peak widths of around 0.8 min with tailing (Figure

2.1A), compared to widths of ~0.06 min for peptides. This problem was caused by the Waters Symmetry C18 trap which uses high purity silica with end capping. Peak broadening was not observed when the sample was directly loaded onto the analytical column which uses a polymeric bonded phase. It is very likely that a significant amount of residual silanol activity existed in the trap column that caused broadening for the basic dansylated metabolites, but not for the peptides. We then switched the trap and column set to the Thermo Scientific PepMap 100 C18 set, which also used high purity silica. However, the PepMap 100 set gave adequate peak widths of 0.2 min with reduced tailing (Figure 2.1B). This set was thus selected for the subsequent experiments. This example illustrates the importance of selecting a proper column and trap combination for profiling labeled metabolites.

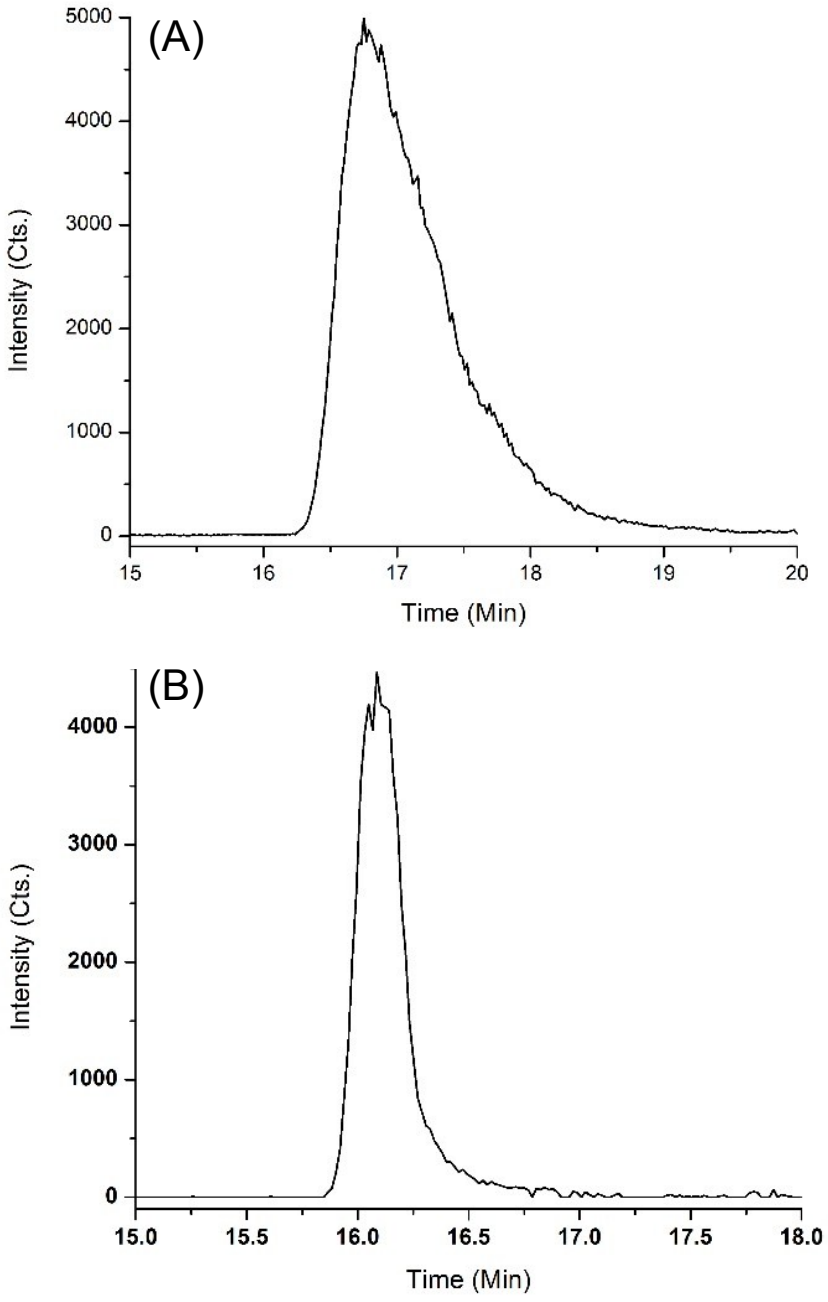

Figure 2.1 Chromatographic peaks of a dansylated amino acid in a labeled urine sample obtained by using (A) Waters nanoACQUITY column set and (B) Thermo Acclaim PepMap column set.

2.3.2 Separation Parameters

Several nLC parameters were optimized to achieve an optimal coverage of the amine/phenol submetabolome profile within the shortest run time. First, analytical flow rates of 500, 350, 150 nL/min were tested. With the three different flow rates, we found no significant differences in the number of peak pairs or metabolites detected. However, while 500 nL/min gave the shortest run time, it could increase the backpressure significantly, resulting in popping the fused-silica capillaries out of their fittings. At the lowest flow rate of 150 nL/min, the analysis time was increased by 10 min. Thus the flow rate of 350 nL/min was chosen as a compromise for the work.

Next we optimized the gradient separation condition. The majority of the labeled metabolites eluted between 15% and 60% mobile phase B (acetonitrile 0.1% formic acid). Thus, a shallow gradient from 25% to 60% over 20 min was used to improve the separation.

The solvent composition of the diluent used to prepare the dansylated samples was also optimized. Initially, the samples were diluted using the same solvent composition as that used for the dansylation labeling reaction, i.e., 1:1 acetonitrile:water (v/v) 0.1% formic acid, to prevent any potential precipitation of highly non-polar dansylated metabolites. This sample plug with a high organic composition greatly reduced the retention of metabolites on the trap column, causing metabolites to be flushed out of the trap column and into the waste. As a result, a significant amount of early eluting peaks were reduced in intensity (Figure 2.2A). After testing a number of different diluents, a diluent composed of 1:9 acetonitrile:water (v/v) 0.1% formic acid gave no sample loss or precipitation for the urine samples studied (Figure 2.2B).

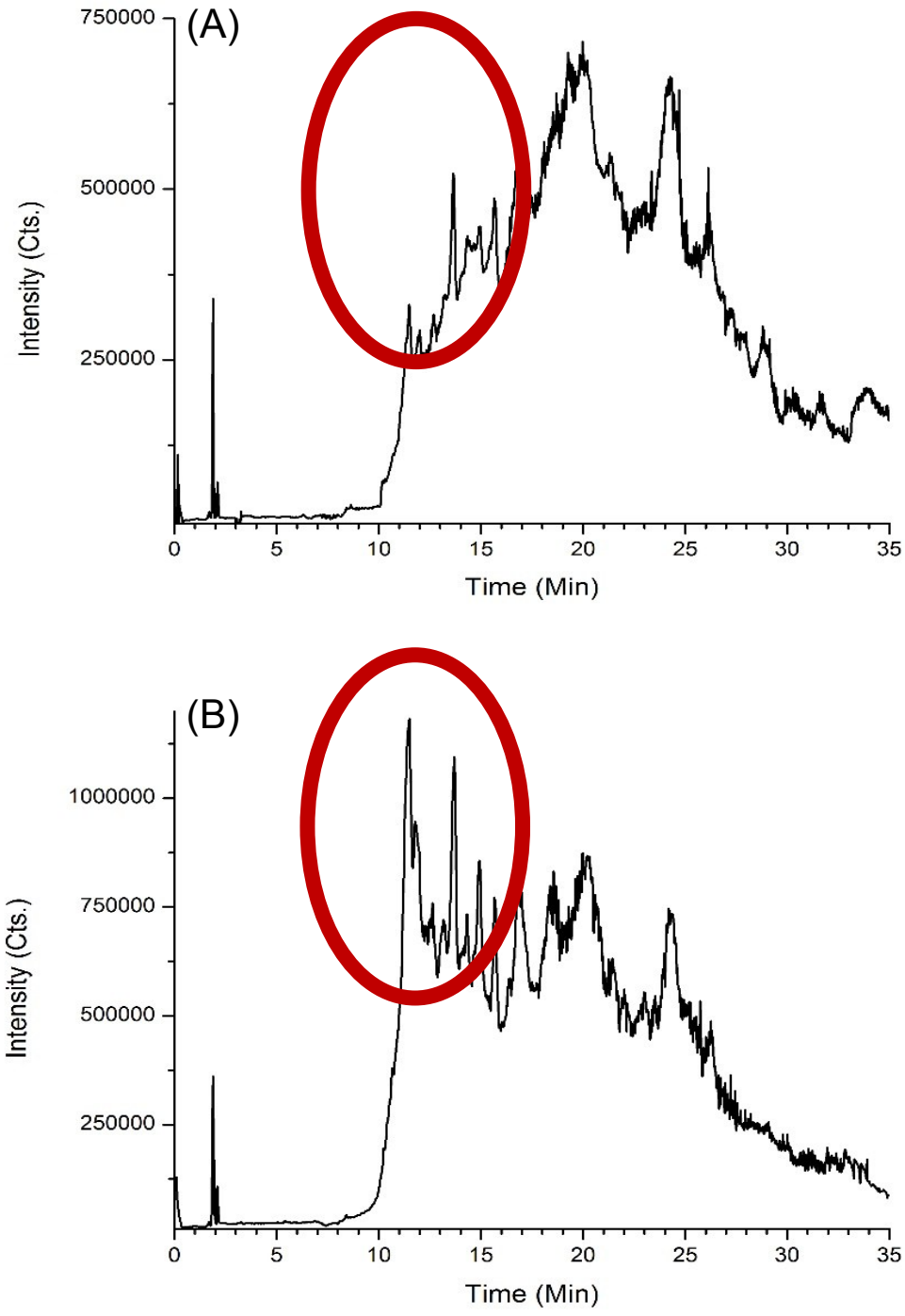

Figure 2.2 Comparison of total-ion chromatograms (TIC) of a dansyl labeled urine sample obtained using (A) 1:1 ACN:H_2O diluent and (B) 1:9 ACN:H_2O diluent. A Significant portion of the early eluting peaks are reduced in intensity when using the 1:1 ACN:H_2O diluent.

2.3.3 Trapping Optimization and Efficiency

A trapping column is an integral part of nLC-MS for injecting a relatively large volume of samples. Traps are not commonly used in mLC-MS, as injection of several microliters of sample is compatible with the high flow rate. In nLC-MS, prior to separating on the analytical column, the sample is first pushed through a short trap column, usually at a higher flow rate compared to the analytical flow rate. Analytes are retained on the trap while extra diluent and other non-retaining matrix components are flushed into the waste. This serves two functions: the first is to remove salts and other interfering chemicals, and the second is to reduce the time it takes for samples to reach the column. As a result, a large volume of sample can be loaded onto the column in a short time. Figure 2.3 shows the chromatograms of the separation of a mixture of dansylated amino acids using a 5 μL injection loop at a flow rate of 350 nL/min. Without the use of the trap column, there was a dead time of 16.67 min and the first retained analyte eluted in 23.63 min (Figure 2.3A). With the trap column, at a trapping flow rate of 7.0 μL/min, the dead time of the sample loop was reduced to 0.71 min leaving only the dead time of the gradient delay which was 7.10 min (Figure 2.3B). Overall, there was a reduction of 16.53 min in run time when the trap was used. Therefore, analyte trapping is essential for reducing the dead time of nLC-MS operating at nanoliter flow rates.

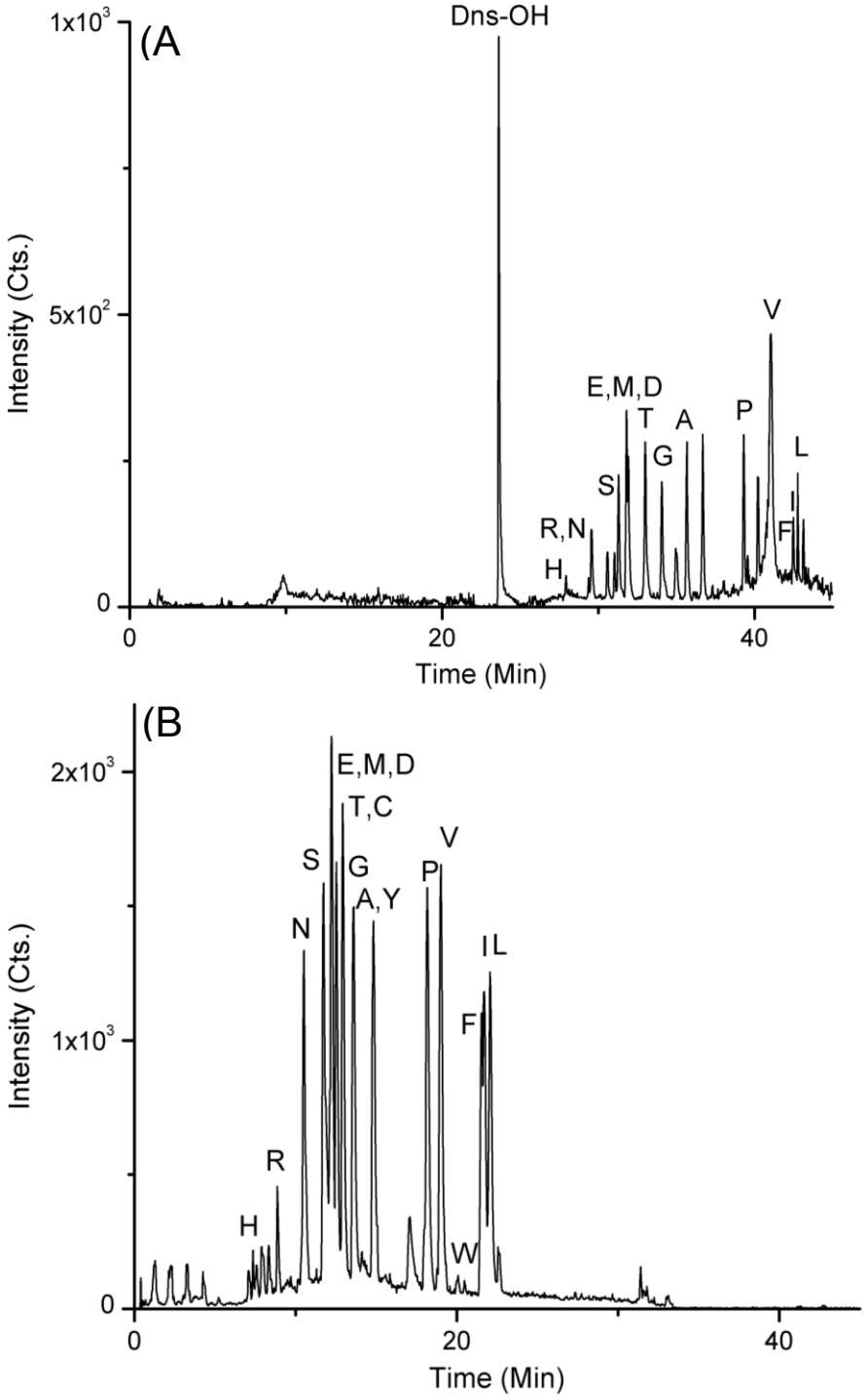

Figure 2.3 nLC-MS chromatograms of a mixture of 18 dansylated amino acids obtained (A) without using a trap column and (B) with the use of a trap column. The peak at 23.63 min was from dansyl-OH, a product of dansyl reagent after quenching with NaOH. This product did not retain on the RP trap column and thus did not show up in (B).

In using the trap, the goal is to have metabolites completely retained on the trap while mobile phase is pushed through at the highest flow rate possible to wash out salts and other non-analytes. The concern is that with higher flow rate there will be more metabolites that are flushed into the waste. Therefore, the trapping flow rate, trapping mobile phase composition and trapping time need to be carefully balanced. Several trapping flow rates ranging from 1 μL/min to 20 μL/min was tested; 20 μL/min was the highest flow rate possible without over pressuring the trap column. By increasing the trap flow rate, the number of peak pairs detected was reduced due to sample loss. Decreasing the flow rate caused a longer dead time and longer overall run time with no significant increase in the peak pair number. The optimal flow rate was 7 μL/min which was the highest flow rate without significant sample loss. The trapping mobile phase composition was optimized to be 2% acetonitrile in water. Increasing the organic composition washed away the sample. Finally, the shortest trapping time to wash the entire sample out of the 5 μL sample loop and onto the trap, in addition to washing out salts, was set at 1 min.

While trapping can increase the detection sensitivity by allowing for the injection of a large volume of dilute sample, there is a greater chance that the analytes might be washed out with larger loading volume. After optimizing the trapping conditions, we investigated the trapping efficiency by injecting a series of diluted dansylated amino acid mixtures where the injection amount was kept constant at 120 fmol by adjusting the injection volume and concentration. There was no observed trend that indicated sample loss from 1000 to 10000 fold diluted samples when looking at the measured peak area for selected dansylated amino acids, as shown in Figure 2.4. This shows that the nLC-MS trapping condition used was efficient at trapping low-concentration and high-injection-volume dansylated samples without affecting chromatographic separation or incurring significant sample loss. It should be noted that we chose the amino acid standards for this trapping

efficiency study, because they represent some of the most polar compounds found in urine, serum or other biological samples. Thus the results of dansyl labeled amino acids on a C18 trap represent the extreme cases of otherwise unretained polar metabolites without labeling. Other metabolites in a biological sample will be more hydrophobic and should be retained on the trap after dansylation even more efficiently.

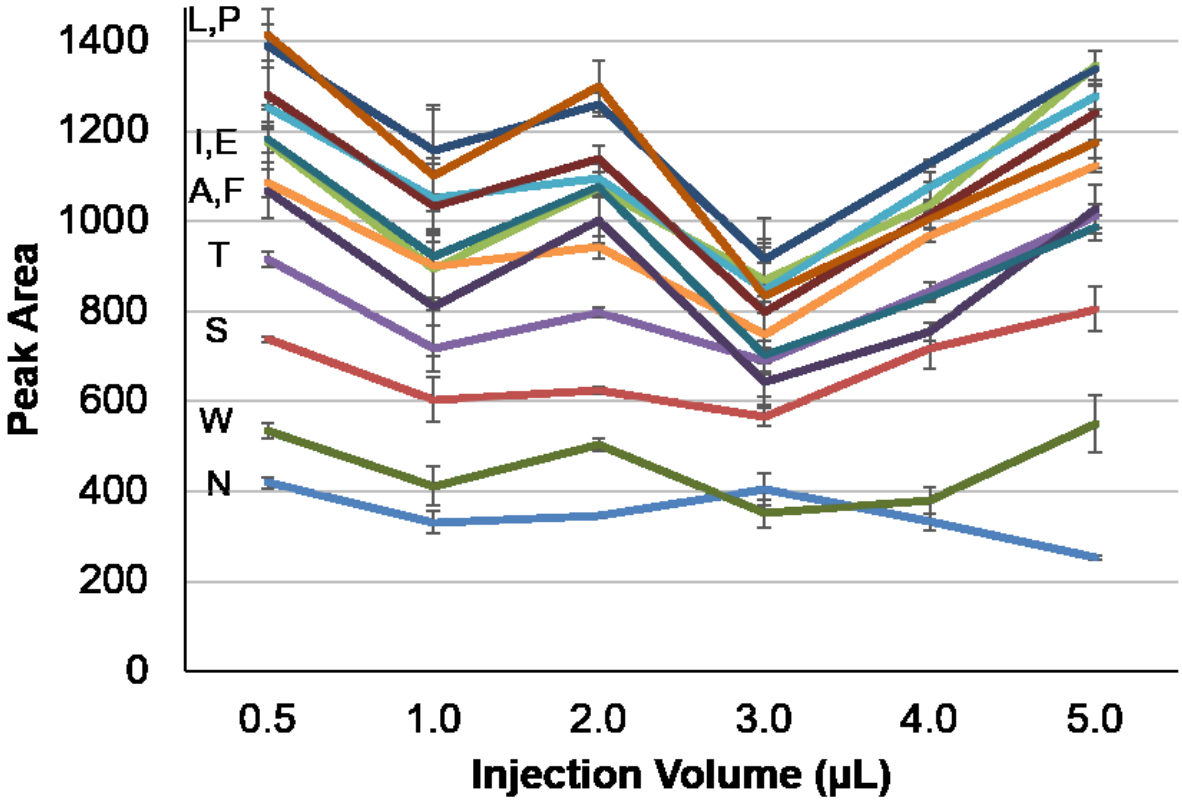

Figure 2.4 Chromatographic peak areas of dansylated amino acids obtained by injecting the same sample amount (120 fmol) while changing the injection volumes for different concentrations of solutions. Error bars are standard deviation (n=3).

2.3.4 Chromatographic Reproducibility

In untargeted metabolomic studies, reproducible retention time is required for data file alignment to generate accurate abundance information across hundreds of samples that are run on different days or even different weeks. Table 2.1 shows the intraday retention time reproducibility of dansylated amino acids measured using the nLC and mLC. The average relative standard

deviation (%RSD) of the nLC retention times was 0.48%, which was significantly worse than the %RSD of the mLC at 0.06%. This confirms reports by other groups that nLC retention time is not as stable as mLC.[29] The lower retention time reproducibility may be due to the reduced quality in stationary phase packing in preparing the nLC columns and a larger flow rate variation with nLC pumps vs. mLC pumps. Retention time stability has a negative effect on the quantification of unlabeled metabolites between different samples and several peak alignment methods have been reported to reduce the effect.[30] However, with CIL, each $^{12}C_2$ dansylated metabolite in a sample is quantified relative to the $^{13}C_2$ dansylated metabolite in a control, and thus precise alignment is not required for relative quantification.

In addition to retention time, the intensity of the metabolites needs to be stable between sample runs for accurate quantification. Table 2.2 shows the intensity %RSDs of the dansylated amino acids. The average %RSD of nLC intensities was similar to that of mLC (3.6% vs. 3.3%). Thus, the quantitative precision of the two systems is similar.

Table 2.1 Relative standard deviations of retention times of dansylated amino acids measured by nLC-MS and mLC-MS (n=3).

	nLC		mLC	
	RSD (%)	σ (s)	RSD (%)	σ (s)
Asparagine	1.1%	7.3	0.00%	0.00
Glutamic Acid	0.84%	6.6	0.18%	0.69
Glycine	0.40%	3.5	0.00%	0.00
Alanine	0.65%	6.3	0.00%	0.00
Proline	0.34%	4.0	0.10%	0.69
Tryptophan	0.21%	2.7	0.09%	0.69
Phenylalanine	0.16%	2.2	0.00%	0.00
Leucine	0.13%	1.8	0.11%	0.92

Table 2.2 Relative standard deviations of peak areas of dansylated amino acids measured by nLC-MS and mLC-MS (n=3).

	nLC			mLC		
	Average Area	SD	RSD	Average Area	SD	RSD
Asparagine	2238.0	153.5	6.9%	49.3	1.3	2.7%
Glutamic Acid	6353.0	98.6	1.6%	121.7	1.4	1.2%
Glycine	6553.0	138.4	2.1%	173.8	9.4	5.4%
Alanine	5684.3	129.8	2.3%	126.7	5.6	4.4%
Proline	5553.6	166.8	3.0%	156.2	1.4	0.9%
Tryptophan	3560.9	99.6	2.8%	49.8	0.7	1.4%
Phenylalanine	4483.3	268.8	6.0%	124.0	3.3	2.7%
Leucine	5514.4	209.5	3.8%	184.0	14.4	7.8%
Average	4992.6	158.1	3.5%	123.2	4.7	3.3%

2.3.5 Sensitivity Improvement

Figure 2.5A shows the plots of peak areas as a function of sample injection amount for nLC- and mLC-MS using dansyl alanine as an example. Signal saturation was observed for nLC-MS when the analyte concentration was over 48 μM, corresponding to 240 pmol with 5 μL injection. In contrast, even at 238 μM, the peak area obtained by mLC-MS was not very high. In fact, it was slightly lower than that obtained using the solution of 0.5 μM in nLC-MS. This result demonstrates a more than 476-fold increase in mass-detection sensitivity at the high concentration region. At the low limit, as Figure 2.5B shows, mass spectral signals were still detectable at S/N 61 with the injection of the 0.005 μM or 5 nM solution, corresponding to 0.025 pmol or 25 fmol amount. The limit of detection (LOD) for dansyl alanine was 1.2 nM in mLC-MS and 0.25 nM in nLC-MS. This sensitivity enhancement for detecting dansyl labeled metabolites using nLC-MS is consistent with what others observed for nano-ESI of other types of molecules due to improvement in ionization efficiency, reduced ion suppression and more efficient ion acceptance to MS.[31,32]

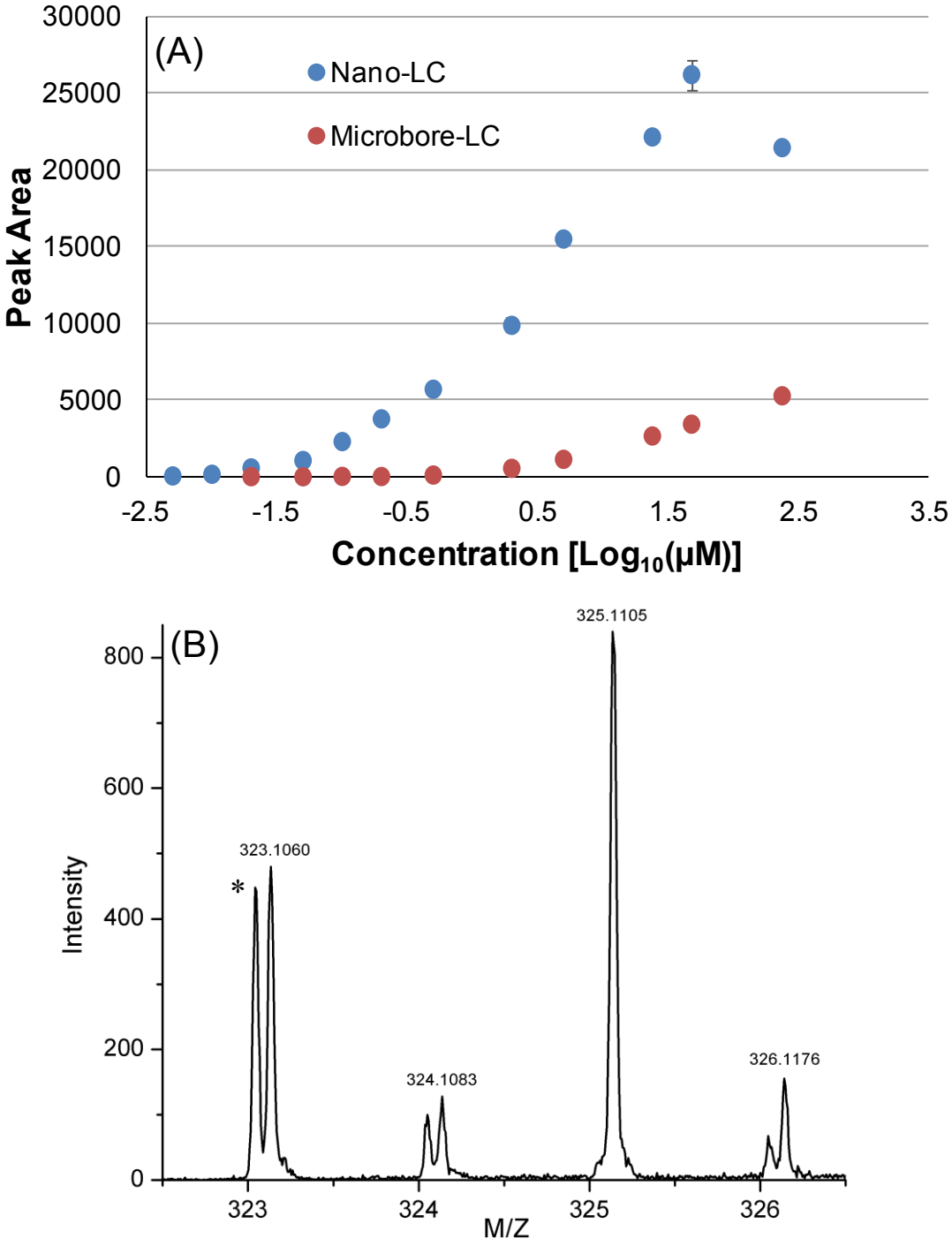

Figure 2.5 (A) Chromatographic peak area of dansyl alanine as a function of injected sample solution concentration for mLC-MS and nLC-MS. Error bar represents one standard deviation (n=3). (B) Molecular ion region of the mass spectrum obtained from 1:2 mixture of ^{12}C-dansyl alanine and ^{13}C-dansyl alanine at 5 nM with an injection of 5 µL solution (i.e., 25 fmol) in nLC-MS. The extra peak (*) next to the ^{12}C-dansyl alanine was from a background species.

For other labeled amino acids tested (Appendix Figure A2.1), injections of 5 nM of dansylated glycine, glutamic acid, asparagine, phenylalanine, leucine and tryptophan gave signals with S/N 130, 120, 11, 30, 150 and 7, respectively, and their corresponding LODs are 0.12 nM in nLC-MS (0.52 nM in mLC-MS), 0.13 nM (0.95 nM), 1.4 nM (>20 nM), 0.5 nM (6.0 nM), 0.10 nM (3.3 nM) and 2.1 nM (8.6 nM). These LODs are significantly lower than those reported using nLC-MS without a trap and with other labeling reagents. LODs of isobaric *N*,*N*-dimethyl leucine labeled alanine, phenylalanine, leucine and tryptophan were 110, 7, 30 and 10 nM, respectively.[21] LODs of isobaric *N*-hydroxysuccinimide ester labeled alanine, glycine, glutamic acid, phenylalanine, leucine and tryptophan were 19, 21, 2, 1, 16 and 2 nM, respectively.[22] Our results illustrate that with a 5-μL loop injection we can now analyze metabolites at <5 nM concentrations with an analyte amount of <25 fmol.

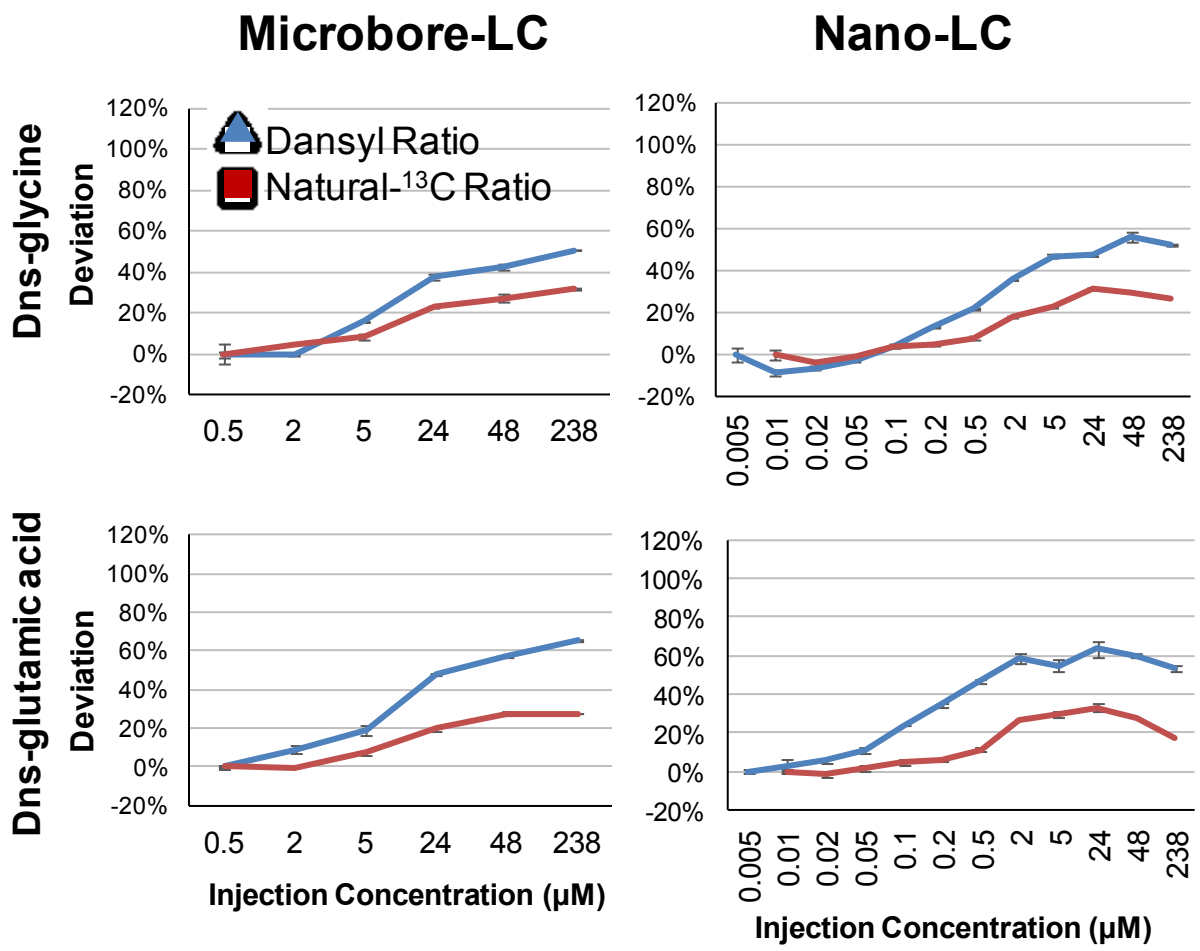

Figure 2.6 Effect of detection saturation on the calculated peak pair ratio in mLC-MS and nLC-MS. Derivation from the expected 1:2 ratio is plotted as a function of the solution concentration of 1:2 mixture of ^{12}C-dansyl amino acid and ^{13}C-dansyl amino acid.

2.3.6 Dynamic Range for Relative Quantification

Quantitative metabolomics rely on relative quantification of all the metabolites in comparative samples, not just one or a few metabolites. In CIL LC-MS, relative quantification of each metabolite is achieved by calculating the peak ratio of the ^{12}C-labeled metabolite in a sample versus the ^{13}C-labeled same metabolite in a control. It is always desirable to detect as many peak pairs as possible in a mass spectrum to quantify the low and high abundance metabolites. However, if a peak pair becomes saturated in a mass spectrum, the highest peak in the pair will become compressed, distorting the measured peak ratio. In our work, the dynamic range for detecting peak

pairs was evaluated by analyzing a series of diluted solutions of a 1:2 mixture of a ^{12}C-labeled amino acid and its ^{13}C-labeled counterpart for several amino acids. The theoretical peak intensity ratio should be 0.5. However, the ^{13}C-labeled peak should be saturated first when the concentration of the mixture increases. Thus, the measured peak ratio will be greater than 0.5 when the ^{13}C-peak is saturated.

Figure 2.6 shows the deviation of the peak ratios of glutamic acid and glycine at different mixture concentrations. Both mLC-MS and nLC-MS showed deviations from the theoretical ratio of 0.5 when the sample concentration increased, showing the effect of detection saturation on the quantification of metabolites. The trends were similar with the other dansyl amino acids. The mLC-MS dansyl peak ratios for glycine and glutamic acid deviated more than 20% at concentrations of > 5 μM, and below 0.5 μM the amino acids were not observed. This means that an accurate peak ratio can only be obtained within 1 order of magnitude in concentration for this mLC-MS setup. The nLC-MS deviated above 20% at 0.5 μM for glycine and 0.1 μM for glutamic acid. The higher sensitivity allowed the lower end concentration to be reduced down to 0.005 μM, giving a concentration range of 2 and 1.3 orders of magnitude for glycine and glutamic acid, respectively.

To extend the dynamic range when the peaks become saturated, the natural-^{13}C peaks can be used to recover the accurate peak ratio because they are of lower intensity and still reflect the sample ratios.[33] Figure 2.6 shows that the natural-^{13}C peak ratios were more resistant to deviation caused by detector saturation. In mLC-MS, the natural-^{13}C peak ratios of glycine deviated above 20% for glycine and glutamic acid at 24 μM, instead of 5 μM, when measuring dansyl peak ratios. The nLC-MS deviated past 20% at 2 μM for both amino acids which was between 4 and 20 times higher concentration than using the dansyl peak ratio. Combining the concentrations that deviated

less than 20% using both dansyl and natural-^{13}C peak ratios, the nLC-MS had a range of 2.6 orders of magnitude, while mLC-MS had 1.7, for both amino acids.

The above results demonstrate that nLC-MS offers a greater dynamic range for detecting peak pairs with accurate quantification, compared to mLC-MS. This result is not surprising as one would expect that mLC-MS which is less sensitive than nLC-MS would have a lower dynamic range of detection.[31,32] If we relax the deviation to ~30%, instead of 20%, the quantitative dynamic range becomes 476-fold (i.e., 0.5 to 238 μM) for mLC-MS and 47600-fold (i.e., 0.005 to 238 μM) for nLC-MS for a 1:2 mixture of ^{12}C-/^{13}C-dansyl glycine or ^{12}C-/^{13}C-dansyl glutamic acid.

2.3.7 Urine Submetabolome Profiling

Dansylated human urine was used for the direct comparison of metabolomic analysis sensitivity between nLC-MS and mLC-MS. A urine sample was split and labeled with ^{12}C- and ^{13}C-dansyl chloride, followed by mixing together in a 1:1 ratio. The total concentration of all dansylated metabolites in urine was quantified to be 48.2 mM. The ^{12}C-/^{13}C-labeled urine mixture was diluted up to 10000-fold and injected in triplicate in decreasing metabolite amounts.

Figure 2.7A shows that the maximum number of detected metabolites in urine using nLC-MS was 4524±37 (n=3) at 26.076 nmol of metabolites injected, while mLC-MS gave a maximum number of 4019±40 at 52.151 nmol injection. Thus, nLC-MS detected about 13% more metabolites than mLC-MS, likely due to the improved dynamic range of detecting peak pairs. This result is consistent with what others have observed in bottom-up proteomics; more peptides or proteins could be detected with nLC-MS.[34] At the optimal injection amount for nLC-MS of 26.076 nmol, mLC-MS detected only 67% of the metabolites (i.e., 3034±161). This means that the optimal injection amount for nLC-MS was 2 times lower than using mLC-MS. The improved sensitivity

of nLC-MS was more apparent at lower sample loading amounts; below 0.522 nmol loading, nLC-MS detected at least 8 times more metabolites than mLC-MS. It is clear that if the sample amount is not limited, mLC-MS can still be used for metabolomic profiling without incurring too large of a drop in the number of metabolites detected. However, as Figure 2.5A shows, sample dilution has a much greater effect on mLC-MS than nLC-MS. For example, injecting 2.6 nmol detected less than 1/3 of the peak pairs found in the 26 nmol injection by mLC-MS, while injecting 0.26 nmol in nLC-MS detected more than half of the peak pairs found in the 2.6 nmol injection. Thus, nLC-MS would have a clear advantage in handling samples of limited amounts or diluted samples.

2.3.8 Sweat Submetabolome Profiling

The advantage of nLC-MS for analyzing a limited amount of sample can be demonstrated in profiling the human sweat metabolome. Typically, only several microliters of sweat can be collected from a subject without needing a prolonged collection and using a very large collection area. For this study, about 10 μL of human sweat was collected from an arm of a healthy individual after exercise. The total concentration of the dansyl labeled metabolites in the sweat was determined to be 8.4 mM using LC-UV, which was 6 times lower than the total concentration of metabolites in urine. For sweat analysis, the lower total concentration and the lower volume require the extra sensitivity offered by the nLC-MS. Figure 2.7B shows that at the maximum injection amount of 5 nmol of dansylated sweat, 3908±62 peak pairs were detected for nLC-MS and 1064±6 peak pairs were detected for mLC-MS, or a 4-fold increase in the number of metabolites detected. Due to the limited amount of sample, it was not possible to inject an optimal amount for mLC-MS similar to Figure 2.7A. The higher sensitivity was again observed at lower sample loading amounts of 1 nmol where nLC-MS has 11-fold higher peak pair values of 3098±16 compared to 275±78 from mLC-MS. We envisage the use of nLC-MS for analyzing many types of metabolomic

samples where the sample amount is limited, such as a microliter of sweat collected naturally, a droplet of blood from a finger prick, etc.

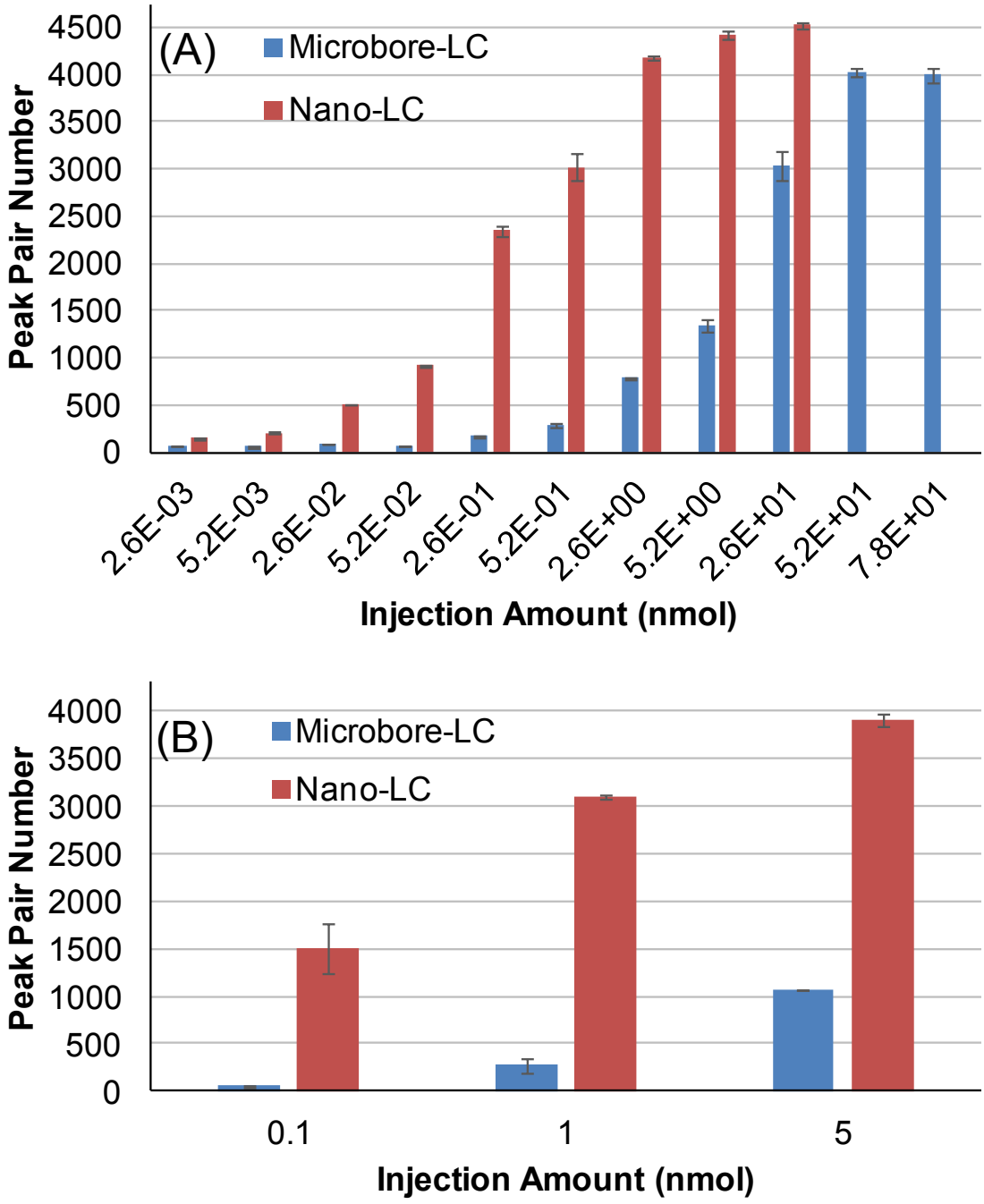

Figure 2.7 Number of peak pairs detected as a function of the sample injection amount from mLC-MS and nLC-MS analysis of (A) ^{12}C-/^{13}C-labeled human urine sample and (B) ^{12}C-/^{13}C-labeled human sweat sample

2.3.9 Robustness

For routine metabolomic analysis, an analytical tool needs to be robust in dealing with a large number of samples. Due to the small inner diameter of fused-silica capillaries, columns, and nESI emitters used in nLC-MS, the entire system is more finicky to maintain, compared to mLC-MS. Firstly, all of the fused-silica components are much more fragile than the polymer and stainless steel components used in mLC-MS and must be handled with care. The small internal diameter also means that the capillaries are more prone to clogging from particulate in the samples and silica fragments from poorly cut and ragged tubing edges. The small nESI emitters are more prone to clogging from sample matrix precipitation and silica particles from the fused-silica, and backpressure must be regularly monitored for clogging.

There are a few precautions that can be taken to significantly reduce the frequency of catastrophic clogging of nLC-MS. In our laboratory, a typical capillary internal diameter of 20 μm and outer diameter of 360 μm was found to be the optimal balance between robustness and chromatographic performance by reducing dead volume. For cutting fused-silica capillaries to the necessary lengths, a rotating diamond cutter is expensive but highly recommended for its ability to reproducibly give clean cuts that are free of capillary clogging particles. Following cutting, new fused-silica columns and capillaries must be flushed and their ends washed with clean solvent to remove any particles. Although the nLC-MS platform can be less robust than mLC-MS platform, by following these precautions and being careful, the system can be operated for months with little downtime. Recent advancements in nLC technology, such as the use of an integrated microfluidic column or capillary cartridge that can be conveniently connected to an MS interface,[35] are expected to make nLC-MS more robust for routine metabolomic analysis.

2.4 Conclusions

We report a nanoflow LC-MS system combined with chemical isotope labeling of metabolites for metabolomic profiling with high coverage. A reversed phase trap column is used to capture the labeled metabolites at 7 μL/min, followed by separation on a capillary RPLC column at 350 nL/min. The sample injection volume is typically at 5 μL, allowing the analysis of a diluted sample solution. Dansylation CIL was demonstrated for sensitive profiling of the amine/phenol submetabolome in human urine and sweat; however, the technique should be applicable to other labeling chemistries where labeled metabolites can be retained on RPLC. Because the configuration of the nLC-MS system described herein is similar to those widely used for shotgun proteome analysis, this metabolomic profiling platform should be readily adapted.

2.5 Literature Cited

(1) Yin, P. Y.; Xu, G. W. *J. Chromatogr. A* **2015**, *1374*, 1-13.

(2) Rainville, P. D.; Theodoridis, G.; Plumb, R. S.; Wilson, I. D. *Trac-Trends Anal. Chem.* **2015**, *61*, 181-191.

(3) Zhou, R.; Huan, T.; Li, L. *Anal. Chim. Acta* **2015**, *881*, 107-116.

(4) Guo, K.; Li, L. *Anal. Chem.* **2009**, *81*, 3919-3932.

(5) Guo, K.; Li, L. *Anal. Chem.* **2010**, *82*, 8789-8793.

(6) Liu, P.; Huang, Y. Q.; Cai, W. J.; Yuan, B. F.; Feng, Y. Q. *Anal. Chem.* **2014**, *86*, 9765-9773.

(7) Tayyari, F.; Gowda, G. A. N.; Gu, H. W.; Raftery, D. *Anal. Chem.* **2013**, *85*, 8715-8721.

(8) Dai, W. D.; Huang, Q.; Yin, P. Y.; Li, J.; Zhou, J.; Kong, H. W.; Zhao, C. X.; Lu, X.; Xu, G. W. *Anal. Chem.* **2012**, *84*, 10245-10251.

(9) Yuan, W.; Anderson, K. W.; Li, S. W.; Edwards, J. L. *Anal. Chem.* **2012**, *84*, 2892-2899.

(10) Song, P.; Mabrouk, O. S.; Hershey, N. D.; Kennedy, R. T. *Anal. Chem.* **2012**, *84*, 412-419.

(11) Zhou, R.; Tseng, C. L.; Huan, T.; Li, L. *Anal. Chem.* **2014**, *86*, 4675-4679.

(12) Huan, T.; Li, L. *Anal. Chem.* **2015**, *87*, 7011-7016.

(13) Guo, K.; Peng, J.; Zhou, R. K.; Li, L. *J. Chromatogr. A* **2011**, *1218*, 3689-3694.

(14) Mirnaghi, F. S.; Caudy, A. A. *Bioanalysis* **2014**, *6*, 3393-3416.

(15) Vuckovic, D. *Anal. Bioanal. Chem.* **2012**, *403*, 1523-1548.

(16) Nilsson, T.; Mann, M.; Aebersold, R.; Yates, J. R.; Bairoch, A.; Bergeron, J. J. M. *Nat. Methods* **2010**, *7*, 681-685.

(17) Jones, D. R.; Wu, Z.; Chauhan, D.; Anderson, K. C.; Peng, J. *Anal. Chem.* **2014**, *86*, 3667-3675.

(18) Chetwynd, A. J.; Abdul-Sada, A.; Hill, E. M. *Anal. Chem.* **2015**, *87*, 1158-1165.

(19) David, A.; Abdul-Sada, A.; Lange, A.; Tyler, C. R.; Hill, E. M. *J. Chromatogr. A* **2014**, *1365*, 72-85.

(20) Uehara, T.; Yokoi, A.; Aoshima, K.; Tanaka, S.; Kadowaki, T.; Tanaka, M.; Oda, Y. *Anal. Chem.* **2009**, *81*, 3836-3842.

(21) Hao, L.; Zhong, X. F.; Greer, T.; Ye, H.; Li, L. J. *Analyst* **2015**, *140*, 467-475.

(22) Yuan, W.; Zhang, J. X.; Li, S. W.; Edwards, J. L. *J. Proteome Res.* **2011**, *10*, 5242-5250.

(23) Ivanisevic, J.; Zhu, Z. J.; Plate, L.; Tautenhahn, R.; Chen, S.; O'Brien, P. J.; Johnson, C. H.; Marletta, M. A.; Patti, G. J.; Siuzdak, G. *Anal. Chem.* **2013**, *85*, 6876-6884.

(24) Contrepois, K.; Jiang, L. H.; Snyder, M. *Mol. Cell. Proteomics* **2015**, *14*, 1684-1695.

(25) Vorkas, P. A.; Isaac, G.; Anwar, M. A.; Davies, A. H.; Want, E. J.; Nicholson, J. K.; Holmes, E. *Anal. Chem.* **2015**, *87*, 4184-4193.

(26) Tulipani, S.; Mora-Cubillos, X.; Jauregui, O.; Llorach, R.; Garcia-Fuentes, E.; Tinahones, F. J.; Andres-Lacueva, C. *Anal. Chem.* **2015**, *87*, 2639-2647.

(27) Mahieu, N. G.; Huang, X. J.; Chen, Y. J.; Patti, G. J. *Anal. Chem.* **2014**, *86*, 9583-9589.

(28) Wu, Y. M.; Li, L. *Anal. Chem.* **2013**, *85*, 5755-5763.

(29) Percy, A. J.; Chambers, A. G.; Yang, J. C.; Domanski, D.; Borchers, C. H. *Anal. Bioanal. Chem.* **2012**, *404*, 1089-1101.

(30) Smith, R.; Ventura, D.; Prince, J. T. *Brief. Bioinform.* **2015**, *16*, 104-117.

(31) Wilm, M.; Mann, M. *Anal. Chem.* **1996**, *68*, 1-8.

(32) Schmidt, A.; Karas, M.; Dulcks, T. *J. Am. Soc. Mass Spectrom.* **2003**, *14*, 492-500.

(33) Zhou, R.; Li, L. *J Proteomics* **2015**, *118*, 130-139.

(34) Ficarro, S. B.; Zhang, Y.; Lu, Y.; Moghimi, A. R.; Askenazi, M.; Hyatt, E.; Smith, E. D.; Boyer, L.; Schlaeger, T. M.; Luckey, C. J.; Marto, J. A. *Anal. Chem.* **2009**, *81*, 3440-3447.

(35) Rainville, P. D.; Langridge, J. I.; Wrona, M. D.; Wilson, I. D.; Plumb, R. S. *Bioanalysis* **2015**, *7*, 1397-1411.

.

Chapter 3 UHPLC Combined with Ultra-High Resolution QTOF-MS for Rapid Lipidomic Profiling of Serum for Discovery of Lipid Biomarkers of Parkinson's Disease

3.1 Introduction

Parkinson's disease (PD) is a universal chronic disorder characterized by the progressive degeneration of dopaminergic neurons in the substantia nigra.[1,2] The death of these dopamine producing neurons causes a wide array of disabling motor symptoms of which PD is most known for. Symptoms include: bradykinesia, rigidity, rest tremors and postural instability.[1,2] In addition to motor impairments, PD is also associated with many non-motor symptoms such as pain, behavioral disorders, depression, loss of cognitive ability, autonomic dysfunction (dysautonomia), sleep disturbances and sensory irregularities.[1,2,3,4] PD typically affects aging individuals of 65 years and older; however there are cases of early onset PD.[5]

According to the World Health Organization, approximately 48 million individuals world-wide were affected by PD in 2015. This disease has many social and economic implications, particularly in an aging population, as it progresses slowly and non-linearly with variable degrees of symptoms among afflicted individuals. Many of the symptoms associated with PD result in the inability for self-care.[6] The quality of life of individuals with PD decreases substantially as the disease progresses.[6,7] PD also places a physical, emotional and financial burden on the patient, their family/caregivers, and the economy.[6] Although it is one of the most common neurodegenerative diseases, the molecular pathology of PD is not entirely understood. To this day there are no objective biological tests for the definitive detection and diagnosis of PD. Clinical information and medical history given by patients along with a neurological test involving the

* I prepared the samples, collected the data, processed the data, and wrote and edited the chapter

observation of the patient for tremors, neck/limb stiffness, movement and ability to right oneself when pulled off balance is used to make a diagnosis of PD.[5] Thus, PD is often left undiagnosed (in the early stages) or misdiagnosed. Many research studies have focused on investigating the different 'omics' of PD including the genome, proteome and metabolome.[8,9,10] Our focus for this study will be on a subset of the metabolome, specifically the lipidome.

Lipidomics is the study of the lipids in a given biological system to better understand their pathways and their interactors (metabolites, proteins, other lipids).[11] Lipid metabolism plays a large role in maintaining physiological homeostasis through energy production, storage and cell signaling. Dysregulation in this area may be a precursor for, or associated with, particular diseases. Recent findings show lipids, specifically lipid peroxidation, to play a role in neurodegenerative diseases, including Parkinson's and Alzheimer's disease.[12,13,14] Genomic and proteomic studies have also identified mutations to the human glucocerebrosidase gene (GBA) that encodes glucocerebrosidase, an enzyme involved in glycolipid metabolism. It has been shown to play a role in the risk and progression of PD to dementia.[10] Thus the investigation of the complete profile of lipids is integral to understanding the molecular pathology of PD. However, reports of high-coverage lipidomic profiling of PD samples are very limited, although some targeted analyses of lipids including peroxidation products have been reported for brain tissues[15-18] and plasma[19], as well as samples of animal models[20]. In metabolomics study of PD with a focus on detecting metabolites, a small fraction of lipids were also detected and some of them could have abundance changes in PD.[21]

In this chapter, I report a study of untargeted lipidomic profiling of plasma samples from 43 control individuals and 43 diseased individuals. The PD individuals were further categorized as early stage PD, and PD with dementia (PDD). Using UHPLC for lipid separation and UHR-

QTOF mass spectrometry for lipid detection and identification, we profiled 4391 lipid features consistently in more than 50% of the samples. Among them, 406 lipids could be identified, spanning 12 different lipid classes. With this high-coverage profiling, we identified panels of lipids for separating PD from controls and PDD from PD with high sensitivity and specificity. This work indicates that lipidomics can be useful in identifying potential biomarkers for PD diagnosis and prognosis as well as investigating the molecular pathology of the disease and disease progression.

3.2 Experimental

3.2.1 Chemicals and Reagents

All chemicals and reagents were from Sigma-Aldrich Canada (Markham, ON, Canada), except those otherwise noted. LC–MS grade water, acetonitrile, methanol, and isopropyl alcohol (IPA) were from Thermo Fisher Scientific (Edmonton, AB, Canada).

3.2.2 Human Samples

Control individuals (H) (n=43) were compared against PD patients (n=43), and the controls were matched in sex and age to the PD patients (Table 3.1). The PD patients were further separated into early stage PD (n=27) and late stage PD with dementia (n=16). The study was done in three phases (18 month intervals) in Edmonton, Alberta, Canada.[22] The patients were recruited from movement disorder clinics, community neurologists and Parkinson's Society of Alberta. The control group was recruited from seniors' centers, magazines, medicine clinics, control contacts and patient contacts.

The University of Alberta health ethics review board approved this study and all participants provided informed consent. PD patients: (1) met standard criteria for PD; (2) did not meet criteria for atypical parkinsonism; and (3) did not have unstable health conditions compromising survival. Participants performed three waves of standardized assessments,

including assessment for cognitive function and dementia. Initially, pairwise comparison of control against PD was done, followed by pairwise analysis of PD against PDD. The PD and PDD samples did not vary greatly by levodopa equivalents and the Unified Parkinson's Disease Rating Scale (Table 3.1).

Table 3.1 Summary of demographic information on the samples used in the final lipidomics comparison.

	Control	**PD**	**PD without dementia**	**PD with dementia**
N	43	43	27	16
Age (years)	71.47 (4.95)	70.71 (4.14)	69.58 (3.55)	72.62 (4.46)
Education (years)	15.09 (3.44)	14.28 (2.98)	14.74 (3.36)	13.50 (2.07)
Gender (F/M)	19/24	19/24	12/15	7/9
MMSE	28.60 (1.48)	28.33 (1.67)	28.85 (1.29)	27.36 (1.91)
Folate (nmol/L)	890.23 (243.22)	842.56 (207.45)	799.00 (185.45)	916.06 (227.41)
Vitamin B12 (pmol/L)	388.53 (198.69)	293.26 (112.82)	295.70 (92.16)	289.13 (144.52)
Levodopa equivalents (mg)	N/A	644.00 (360.06)	611.83 (392.94)	703.76 (293.41)
UPDRS part 3	N/A	16.12 (7.90)	16.67 (8.08)	15.19 (7.77)

Note. PD, adults with Parkinson's disease; MMSE, Mini Mental State Exam; UPDRS, Unified Parkinson's Disease Rating Scale

3.2.3 Sample Preparation

Ten µL of human serum was extracted using modified Bligh-Dyer method.[23] Briefly, 67 µL of methanol was added and vortexed, followed by the addition of 133 µL of dichloromethane and vortexed. Forty µL of water was then added to induce phase separation. After a 10 min spin-down at 14000 rpm the bottom layer was removed and dried down using SpeedVac. The sample was re-dissolved in 15 µL of 6:4 mobile phase A/mobile phase B. Experimental duplicates were performed for each sample.

3.2.4 Instrumentation

Chromatographic separation was performed using a Dionex UltiMate 3000 (Dionex, Sunnyvale, CA, USA) equipped with a Phenomenex Coreshell C18 Column (100 mm x 2.1 mm, 2.7 µm). The mobile phase A was ACN/MeOH/Water (19:19:2, v/v/v). Mobile Phase B was IPA. Both mobile phases contained 20 mM ammonium formate and 5 mM formic acid. An 18-min gradient was implemented: 0 min (5% B), 0-1.8 (5% B), 1.8-8.5 min (5-30% B), 8.5-16.5 min (30-90% B), 16.5-18 min (90% B). The flow rate was 250 µL/min and the sample injection volume was 2.0 µL. The column was re-equilibrated with the initial mobile phase conditions for 10 min at 300 µL/min prior to the next sample run. The column compartment was held at 40 °C for all runs.

A quality control (QC) sample was prepared by combining 2 µL of serum from each sample. The QC sample was extracted using the modified Bligh and Dyer method.[23] To ensure enough sample volume for all the runs, the QC was reconstituted in 30 µL of 6:4 solvent A and Solvent B. Initially the QC sample was injected ten times to stabilize retention time and MS signal, then injected every ten runs. Two µL of the QC sample were injected.

A Bruker maXis II UHR-QTOF instrument equipped with an ESI source was used for the analysis. The following source settings were used: nebulizer gas 1.0 bar, dry gas 8.0 L min^{-1}, dry

gas heater 300 °C, capillary voltage 4500 V, end plate offset -500 V, and the mass range was set at *m*/*z* 50–1500. All of the MS and MS/MS scans were performed in the positive mode. MS spectra were collected at a spectral rate of 2 Hz. In the MS/MS scan, the cycle time was 6.0 s and active exclusion was 0.15 min. The lower mass range (150 m/z) was 30 collision energy (CE) and higher mass range (1500 m/z) were 25 CE. The collision energy was ramped from 50% - 150% of the CE. Lower intensity (<10000) MS/MS spectra were collected at 5 Hz and the higher intensity spectra (>500000) were collected at 10 Hz.

3.2.5 Data Processing

All data was calibrated, processed and aligned using Profile Analysis (Bruker). Principal component analysis (PCA), partial least squares discriminant analysis (PLS-DA), orthogonal partial least squares discriminant analysis (OPLS-DA), and model cross-validation were done using Simca 12.0. Receiver operator characteristic (ROC) curves were created using Metaboanalyst using the random forest algorithm. Lipid Bank, Human Metabolome Database (HMDB), and MyCompoundID (MCID) were used for putative identification based on accurate mass. Positive identification was done using MS/MS matching with Lipid Blast and MS Dial.

3.3 Results and Discussion

3.3.1 Lipid Extraction

A Modified Bligh and Dyer[23] method was utilized to extract lipids from the serum samples. Initially, lipids were extracted from 30 µL of serum which was then reconstituted in 25 µL of 6:4 solvent A and B. To generate the highest separation efficiency and prevent MS signal saturation, an injection volume of 2 µL was determined to be optimal. Since only 2 µL of the prepared sample was used, the remaining 23 µL of sample would go to waste. To prevent wasting of original samples, the extraction method was scaled down by a third. By extracting 10 µL of serum, we

were able to inject the same amount of sample while keeping the peak resolution high and MS signal comparable to the 30 µL extraction (Figure 3.1). This method could be further reduced to use even less sample if necessary.

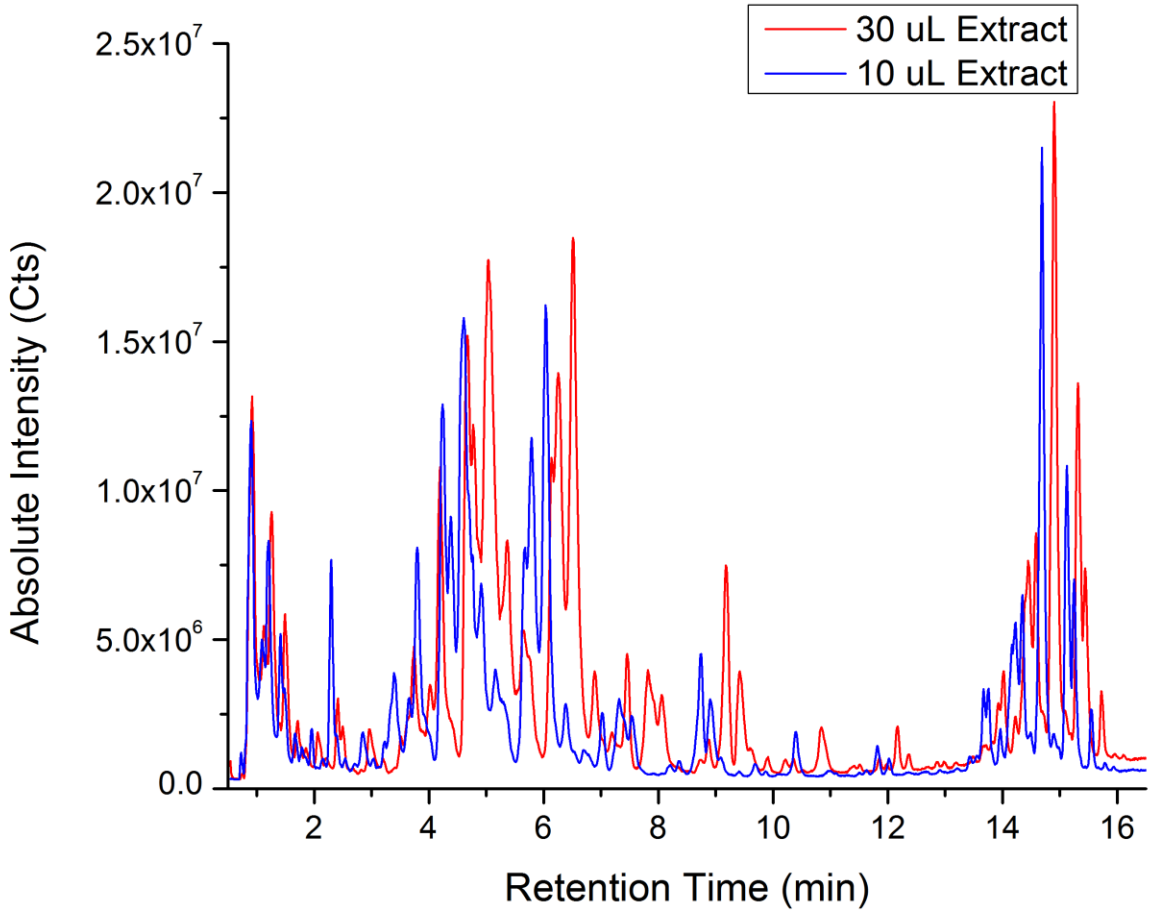

Figure 3.1 Total ion chromatographs (TIC) of 2 µL injections of 10 µL (blue) and 30 µL (red) extracted serum, extracted using modified Bligh and Dyer method.[23]

3.3.2 Column Optimization

Initially a UHPLC column (100 mm x 2.1 mm, 1.8 µm) was used to provide the highest peak resolution for separating the lipid species. IPA was used as solvent B at 80 µL/min. Due to IPA's viscous nature a high back pressure was observed during the LC-MS run. However, the need for IPA is crucial when running lipid samples. Without IPA the peak resolution using a C18

column is reduced and the analysis of larger lipids becomes difficult. Running at 80 µL/min resulted in a total run time of 120 min including equilibrium. This long runtime limits the sample throughput when analyzing 100's of samples in a lipidomics study. To increase the throughput and maintain similar UHPLC separation efficiency, we decided to use a coreshell C18 column (100 mm x 2.1 mm, 2.7 µm). This allowed for the reduction of back pressure on the LC system while providing the resolution of a UHPLC column. With the coreshell column we could use flow rates of 250-300 µL/min. The overall run time was decreased to 28 min including column equilibrium, thereby greatly increasing the sample throughput.

3.3.3 Lipid Feature Extraction

Profile Analysis (Bruker) was used for alignment and feature extraction. The software package offers feature extraction and statistical analysis. To include the highest number of features in our analysis while decreasing the chance of false-positive findings, two parameters were adjusted. Firstly, a signal-to-noise ratio (S/N) cut-off of three was used. Secondly, each feature was required to show up in ≥ 7 spectra. Features that showed up in greater than 50% of the samples were kept and minimum peak area of the sample group was used to fill missing values.

3.3.4 Lipid Identification

MS/MS spectra were matched to two complementary lipid MS/MS libraries: LipidBlast[24] (<10 ppm) and MS Dial[25] (<10 ppm) (Appendix Table A3.1). Both use a version of the LipidBlast library. However, the additional libraries provided by LipidBlast increased the coverage of the cholesterol species and triacylglycerols (TG), while the use of MS Dial increased the coverage of phosphatidylcholines (PC). Due to the rapid collection rate of the QTOF instrument, multiple MS/MS spectra of the same precursor can be acquired, even when active exclusion is used. This leads to duplicate MS/MS matches. Thus manual checking of the data is required, which is time

consuming. In the MS Dial program a retention time window can be set to prevent this duplicate matching. The average LC peak width was determined to be 0.3 min, and thus this was used as the retention time window. The MS/MS spectra were also manually interpreted to generate more positive IDs while reducing false positive IDs.

The QC sample was representative of all the samples and was used for most of the lipid identifications. Some features could not be identified from the QC sample and we suspect there were two reasons for this. In the first case, the feature was fragmented and a MS/MS spectrum was acquired. However, the acquired spectrum could not be matched to the library, or had a low matching score. For the second case, the feature was suppressed in the QC sample and a MS/MS spectrum could not be acquired. We attempted to manually interpret or match the feature to other libraries in the first case. In the second case we identified samples with the highest concentration of the missed feature(s) and reran the MS/MS experiment focusing on the particular feature(s), using scheduled MS/MS.

For manual interpretation of the MS/MS spectra, we used their characteristic fragments such as 184.074 or 369.352 m/z for PC and cholesterol species. Using manual interpretation we identified 22 additional cholesterol species. Some of those were identified by accurate mass, while others that could not be identified were denoted as cholesterol species (Appendix Table A3.2). Numerous PC species were also identified; however there were too many to manually curate. Also, not all lipids have these types of characteristic fragments, making them difficult to identify. The use of standards or the expansion of lipid libraries in MS and MS/MS database would be required for their identification.

The ID results from the two library searches were combined and duplicates were removed. The results were then further refined using accurate mass and retention time. In total we were able

to positively identify 406 lipids spanning 12 different lipid classes using MS/MS matching and manual interpretation (Table 3.2).

Not all features could be positively identified using MS/MS matching. However, they could be putatively identified or matched to some lipid structures based on accurate mass search. Putative identification was done using Lipid Maps[26] (<10 ppm), HMDB[27] (< 5 ppm), and MCID[28] (<5 ppm). The identification was done in 3 tiers. Lipid Maps was searched first. The features that could not be identified were then searched against HMDB. If the features were still not identified by HMDB, they were searched against MCID using the one reaction predicted metabolite library. The putative results were further refined by examining the retention characteristics of the match as larger lipids would retain longer on the column. This further increased confidence in the putative matches.

Table 3.2 Twelve lipid classes positively identified using MS/MS. MS/MS spectra were matched to LipidBlast, MS Dial and manually interpreted. Matching parameters used were precursor match 10 ppm or less and matching score greater than 650. A retention window tolerance of 0.3 minutes was used.

Lipid Class	**MS/MS Identified**
Sphingomyelin (SM)	60
Lysophosphatidylcholine (LysoPC)	13
Lysophosphatidylethanolamine (LysoPE)	2
Ceramide (Cer)	13
Phosphatidylcholine (PC)	106
Phosphatidylethanolamine (PE)	13
Plasmenyl-PC	31
Plasmenyl-PE	19
Diacylglycerol (DG)	16
Triacylglycerol (TG)	98
Cholesterol Esters (CE)	15
Cholesterol Species	20
Total	**406**

3.3.5 High Resolution

The maXis II instrument provided ultra-high resolution for lipid analysis with a resolving power of 60000 or greater observed for most lipid species. An example of the MS and MS/MS spectra obtained by this UHR-QTOF-MS instrument are shown in Figure 3.2. The MS/MS spectrum shown was obtained when the instrument was operating at a spectral acquisition rate of 10 Hz. The resolving power of the fragment ions was over 60000 FWHM. For UHPLC separation, higher spectral acquisition rate benefits the detection of high-resolution peaks. The need for ultra-high mass resolution becomes apparent in lipidomics analysis, as most lipids have multiple isomers or similar species. Higher resolution provides increased confidence in MS/MS matching and higher mass accuracy. Even though a mass window of 10 ppm was used, the majority of the matches had mass errors of less than 5 ppm. Out of the 210 positive LipidBlast matches, 205 were matched at $\leq$ 5 ppm and 87 of those at $\leq$ 1 ppm. In this work, external mass calibration was used. Future work of implementing a convenient way of performing internal mass calibration in conjunction with UHPLC separation will likely improve the mass accuracy obtained to less than 5 ppm.

Ultra-high resolution is not only useful for MS/MS matching, but can also provide increased confidence in the putative matching. The increased mass accuracy allows for increased confidence in the matching, narrowing dozens of hits down to two or three. This was confirmed by comparing lipids that were already identified by MS/MS matching to their putative match. In most cases the putative matches were either a direct match to the positive ID or matched to its respective lipid class. In the volcano plot analysis (see below), 30 of the 38 positive IDs were matched with their putative ID or lipid class. Thus, the putative match accuracy was 80%. Of

interest, the mismatched ones were mainly from the ones with M^+ such as sphingomyelin (SM), instead of $[M+H]^+$ or other adduct ions.

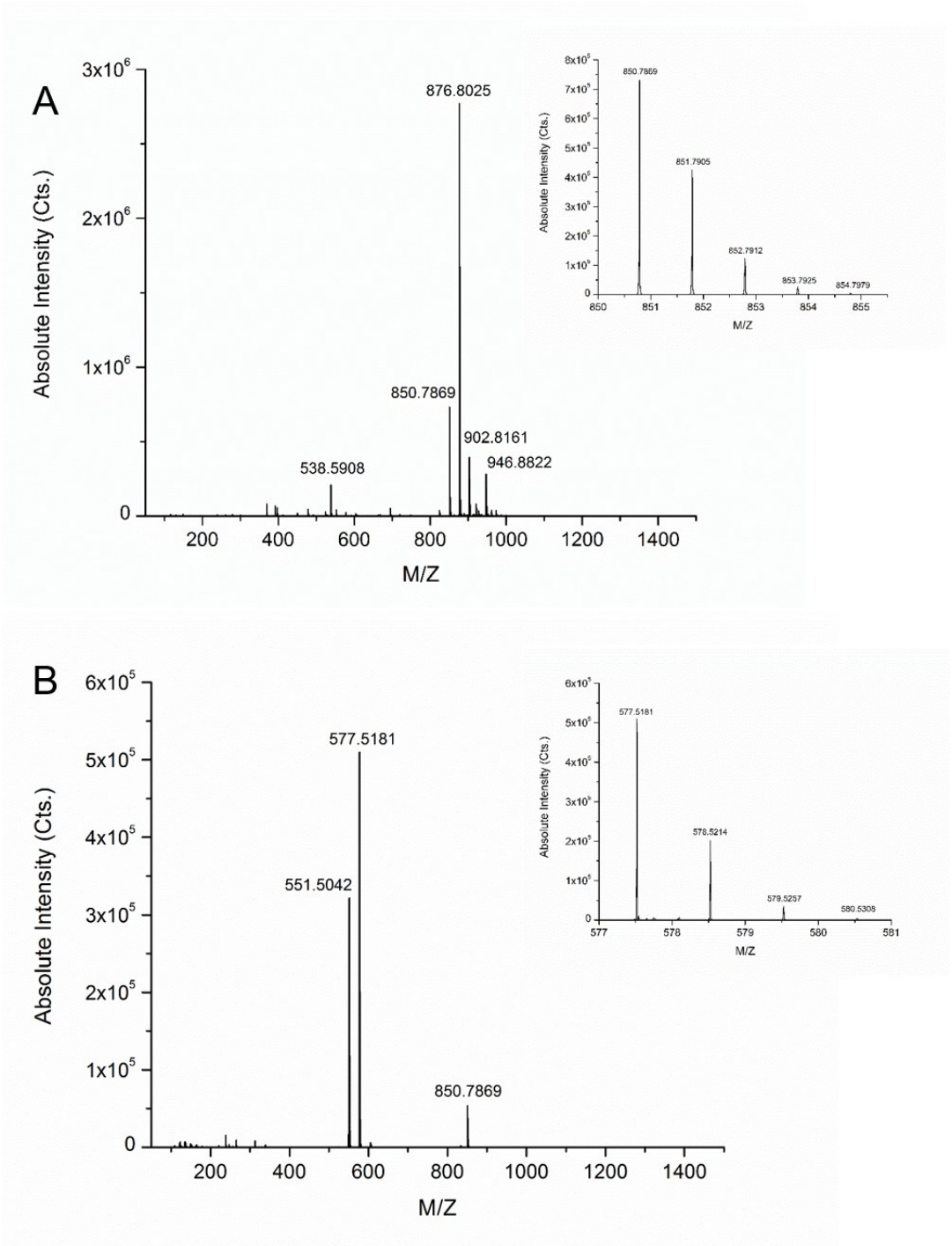

Figure 3.2 (A) MS spectrum at > 60000 resolving power (FWHM). (B) MS/MS spectrum of 850.7869 at > 60000 resolving power acquired at 10 Hz.

3.3.6 Statistical Analysis

Multivariate and univariate analyses were used to examine changes between the disease and control group. Table 3.3 lists the average retention time of five random peaks and Table 3.4 lists the average peak area for the same five peaks. For each retention time and peak area, standard deviation and %RSD where calculated to show the reproducibility of our LC-MS method.

We found no visual separation in the PCA plot for the comparison of the control samples against the disease samples. Using PLS-DA, the score plot showed good separation, with R^2 of 0.86 and Q^2 of 0.68 (Figure 3.3A). The R^2 is a goodness of fit and the Q^2 is the predication power of the model. This plot was validated using 100 permutations which gave an R^2 of 0.70 and Q^2 of 0.04. OPLS-DA was also performed and the score plot showed clear separation between the two classes with R^2 and Q^2 of 0.98, and 0.74 (Figure 3.3B).

Table 3.3 Average retention times of 5 random peaks extracted from the QC samples (n=18).

M/Z	Average Retention Time (min)	σ (min)	%RSD
158.154	0.796	0.005	0.62
675.677	2.31	0.01	0.51
343.286	4.44	0.04	0.80
786.601	6.12	0.06	0.95
874.786	14.72	0.02	0.17

Table 3.4 Average peak areas of 5 random peaks extracted from the QC samples (n=18).

M/Z	Average Peak Area (Cts.)	σ (Cts.)	%RSD
158.154	5.4E+04	3.7E+03	6.8
675.677	4.5E+06	2.0E+05	4.3
343.286	9.8E+04	5.5E+03	5.6
786.601	1.0E+07	2.9E+05	2.9
874.786	6.6E+06	1.9E+05	2.9

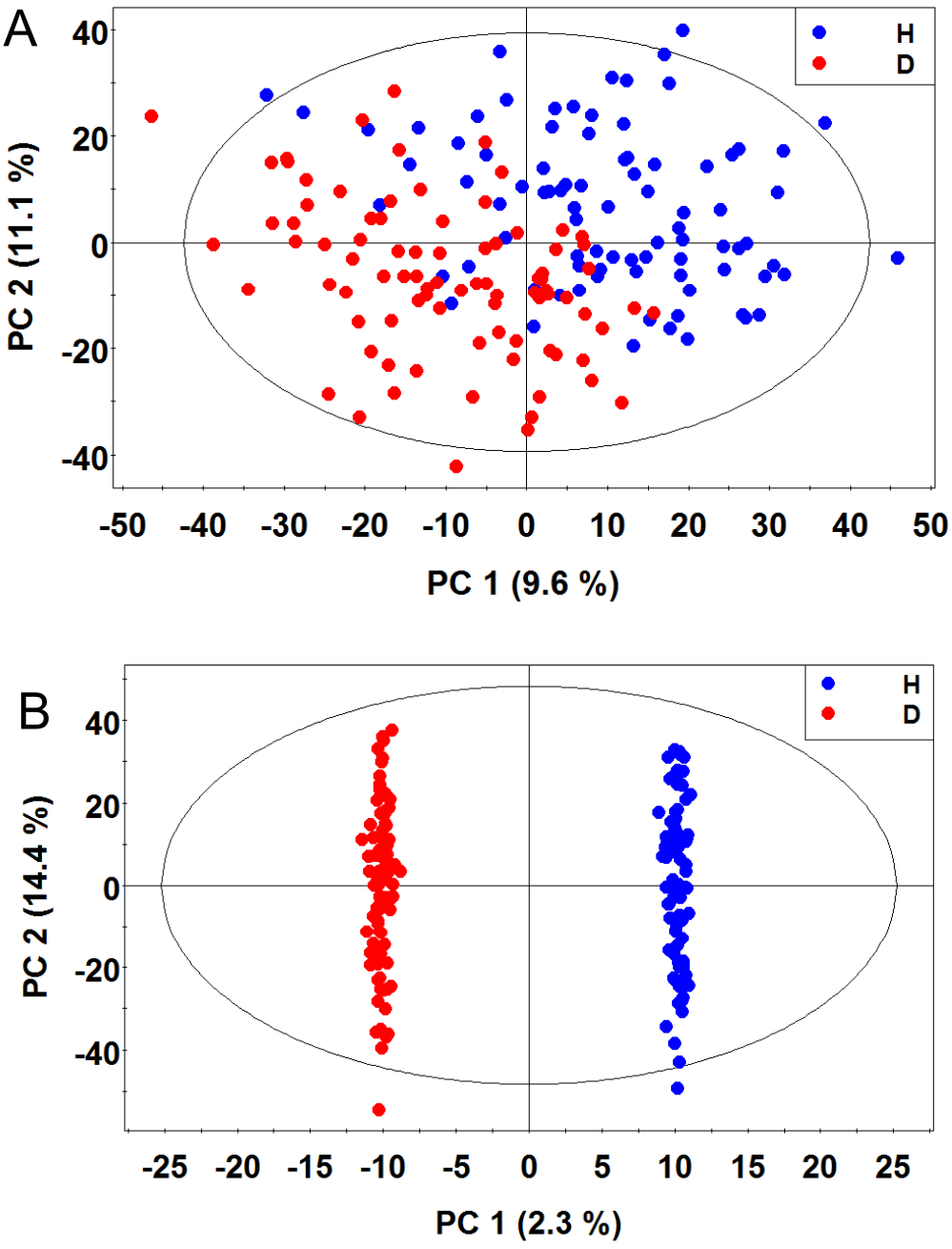

Figure 3.3 (A) PLS-DA score plot and (B) OPLS-DA score plot of lipidomic LC-MS data of 43 control samples (blue) and 43 PD and PDD samples (red). The PLS-DA score plot had an R^2 of 0.86 and Q^2 of 0.68. The OPLS-DA had R^2 of 0.98 and Q^2 of 0.74. PLS-DA was validated using 100 permutations.

Univariate analysis was done using volcano plots to find any features that had significantly increased or decreased in concentration relative to the disease group (Figure 3.4A). A significant increase is defined by any feature with a fold change (FC) larger than 1.5 and p-value of less than 0.05. Significant decrease was determined by any feature with FC of less than 0.67 and p-value of less than 0.05. In Figure 3.4A for the comparison of disease group (PD) against the control (H) group, 29 features were significantly increased in concentration and 30 features were significantly decreased relative to the disease group.

The significant features were identified either positively or putatively (Appendix Table A3.3). Of the 29 increased features, seven were positively identified as SMs and one as a TG. We were able to putatively identify 21 other features. Of the 30 decreased features, 1 was positively identified as a PC and 22 were putatively identified.

In the third phase of the longitudinal study, some patients developed signs of dementia (PDD). This gave us an opportunity to study the progression of early stage PD to late stage PD with dementia. The analysis of this progression would allow us to account for drug effects seen only in the PD patients that could cause artificial variance between the control and disease samples. We used PLS-DA and OPLS-DA (Figure 3.5A & B) to determine any variance between the two disease groups PD and PDD. The PLS-DA score plot shows good separation, with R^2 and Q^2 of 0.99, and 0.80. This plot was validated with 100 permutations achieving an R^2 and Q^2 of 0.96, and 0.02. OPLS-DA score plot also showed clear separation between the two groups with R^2 and Q^2 of 0.99, and 0.88.

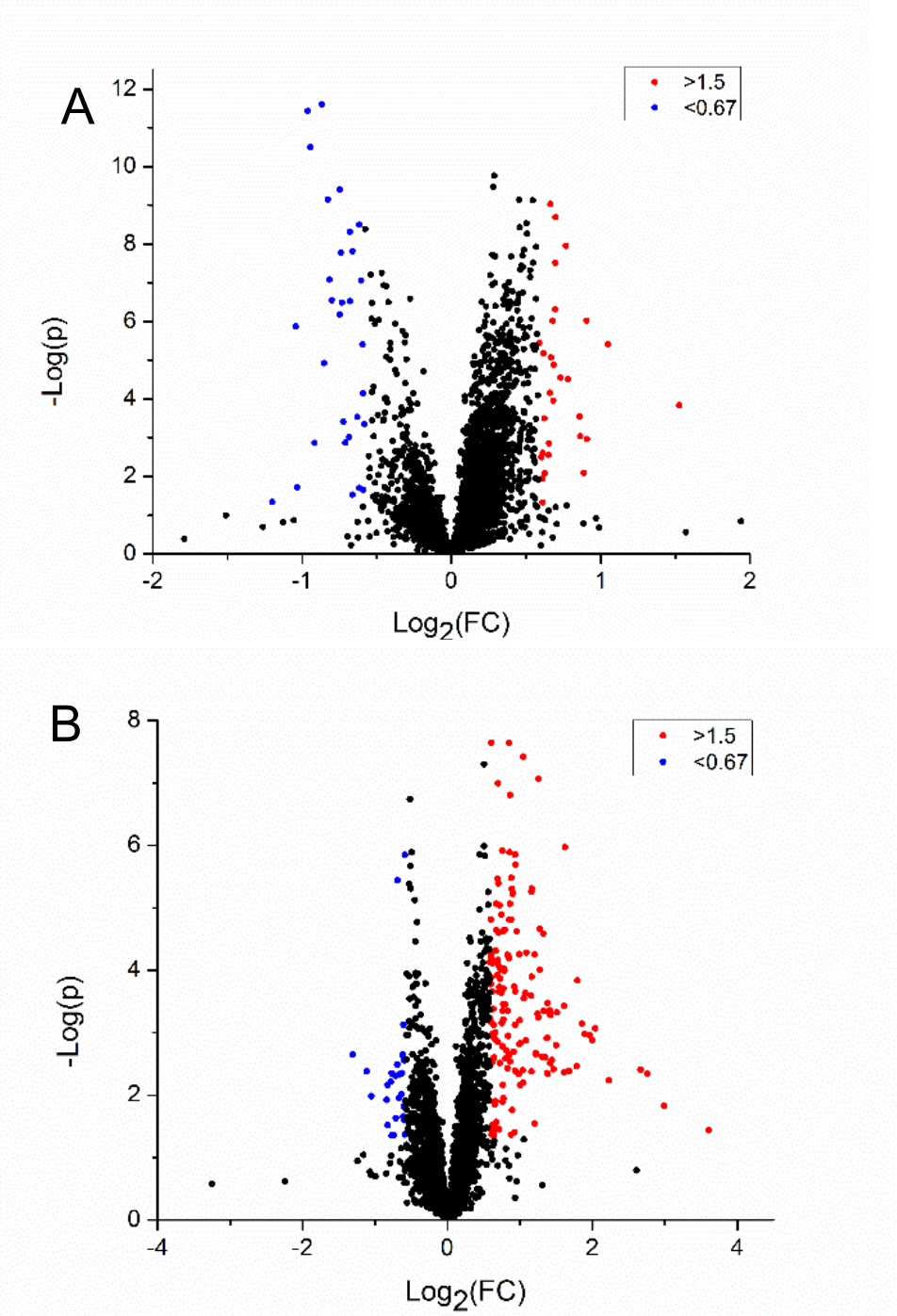

Figure 3.4 (A) Volcano plot comparison of healthy control and PD patients showed an increase of 29 features with FC > 1.5, p-value < 0.05 (red) and a decrease of 30 features with FC < 0.67, p-value < 0.05 (blue) relative to the disease group. (B) Volcano plot comparison of PD and PDD patients showed increase of 164 features with FC > 1.5, p-value < 0.05 (red) and a decrease of 27 features with FC < 0.67, p-value < 0.05 (blue) relative to the PDD group.

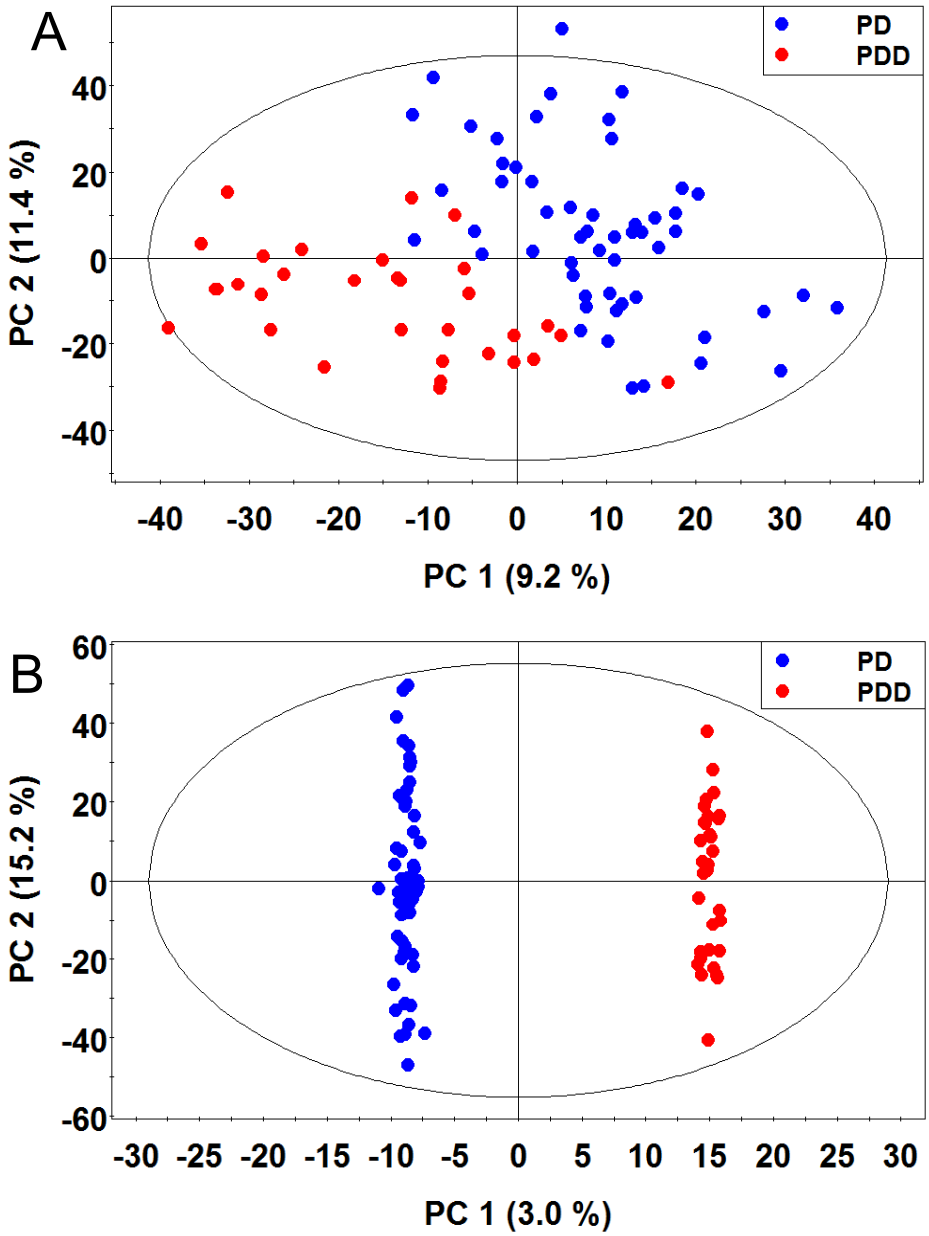

Figure 3.5 (A) PLS-DA score plot and (B) OPLS-DA score plot of lipidomic LC-MS data of 27 PD samples (blue) and 16 PDD samples (red). The PLS-DA score plot had an R^2 of 0.99 and Q^2 of 0.88. The OPLS-DA had R^2 of 0.98 and Q^2 of 0.69. PLS-DA was validated using 100 permutations.

Univariate analysis was done using the same parameters as before (Figure 3.4B). Relative to the PDD group we found 164 features had increased in concentration, with FC > 1.5 and $p < 0.05$ and 27 features had decreased in concentration with FC < 0.67 and $p < 0.05$ (Figure. 3B). For Figure 3.4B of the 27 decreasing in concentration one lipid was positively identified as a Lyso-PC and 24 were putatively identified. Of the 164 that increased, 26 were definitively identified as TG, DG and SM, and 122 of them were putatively identified (Appendix Table A3.4). The TG and DG levels in the blood can vary depending on weight of patient, if statins were used and time of blood collection.

3.3.7 ROC Analysis

Receiver operator characteristic (ROC) curves can be used to distinguish the separation power of one particular feature or a combination of features from control to disease. This allows us to screen for potential biomarkers in our experiments. Metaboanalyst 3.0[29] was used to generate ROC curves for the top candidates. The common features that showed significant increase or decrease in both pairwise analyses were mined from PLS-DA and the volcano plots and were combined for ROC. The common features were ranked using their individual area under the curve (AUC) values. All ROC curves were generated using the random forest algorithm.

The top five features that had the highest individual AUC were selected. The top 5 compounds that separated control from disease samples were: Cer(d18:0/25:0) [+$C_5H_5N_5$ -H_2O]* (AUC = 0.782), phosphtatidylglycerols(53:1) (PG)* (0.773), PC species (0.766), PG(32:1)* (0.763), sphingoid base(d20:1) (Sph)* (0.751) (*Putative ID). The highest AUC lipid, Cer(d18:0/25:0) [+$C_5H_5N_5$ -H_2O], had a sensitivity of 60% and specificity of 100%. The 5 compounds were then combined in a biomarker screen and were used to generate a ROC curve.

The AUC was 0.980 with a sensitivity and specificity of 98 % and 94 % with confidence interval at 95 % of 0.945-1 (Figure 3.6A).

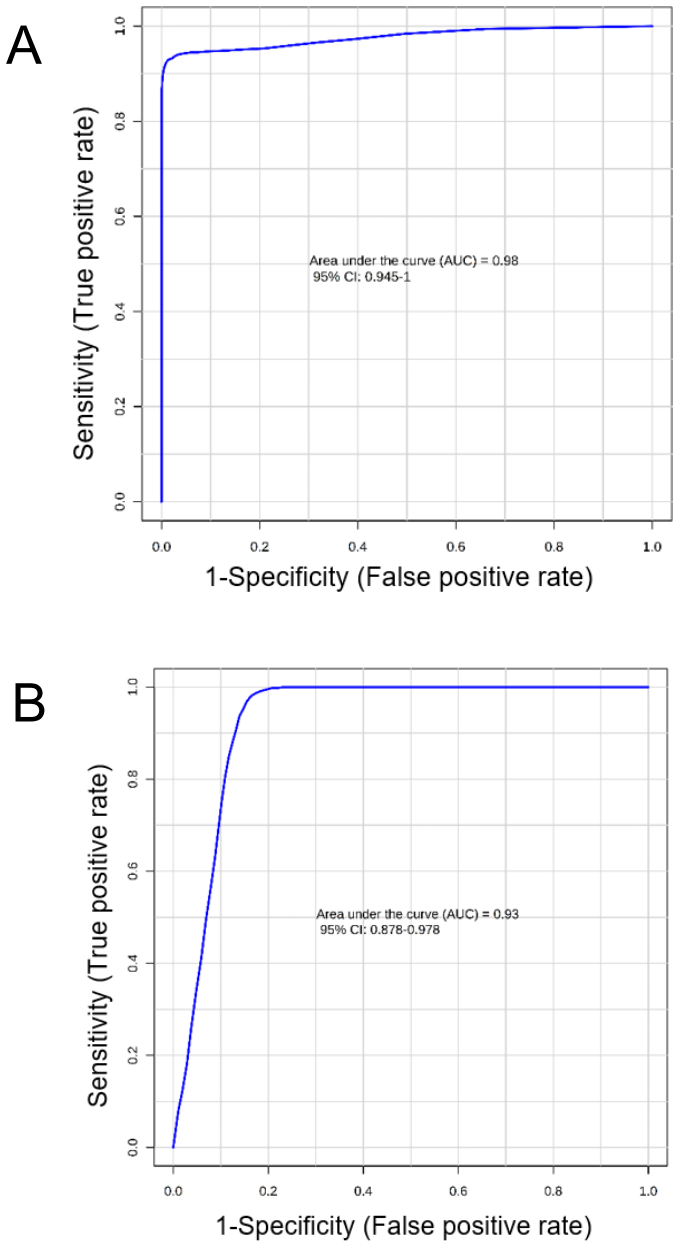

Figure 3.6 (A) ROC curve generated by the random forest model using 5 metabolite biomarker candidates: Cer(d18:0/25:0) [+$C_5H_5N_5$ -H_2O]*, Phosphtatidylglycerols(53:1) (PG)*, PC, PG(32:1)*, Sphingoid bases(d20:1) (Sph)*, (*Putative ID) between control and disease. (B) ROC curve generated by the random forest model using 6 metabolite biomarker candidates. The same five above with the addition of 784.739 m/z (Unidentified) between PD and PDD.

To find biomarkers that could be used to monitor progression of the disease, we combined the five features from Figure 3.6A with one other feature that showed the highest AUC value for separation of PD from PDD. The top 6 candidates were: 784.739 m/z (unidentified) (0.779), phosphtatidylglycerols (53:1) (PG)* (0.767), Cer(d18:0/25:0) [+$C_5H_5N_5$ -H_2O]* (0.759), PC species (0.740), PG(32:1)* (0.722), sphingoid bases (d20:1) (Sph)* (0.712). The top ROC candidate, 784.739 m/z (unidentified) had a sensitivity of 60% and specificity of 100%. The 5 compounds were then combined as a biomarker panel, which generated an AUC of 0.930 and sensitivity and specificity of 84 % and 98 % with 95 % confidence interval (CI) of 0.878-0.978 (Figure 3.6B). Box plots of all six features were shown in Figure 3.7. We see an increasing trend in all six features from control to PDD.

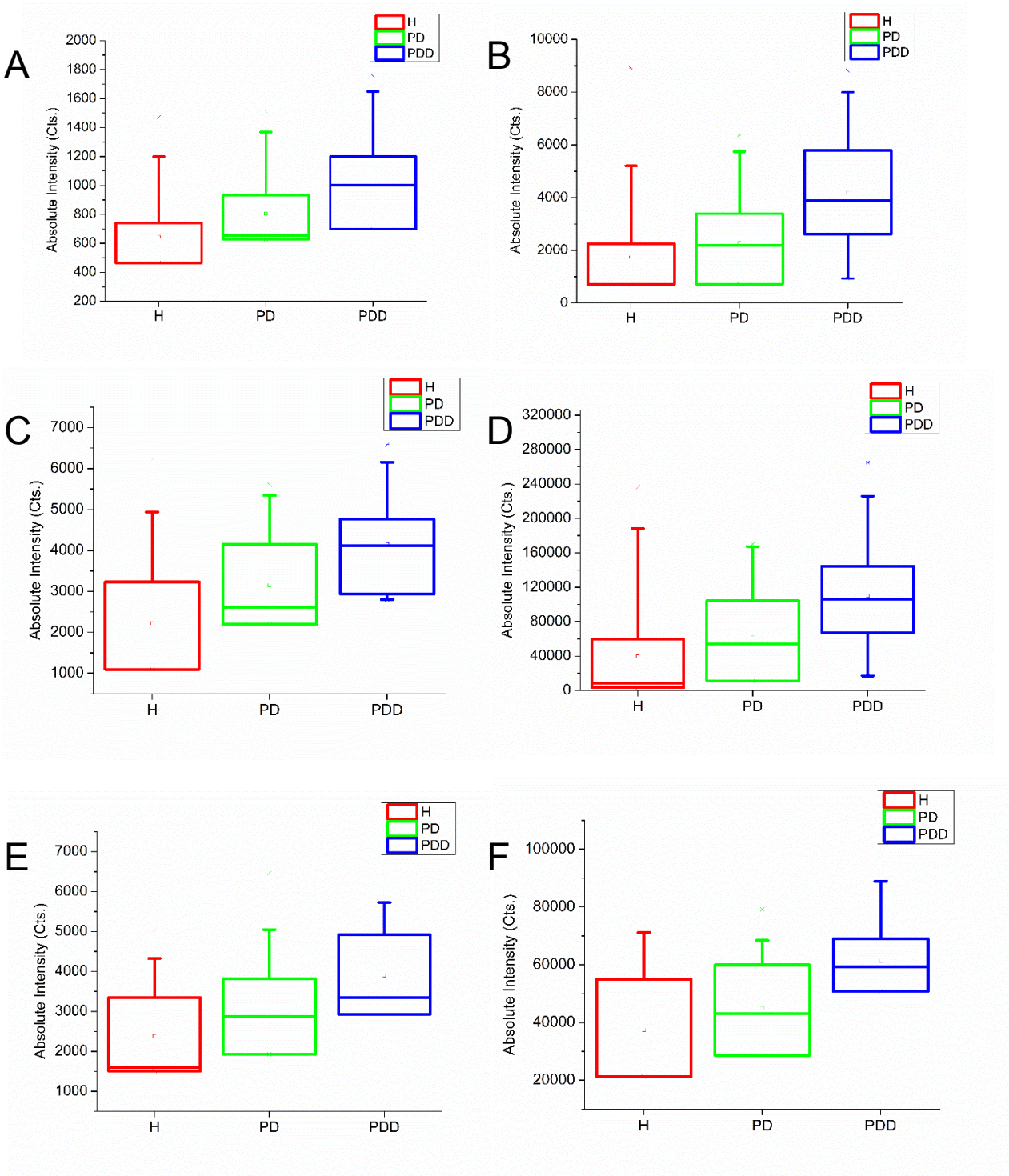

Figure 3.7 Box plot of all six ROC candidates. (A) Cer(d18:0/25:0) [+$C_5H_5N_5$ -H_2O], (B) PG(53:1), (C) PC species, (D) PG(32:1), (E) Sph(d20:1), (F) 784.739 m/z.

Some features were significant in only one pairwise analysis; these were also used for ROC analysis. The top 5 compounds that were used to separate control from disease: N-(3-aminopropyl)-2-pyrrolidinone* (0.784), wax ester (WE) (37:6)* (0.738), ceramide phosphoinositol (PI-Cer) (d33-0) (0.734), GPCho(17:0/22:6(4Z,7Z,10Z,13Z,16Z,19Z)) (0.706), PC species (0.694). The highest AUC feature, N-(3-aminopropyl)-2-pyrrolidinone, had a sensitivity of 60% and specificity of 100%. The 5 compounds were then combined in a biomarker screen with AUC of 0.976, a sensitivity and specificity of 92% and 90%, with confidence interval at 95% of 0.948-1 (Figure 3.8A).

Figure 3.8A has similar AUC to Figure 3.6A. However the features used in Figure 3.8A could be used for disease diagnosis rather than tracking progression. The top candidate for Figure 3.8A is N-(3-aminopropyl)-2-pyrrolidinone, which is a metabolite of spermidine.[30] Spermidine has been shown to play a role in anti-aging and lipid metabolism, possibly preventing aging physiology and loss of locomotor skills.[31] We found the metabolite to be decreased in concentration the disease group with a fold change of 0.598 and a p-value of 1.66E-08. The decrease could be accounted for in PD patients due to their loss of locomotor skills, which may be correlated to the decreased amounts of spermidine and its metabolites.

Features that were significant for PD and PDD were also used to generate ROC curves. The top 5 candidates were: plasmenyl-PE 36:3; PE(P-16:0/20:3(8Z,11Z,14Z)) (0.883), 2,6,10,14-tetramethyl-6,7-epoxy-9-(3-methyl-pentyl)-pentadecane (0.866), plasmenyl-PC 42:2; PC(P-16:0/26:2(5E,9Z)) (0.847), TG 52:0; TG(16:0/18:0/18:0) (0.834), SM(d18:1/26:0)* (0.833). Plasmenyl-PE 36:3 had a sensitivity of 100% and specificity of 80%. The 5 compounds were then combined as a biomarker panel and processed using random forest, which generated an AUC of 0.958 and sensitivity and specificity of 87% and 94% with 95 % CI of 0.828-1 (Figure 3.8B).

Figure 3.8B shows a better AUC with less features than Figure 3.6B. The top feature was Plasmenyl-PE 36:3, which can be classified as a plasmalogen. Plasmalogens such as plasmenyl-PE and plasmenyl-PC are found in numerous human tissues such as the cardio vascular, immune and nervous systems.[32] The main functions of plasmalogens are not well known. However they could play a role in protecting the cells against reactive oxygen species, cell signalling, and controlling membrane dynamics.[33]

Plasmalogens have also been associated with Alzheimer's disease (AD) and Down's syndrome[33]. In AD patients[34,35] a decrease in plasmalogens was observed. We see a similar trend with a decrease from PD to PDD with a fold change and p-value of 0.743, 1.66E-04 and 0.698, 1.83E-07 for plasmenyl-PE 36:3 and plasmenyl-PC 42:2.

A significant change from the control to disease group for plasmenyl-PC 42:2 was not observed. However, for plasmenyl-PE 36:3, a significant decrease with a FC of 0.886 and a p-value of 3.76E-02 relative to the disease was observed. Further analysis is needed on plasmenyl-PEs to determine if they could be used as biomarkers of PD progression. In addition, we see a consistent trend for the PC and PE species decreasing from control to PDD samples in Figure 3.8B and the univariate analysis.

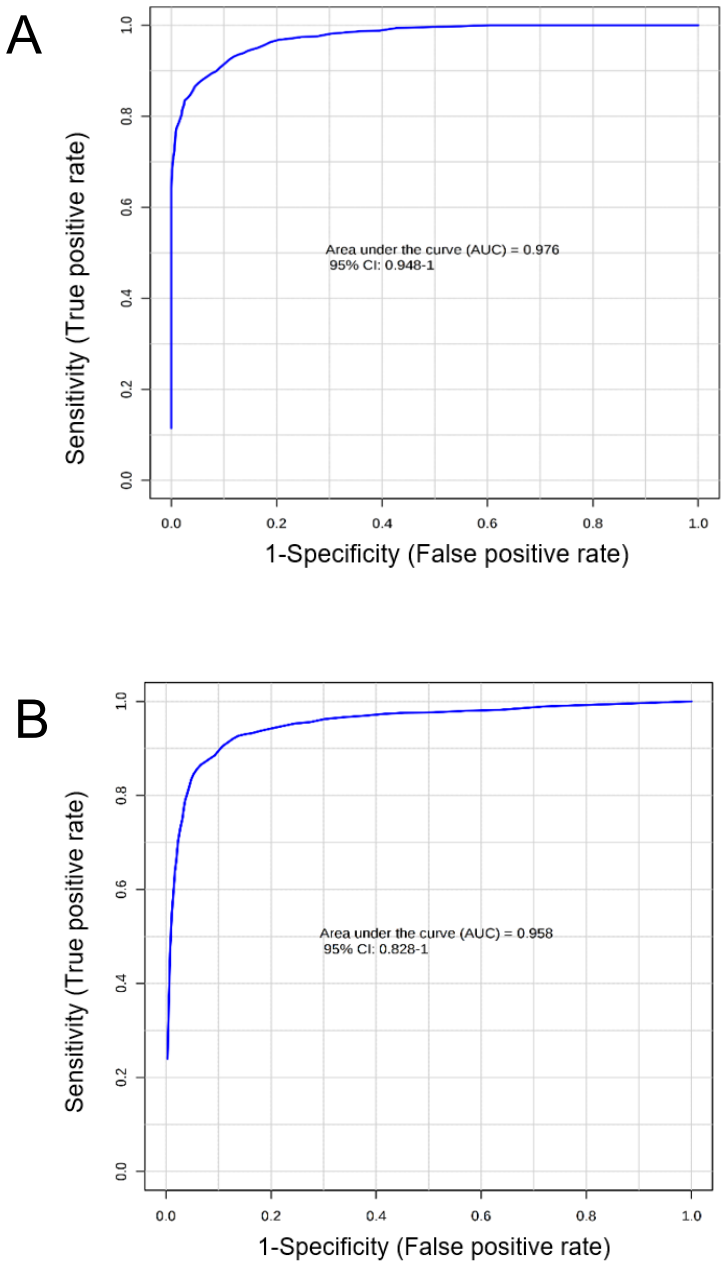

Figure 3.8 (A) ROC curve generated by the random forest model using 5 metabolite biomarker candidates: N-(3-Aminopropyl)-2-pyrrolidinone*, wax esters (WE) (37:6)*, Ceramide-phosphoinositol (PI-Cer) (d33-0)*, PC 39:6; GPCho(17:0/22:6(4Z,7Z,10Z,13Z,16Z,19Z)), PC, (*Putative ID) between control and disease. (B) ROC curve generated by the random forest model using 5 metabolite biomarker candidates: plasmenyl-PE 36:3; PE(P-16:0/20:3(8Z,11Z,14Z)), 2,6,10,14-tetramethyl-6,7-epoxy-9-(3-methyl-pentyl)-pentadecane, plasmenyl-PC 42:2; PC(P-16:0/26:2(5E,9Z)), TG 52:0; TG(16:0/18:0/18:0), SM(d18:1/26:0)* (*Putative ID) between PD and PDD.

3.3.8 Cholesterol Analysis

Previous research findings have shown a correlation between cholesterol and PD.[36,37] In our study, the fold change of cholesterol from healthy to disease group was examined. The cholesterol peak had a FC of 0.88 and a p-value of 1.9E-05, corresponding to a significant decrease in the disease group. This similar trend was also noted by Huang et al and others.[36,37] However, when examining the PD samples against PDD samples we found no significant change between the two sets of data. Cholesterol is a potential risk factor for PD, although further validation is needed.

3.4 Conclusions

Using UHPLC connected to UHR-QTOF we profiled 43 control and 43 Parkinson's disease patients to find biomarkers representative of the disease. Using statistical tools we discovered five biomarkers distinguishing disease from healthy individuals. These were Cer(d18:0/25:0) [+$C_5H_5N_5$ -H_2O], PG(53:1), PC species, PG(32:1), Sph(d20:1). These same five biomarkers plus an unidentified sixth feature were used to further distinguish PD from PDD with high sensitivity and specificity. Using ultra high resolution MS we were able to identify over 400 lipid molecules with high confidence. We see similar decreasing trends in plasmenyl PE and cholesterol in the healthy control samples against the PD samples. In the future we would like to use HILIC to further examine polar lipids and analyze lipids evident only in negative ion mode. This further examination of the lipidome could provide greater insights into PD.

3.5 Literature Cited

(1) Fil, A.; Cano-de-la-Cuerda, R.; Munoz-Hellin, E.; Vela, L.; Ramiro-Gonzalez, M.; Fernandez-de-Las-Penas, C. *Parkinsonism Relat. Disord.* **2013**, *19*, 285-294.

(2) Davie, C. A. *Br. Med. Bull.* **2008**, *86*, 109-127.

(3) Park, A.; Stacy, M. *J. Neurol.* **2009**, *256 Suppl 3*, 293-298.

(4) Seppi, K.; Weintraub, D.; Coelho, M.; Perez-Lloret, S.; Fox, S. H.; Katzenschlager, R.; Hametner, E. M.; Poewe, W.; Rascol, O.; Goetz, C. G.; Sampaio, C. *Mov. Disord.* **2011**, *26 Suppl 3*, S42-80.

(5) Rizek, P.; Kumar, N.; Jog, M. S. *CMAJ* **2016**.

(6) Corallo, F.; De Cola, M. C.; Buono, V. L.; Di Lorenzo, G.; Bramanti, P.; Marino, S. *Psychogeriatrics* **2016**.

(7) Nutt, J. G.; Siderowf, A. D.; Guttman, M.; Schmidt, P. N.; Zamudio, J. I.; Wu, S. S.; Okun, M. S.; Simuni, T.; Parashos, S. A.; Dahodwala, N. A.; Davis, T. L.; Giladi, N.; Gurevich, T.; Hauser, R. A.; Jankovic, J.; Lyons, K. E.; Marsh, L.; Miyasaki, J. M.; Morgan, J. C.; Santiago, A. J.; Tarsy, D.; Mari, Z.; Malaty, I. A.; Nelson, E. C.; National Parkinson Foundation Quality Improvement Initiative, I. *Parkinsonism Relat. Disord.* **2014**, *20*, 274-279.

(8) Wang, Q.; Zhou, Q.; Zhang, S.; Shao, W.; Yin, Y.; Li, Y.; Hou, J.; Zhang, X.; Guo, Y.; Wang, X.; Gu, X.; Zhou, J. *Front Aging Neurosci* **2016**, *8*, 197.

(9) Biernacka, J. M.; Chung, S. J.; Armasu, S. M.; Anderson, K. S.; Lill, C. M.; Bertram, L.; Ahlskog, J. E.; Brighina, L.; Frigerio, R.; Maraganore, D. M. *Parkinsonism Relat. Disord.* **2016**.

(10) Anandhan, A.; Lei, S.; Levytskyy, R.; Pappa, A.; Panayiotidis, M. I.; Cerny, R. L.; Khalimonchuk, O.; Powers, R.; Franco, R. *Mol. Neurobiol.* **2016**.

(11) Wenk, M. R. *Nat. Rev. Drug Discov.* **2005**, *4*, 594-610.

(12) de Farias, C. C.; Maes, M.; Bonifacio, K. L.; Bortolasci, C. C.; de Souza Nogueira, A.; Brinholi, F. F.; Matsumoto, A. K.; do Nascimento, M. A.; de Melo, L. B.; Nixdorf, S. L.; Lavado, E. L.; Moreira, E. G.; Barbosa, D. S. *Neurosci. Lett.* **2016**, *617*, 66-71.

(13) Skoumalova, A.; Ivica, J.; Santorova, P.; Topinkova, E.; Wilhelm, J. *Exp. Gerontol.* **2011**, *46*, 38-42.

(14) Ruiperez, V.; Darios, F.; Davletov, B. *Prog. Lipid Res.* **2010**, *49*, 420-428.

(15) Boutin, M.; Sun, Y.; Shacka, J. J.; Auray-Blais, C. *Anal. Chem.* **2016**, *88*, 1856-1863.

(16) Cheng, D.; Jenner, A. M.; Shui, G. H.; Cheong, W. F.; Mitchell, T. W.; Nealon, J. R.; Kim, W. S.; McCann, H.; Wenk, M. R.; Halliday, G. M.; Garner, B. *PLoS One* **2011**, *6*, 17.

(17) Fabelo, N.; Martin, V.; Santpere, G.; Marin, R.; Torrent, L.; Ferrer, I.; Diaz, M. *Mol. Med.* **2011**, *17*, 1107-1118.

(18) Abbott, S. K.; Jenner, A. M.; Spiro, A. S.; Batterham, M.; Halliday, G. M.; Garner, B. *J. Parkinsons Dis.* **2015**, *5*, 175-185.

(19) Mielke, M. M.; Maetzler, W.; Haughey, N. J.; Bandaru, V. V. R.; Savica, R.; Deuschle, C.; Gasser, T.; Hauser, A. K.; Graber-Sultan, S.; Schleicher, E.; Berg, D.; Liepelt-Scarfone, I. *PLoS One* **2013**, *8*, 6.

(20) Farmer, K.; Smith, C. A.; Hayley, S.; Smith, J. *Int. J. Mol. Sci.* **2015**, *16*, 18865-18877.

(21) Schulte, E. C.; Altmaier, E.; Berger, H. S.; Do, K. T.; Kastenmuller, G.; Wahl, S.; Adamski, J.; Peters, A.; Krumsiek, J.; Suhre, K.; Haslinger, B.; Ceballos-Baumann, A.; Gieger, C.; Winkelmann, J. *PLoS One* **2016**, *11*, 12.

(22) Johansen, K. K.; Wang, L.; Aasly, J. O.; White, L. R.; Matson, W. R.; Henchcliffe, C.; Beal, M. F.; Bogdanov, M. *PLoS One* **2009**, *4*, e7551.

(23) Iverson, S. J.; Lang, S. L.; Cooper, M. H. *Lipids* **2001**, *36*, 1283-1287.

(24) Kind, T.; Liu, K. H.; Lee do, Y.; DeFelice, B.; Meissen, J. K.; Fiehn, O. *Nat. Methods* **2013**, *10*, 755-758.

(25) Tsugawa, H.; Cajka, T.; Kind, T.; Ma, Y.; Higgins, B.; Ikeda, K.; Kanazawa, M.; VanderGheynst, J.; Fiehn, O.; Arita, M. *Nat. Methods* **2015**, *12*, 523-+.

(26) Sud, M.; Fahy, E.; Cotter, D.; Brown, A.; Dennis, E. A.; Glass, C. K.; Merrill, A. H., Jr.; Murphy, R. C.; Raetz, C. R.; Russell, D. W.; Subramaniam, S. *Nucleic Acids Res.* **2007**, *35*, D527-532.

(27) Wishart, D. S.; Jewison, T.; Guo, A. C.; Wilson, M.; Knox, C.; Liu, Y.; Djoumbou, Y.; Mandal, R.; Aziat, F.; Dong, E.; Bouatra, S.; Sinelnikov, I.; Arndt, D.; Xia, J.; Liu, P.; Yallou, F.; Bjorndahl, T.; Perez-Pineiro, R.; Eisner, R.; Allen, F.; Neveu, V.; Greiner, R.; Scalbert, A. *Nucleic Acids Res.* **2013**, *41*, D801-807.

(28) Li, L.; Li, R.; Zhou, J.; Zuniga, A.; Stanislaus, A. E.; Wu, Y.; Huan, T.; Zheng, J.; Shi, Y.; Wishart, D. S.; Lin, G. *Anal. Chem.* **2013**, *85*, 3401-3408.

(29) Xia, J.; Broadhurst, D. I.; Wilson, M.; Wishart, D. S. *Metabolomics* **2013**, *9*, 280-299.

(30) Vandenberg, G. A.; Muskiet, F. A. J.; Kingma, A. W.; Vanderslik, W.; Halie, M. R. *Clin. Chem.* **1986**, *32*, 1930-1937.

(31) Minois, N. *Gerontology* **2014**, *60*, 319-326.

(32) Nagan, N.; Zoeller, R. A. *Prog. Lipid Res.* **2001**, *40*, 199-229.

(33) Brites, P.; Waterham, H. R.; Wanders, R. J. A. *Bba-Mol. Cell. Biol. L.* **2004**, *1636*, 219-231.

(34) Ginsberg, L.; Rafique, S.; Xuereb, J. H.; Rapoport, S. I.; Gershfeld, N. L. *Brain Res.* **1995**, *698*, 223-226.

(35) Han, X. L.; Holtzman, D. M.; McKeel, D. W. *J. Neurochem.* **2001**, *77*, 1168-1180.

(36) Guo, X.; Song, W.; Chen, K.; Chen, X.; Zheng, Z.; Cao, B.; Huang, R.; Zhao, B.; Wu, Y.; Shang, H. F. *Int. J. Neurosci.* **2015**, *125*, 838-844.

(37) Huang, X.; Auinger, P.; Eberly, S.; Oakes, D.; Schwarzschild, M.; Ascherio, A.; Mailman, R.; Chen, H.; Parkinson Study Group, D. I. *PLoS One* **2011**, *6*, e22854.

Chapter 4 Conclusions and Future Work

4.1 Thesis Summary

Liquid chromatography mass spectrometry (LC-MS) in the field of metabolomics and lipidomics has increased coverage and sensitivity, allowing the analysis of small volume and unique samples. In Chapter 2, nLC-MS was combined with chemical isotope labeling (CIL) metabolomics profiling for increased sensitivity. Samples were diluted and trapped using a reverse phase column, while still retaining their detectability. This showed that we can analyze low concentration samples and that samples could be diluted for multiple experiments. Dansylation CIL increased the metabolome coverage of sweat and urine by more than 4 fold and 13 % over mLC-MS.

In Chapter 3, I used an UHR-QTOF instrument connected to UHPLC to profile Parkinson's disease (PD) samples, to identify potential biomarkers. I identified over 4391 lipid features in more than 50% of the samples. I were able to positively identify 406 lipids that spanned 12 different lipid classes. With the use of UHR-QTOF I was able to identify potential biomarkers that could be used to track the progression of PD from control (H) to PD with dementia (PDD). These potential biomarkers were: Cer(d18:0/25:0) [+$C_5H_5N_5$ -H_2O], PG(53:1), PC species, PG(32:1), Sph(d20:1), 784.739 m/z. We also identified cholesterol and plasmalogens that could be used to monitor, diagnose, or be used as risk factors for PD.

4.2 Future Work

The use of nLC provides unprecedented sensitivity and reduced sample consumption. However the advantages are weighed down by the finicky nature of nLC. nLC uses sprayer tips that clog easily, as well as connections that can pop due to high pressure, hindering the widespread

use of this technique. Despite these issues, new technologies have been developed by companies and experts in the field that improve on nLC-MS. These technologies include integrated chip systems, where the sprayer tip and column are combined into one easy to use system developed by Waters and New Objectives. Additionally, new types of nano sources such as the Captive spray developed by Bruker, make nLC-MS more robust. Furthermore we can apply nLC-MS CIL metabolomics to finger blood sampling, sweat analysis, and microdialysis fluid profiling. The future lies in applying these new technologies to nLC-MS CIL metabolomics, and further optimizing this technique for other applications.

Finally, the PD project can be expanded using different LC-MS techniques and recruiting more patients for validation and further biomarker analysis. Using other LC-MS techniques, we can profile in the negative mode and use different column phases to target different groups of lipids. nLC-MS could also be applied to increase coverage through higher sensitivity, and allow the analysis of low volume/concentration samples, such as cerebral spinal fluid and mircodialysis fluid. This more comprehensive analysis will increase coverage of the lipidome and provide further insight into PD.

The development of mass spectrometry for the fields of metabolomics and lipidomics has grown rapidly. With the use of these techniques in my thesis, I hope to see these fields developed even further, allowing for the opening of new frontiers in the fields of health and medicine.

Bibliography

(1) Abbott, S. K.; Jenner, A. M.; Spiro, A. S.; Batterham, M.; Halliday, G. M.; Garner, B. *J. Parkinsons Dis.* **2015**, *5*, 175-185.

(2) Adibhatla, R. M.; Hatcher, J. F.; Dempsey, R. J. *AAPS J.* **2006**, *8*, E314-321.

(3) Anandhan, A.; Lei, S.; Levytskyy, R.; Pappa, A.; Panayiotidis, M. I.; Cerny, R. L.; Khalimonchuk, O.; Powers, R.; Franco, R. *Mol. Neurobiol.* **2016**.

(4) Awad, H.; Khamis, M. M.; El-Aneed, A. *Appl. Spectrosc. Rev.* **2015**, *50*, 158-175.

(5) Biernacka, J. M.; Chung, S. J.; Armasu, S. M.; Anderson, K. S.; Lill, C. M.; Bertram, L.; Ahlskog, J. E.; Brighina, L.; Frigerio, R.; Maraganore, D. M. *Parkinsonism Relat. Disord.* **2016**.

(6) Bimurzaev, S. B. *Tech. Phys. Lett.* **2014**, *40*, 108-111.

(7) Boutin, M.; Sun, Y.; Shacka, J. J.; Auray-Blais, C. *Anal. Chem.* **2016**, *88*, 1856-1863.

(8) Brites, P.; Waterham, H. R.; Wanders, R. J. A. *Bba-Mol. Cell. Biol. L.* **2004**, *1636*, 219-231.

(9) Caprioli, G.; Giusti, F.; Ballini, R.; Sagratini, G.; Vila-Donat, P.; Vittori, S.; Fiorini, D. *Food Chem.* **2016**, *192*, 965-971.

(10) Chen, X. J.; Bichoutskaia, E.; Stace, A. J. *J. Phys. Chem. A* **2013**, *117*, 3877-3886.

(11) Cheng, D.; Jenner, A. M.; Shui, G. H.; Cheong, W. F.; Mitchell, T. W.; Nealon, J. R.; Kim, W. S.; McCann, H.; Wenk, M. R.; Halliday, G. M.; Garner, B. *PLoS One* **2011**, *6*, 17.

(12) Chernushevich, I. V.; Loboda, A. V.; Thomson, B. A. *J. Mass Spectrom.* **2001**, *36*, 849-865.

(13) Chetwynd, A. J.; Abdul-Sada, A.; Hill, E. M. *Anal. Chem.* **2015**, *87*, 1158-1165.

(14) Cifkova, E.; Holcapek, M.; Lisa, M.; Vrana, D.; Melichar, B.; Student, V. *J. Chromatogr. B Analyt. Technol. Biomed. Life. Sci.* **2015**, *1000*, 14-21.

(15) Contrepois, K.; Jiang, L. H.; Snyder, M. *Mol. Cell. Proteomics* **2015**, *14*, 1684-1695.

(16) Corallo, F.; De Cola, M. C.; Buono, V. L.; Di Lorenzo, G.; Bramanti, P.; Marino, S. *Psychogeriatrics* **2016**.

(17) Dai, W. D.; Huang, Q.; Yin, P. Y.; Li, J.; Zhou, J.; Kong, H. W.; Zhao, C. X.; Lu, X.; Xu, G. W. *Anal. Chem.* **2012**, *84*, 10245-10251.

(18) David, A.; Abdul-Sada, A.; Lange, A.; Tyler, C. R.; Hill, E. M. *J. Chromatogr. A* **2014**, *1365*, 72-85.

(19) Davie, C. A. *Br. Med. Bull.* **2008**, *86*, 109-127.

(20) de Farias, C. C.; Maes, M.; Bonifacio, K. L.; Bortolasci, C. C.; de Souza Nogueira, A.; Brinholi, F. F.; Matsumoto, A. K.; do Nascimento, M. A.; de Melo, L. B.; Nixdorf, S. L.; Lavado, E. L.; Moreira, E. G.; Barbosa, D. S. *Neurosci. Lett.* **2016**, *617*, 66-71.

(21) de la Mora, J. F. *Annu. Rev. Fluid Mech.* **2007**, *39*, 217-243.

(22) Deininger, S. O.; Cornett, D. S.; Paape, R.; Becker, M.; Pineau, C.; Rauser, S.; Walch, A.; Wolski, E. *Anal. Bioanal. Chem.* **2011**, *401*, 167-181.

(23) Dempster, A. J. *Physical Review* **1918**, *11*, 316-325.

(24) Fabelo, N.; Martin, V.; Santpere, G.; Marin, R.; Torrent, L.; Ferrer, I.; Diaz, M. *Mol. Med.* **2011**, *17*, 1107-1118.

(25) Fahy, E.; Subramaniam, S.; Brown, H. A.; Glass, C. K.; Merrill, A. H., Jr.; Murphy, R. C.; Raetz, C. R.; Russell, D. W.; Seyama, Y.; Shaw, W.; Shimizu, T.; Spener, F.; van Meer, G.; VanNieuwenhze, M. S.; White, S. H.; Witztum, J. L.; Dennis, E. A. *J. Lipid Res.* **2005**, *46*, 839-861.

(26) Fan, T. W. M.; Lane, A. N. *Prog. Nucl. Magn. Reson. Spectrosc.* **2016**, *92-93*, 18-53.

(27) Farmer, K.; Smith, C. A.; Hayley, S.; Smith, J. *Int. J. Mol. Sci.* **2015**, *16*, 18865-18877.

(28) Ficarro, S. B.; Zhang, Y.; Lu, Y.; Moghimi, A. R.; Askenazi, M.; Hyatt, E.; Smith, E. D.; Boyer, L.; Schlaeger, T. M.; Luckey, C. J.; Marto, J. A. *Anal. Chem.* **2009**, *81*, 3440-3447.

(29) Fil, A.; Cano-de-la-Cuerda, R.; Munoz-Hellin, E.; Vela, L.; Ramiro-Gonzalez, M.; Fernandez-de-Las-Penas, C. *Parkinsonism Relat. Disord.* **2013**, *19*, 285-294; discussion 285.

(30) Ginsberg, L.; Rafique, S.; Xuereb, J. H.; Rapoport, S. I.; Gershfeld, N. L. *Brain Res.* **1995**, *698*, 223-226.

(31) Godzien, J.; Ciborowski, M.; Martinez-Alcazar, M. P.; Samczuk, P.; Kretowski, A.; Barbas, C. *J. Proteome Res.* **2015**, *14*, 3204-3216.

(32) Goldenberg, N. A.; Everett, A. D.; Graham, D.; Bernard, T. J.; Nowak-Gottl, U. *Proteomics Clin. Appl.* **2014**, *8*, 828-836.

(33) Grimm, R. L.; Beauchamp, J. L. *J. Phys. Chem. A* **2010**, *114*, 1411-1419.

(34) Guo, K.; Li, L. *Anal. Chem.* **2009**, *81*, 3919-3932.

(35) Guo, K.; Li, L. *Anal. Chem.* **2010**, *82*, 8789-8793.

(36) Guo, K.; Peng, J.; Zhou, R. K.; Li, L. *J. Chromatogr. A* **2011**, *1218*, 3689-3694.

(37) Guo, X.; Song, W.; Chen, K.; Chen, X.; Zheng, Z.; Cao, B.; Huang, R.; Zhao, B.; Wu, Y.; Shang, H. F. *Int. J. Neurosci.* **2015**, *125*, 838-844.

(38) Han, X. L.; Holtzman, D. M.; McKeel, D. W. *J. Neurochem.* **2001**, *77*, 1168-1180.

(39) Hao, L.; Zhong, X. F.; Greer, T.; Ye, H.; Li, L. J. *Analyst* **2015**, *140*, 467-475.

(40) Huan, T.; Li, L. *Anal. Chem.* **2015**, *87*, 7011-7016.

(41) Huan, T.; Wu, Y.; Tang, C.; Lin, G.; Li, L. *Anal. Chem.* **2015**, *87*, 9838-9845.

(42) Huang, X.; Auinger, P.; Eberly, S.; Oakes, D.; Schwarzschild, M.; Ascherio, A.; Mailman, R.; Chen, H.; Parkinson Study Group, D. I. *PLoS One* **2011**, *6*, e22854.

(43) Hussain, J.; Liu, Y.; Lopes, W. A.; Druzian, J. I.; Souza, C. O.; Carvalho, G. C.; Nascimento, I. A.; Liao, W. *Appl. Biochem. Biotechnol.* **2015**, *175*, 3048-3057.

(44) Iribarne, J. V.; Thomson, B. A. *J. Chem. Phys.* **1976**, *64*, 2287-2294.

(45) Ivanisevic, J.; Zhu, Z. J.; Plate, L.; Tautenhahn, R.; Chen, S.; O'Brien, P. J.; Johnson, C. H.; Marletta, M. A.; Patti, G. J.; Siuzdak, G. *Anal. Chem.* **2013**, *85*, 6876-6884.

(46) Iverson, S. J.; Lang, S. L.; Cooper, M. H. *Lipids* **2001**, *36*, 1283-1287.

(47) Johansen, K. K.; Wang, L.; Aasly, J. O.; White, L. R.; Matson, W. R.; Henchcliffe, C.; Beal, M. F.; Bogdanov, M. *PLoS One* **2009**, *4*, e7551.

(48) Jones, D. R.; Wu, Z.; Chauhan, D.; Anderson, K. C.; Peng, J. *Anal. Chem.* **2014**, *86*, 3667-3675.

(49) Kang, Y. P.; Lee, W. J.; Hong, J. Y.; Lee, S. B.; Park, J. H.; Kim, D.; Park, S.; Park, C. S.; Park, S. W.; Kwon, S. W. *J. Proteome Res.* **2014**, *13*, 3919-3929.

(50) Kind, T.; Liu, K. H.; Lee do, Y.; DeFelice, B.; Meissen, J. K.; Fiehn, O. *Nat. Methods* **2013**, *10*, 755-758.

(51) Li, L.; Li, R.; Zhou, J.; Zuniga, A.; Stanislaus, A. E.; Wu, Y.; Huan, T.; Zheng, J.; Shi, Y.; Wishart, D. S.; Lin, G. *Anal. Chem.* **2013**, *85*, 3401-3408.

(52) Liu, P.; Huang, Y. Q.; Cai, W. J.; Yuan, B. F.; Feng, Y. Q. *Anal. Chem.* **2014**, *86*, 9765-9773.

(53) Lu, Z.; Peart, T. E.; Cook, C. J.; De Silva, A. O. *J. Chromatogr. A* **2016**.

(54) Mahieu, N. G.; Huang, X. J.; Chen, Y. J.; Patti, G. J. *Anal. Chem.* **2014**, *86*, 9583-9589.

(55) Mielke, M. M.; Maetzler, W.; Haughey, N. J.; Bandaru, V. V. R.; Savica, R.; Deuschle, C.; Gasser, T.; Hauser, A. K.; Graber-Sultan, S.; Schleicher, E.; Berg, D.; Liepelt-Scarfone, I. *PLoS One* **2013**, *8*, 6.

(56) Millan, L.; Sampedro, M. C.; Sanchez, A.; Delporte, C.; Van Antwerpen, P.; Goicolea, M. A.; Barrio, R. J. *J. Chromatogr. A* **2016**, *1454*, 67-77.

(57) Minois, N. *Gerontology* **2014**, *60*, 319-326.

(58) Mirnaghi, F. S.; Caudy, A. A. *Bioanalysis* **2014**, *6*, 3393-3416.

(59) Mohamed, R.; Varesio, E.; Ivosev, G.; Burton, L.; Bonner, R.; Hopfgartner, G. *Anal. Chem.* **2009**, *81*, 7677-7694.

(60) Nagan, N.; Zoeller, R. A. *Prog. Lipid Res.* **2001**, *40*, 199-229.

(61) Narvaez-Rivas, M.; Zhang, Q. *J. Chromatogr. A* **2016**, *1440*, 123-134.

(62) Nilsson, T.; Mann, M.; Aebersold, R.; Yates, J. R.; Bairoch, A.; Bergeron, J. J. M. *Nat. Methods* **2010**, *7*, 681-685.

(63) Nutt, J. G.; Siderowf, A. D.; Guttman, M.; Schmidt, P. N.; Zamudio, J. I.; Wu, S. S.; Okun, M. S.; Simuni, T.; Parashos, S. A.; Dahodwala, N. A.; Davis, T. L.; Giladi, N.; Gurevich, T.; Hauser, R. A.; Jankovic, J.; Lyons, K. E.; Marsh, L.; Miyasaki, J. M.; Morgan, J. C.; Santiago, A. J.; Tarsy, D.; Mari, Z.; Malaty, I. A.; Nelson, E. C.; National Parkinson Foundation Quality Improvement Initiative, I. *Parkinsonism Relat. Disord.* **2014**, *20*, 274-279.

(64) Otter, D.; Cao, M.; Lin, H. M.; Fraser, K.; Edmunds, S.; Lane, G.; Rowan, D. *J. Biomed. Biotechnol.* **2011**, *2011*, 974701.

(65) Ovcacikova, M.; Lisa, M.; Cifkova, E.; Holcapek, M. *J. Chromatogr. A* **2016**, *1450*, 76-85.

(66) Park, A.; Stacy, M. *J. Neurol.* **2009**, *256 Suppl 3*, 293-298.

(67) Percy, A. J.; Chambers, A. G.; Yang, J. C.; Domanski, D.; Borchers, C. H. *Anal. Bioanal. Chem.* **2012**, *404*, 1089-1101.

(68) Rainville, P. D.; Langridge, J. I.; Wrona, M. D.; Wilson, I. D.; Plumb, R. S. *Bioanalysis* **2015**, *7*, 1397-1411.

(69) Rainville, P. D.; Theodoridis, G.; Plumb, R. S.; Wilson, I. D. *Trac-Trends Anal. Chem.* **2015**, *61*, 181-191.

(70) Ran, C.; Brodin, L.; Forsgren, L.; Westerlund, M.; Ramezani, M.; Gellhaar, S.; Xiang, F.; Fardell, C.; Nissbrandt, H.; Soderkvist, P.; Puschmann, A.; Ygland, E.; Olson, L.; Willows, T.; Johansson, A.; Sydow, O.; Wirdefeldt, K.; Galter, D.; Svenningsson, P.; Belin, A. C. *Neurobiol. Aging* **2016**.

(71) Rizek, P.; Kumar, N.; Jog, M. S. *CMAJ* **2016**.

(72) Robotti, E.; Marengo, E. *Methods Mol. Biol.* **2016**, *1384*, 237-267.

(73) Ruiperez, V.; Darios, F.; Davletov, B. *Prog. Lipid Res.* **2010**, *49*, 420-428.

(74) Saccenti, E.; Timmerman, M. E. *J. Proteome Res.* **2016**.

(75) Sas, K. M.; Nair, V.; Byun, J.; Kayampilly, P.; Zhang, H.; Saha, J.; Brosius, F. C., 3rd; Kretzler, M.; Pennathur, S. *J. Proteomics Bioinform.* **2015**, *Suppl 14*.

(76) Schmidt, A.; Karas, M.; Dulcks, T. *J. Am. Soc. Mass Spectrom.* **2003**, *14*, 492-500.

(77) Schulte, E. C.; Altmaier, E.; Berger, H. S.; Do, K. T.; Kastenmuller, G.; Wahl, S.; Adamski, J.; Peters, A.; Krumsiek, J.; Suhre, K.; Haslinger, B.; Ceballos-Baumann, A.; Gieger, C.; Winkelmann, J. *PLoS One* **2016**, *11*, 12.

(78) Seppi, K.; Weintraub, D.; Coelho, M.; Perez-Lloret, S.; Fox, S. H.; Katzenschlager, R.; Hametner, E. M.; Poewe, W.; Rascol, O.; Goetz, C. G.; Sampaio, C. *Mov. Disord.* **2011**, *26 Suppl 3*, S42-80.

(79) Shen, Q.; Dai, Z.; Huang, Y. W.; Cheung, H. Y. *Food Chem.* **2016**, *205*, 89-96.

(80) Shevchenko, A.; Chernushevich, I.; Ens, W.; Standing, K. G.; Thomson, B.; Wilm, M.; Mann, M. *Rapid Commun. Mass Spectrom.* **1997**, *11*, 1015-1024.

(81) Skoumalova, A.; Ivica, J.; Santorova, P.; Topinkova, E.; Wilhelm, J. *Exp. Gerontol.* **2011**, *46*, 38-42.

(82) Smith, R.; Ventura, D.; Prince, J. T. *Brief. Bioinform.* **2015**, *16*, 104-117.

(83) Song, P.; Mabrouk, O. S.; Hershey, N. D.; Kennedy, R. T. *Anal. Chem.* **2012**, *84*, 412-419.

(84) Sud, M.; Fahy, E.; Cotter, D.; Brown, A.; Dennis, E. A.; Glass, C. K.; Merrill, A. H., Jr.; Murphy, R. C.; Raetz, C. R.; Russell, D. W.; Subramaniam, S. *Nucleic Acids Res.* **2007**, *35*, D527-532.

(85) Tayyari, F.; Gowda, G. A. N.; Gu, H. W.; Raftery, D. *Anal. Chem.* **2013**, *85*, 8715-8721.

(86) Tenenboim, H.; Burgos, A.; Willmitzer, L.; Brotman, Y. *Biochimie* **2016**.

(87) Tsugawa, H.; Cajka, T.; Kind, T.; Ma, Y.; Higgins, B.; Ikeda, K.; Kanazawa, M.; VanderGheynst, J.; Fiehn, O.; Arita, M. *Nat. Methods* **2015**, *12*, 523-+.

(88) Tulipani, S.; Mora-Cubillos, X.; Jauregui, O.; Llorach, R.; Garcia-Fuentes, E.; Tinahones, F. J.; Andres-Lacueva, C. *Anal. Chem.* **2015**, *87*, 2639-2647.

(89) Turkoglu, O.; Zeb, A.; Graham, S.; Szyperski, T.; Szender, J. B.; Odunsi, K.; Bahado-Singh, R. *Metabolomics* **2016**, *12*.

(90) Uehara, T.; Yokoi, A.; Aoshima, K.; Tanaka, S.; Kadowaki, T.; Tanaka, M.; Oda, Y. *Anal. Chem.* **2009**, *81*, 3836-3842.

(91) Vandenberg, G. A.; Muskiet, F. A. J.; Kingma, A. W.; Vanderslik, W.; Halie, M. R. *Clin. Chem.* **1986**, *32*, 1930-1937.

(92) Vissers, J. P. *J. Chromatogr. A* **1999**, *856*, 117-143.

(93) Vissers, J. P. C.; Claessens, H. A.; Cramers, C. A. *J. Chromatogr. A* **1997**, *779*, 1-28.

(94) Vorkas, P. A.; Isaac, G.; Anwar, M. A.; Davies, A. H.; Want, E. J.; Nicholson, J. K.; Holmes, E. *Anal. Chem.* **2015**, *87*, 4184-4193.

(95) Vuckovic, D. *Anal. Bioanal. Chem.* **2012**, *403*, 1523-1548.

(96) Waikar, S. S.; Sabbisetti, V. S.; Bonventre, J. V. *Kidney Int.* **2010**, *78*, 486-494.

(97) Wang, Q.; Zhou, Q.; Zhang, S.; Shao, W.; Yin, Y.; Li, Y.; Hou, J.; Zhang, X.; Guo, Y.; Wang, X.; Gu, X.; Zhou, J. *Front Aging Neurosci* **2016**, *8*, 197.

(98) Wells, J. M.; McLuckey, S. A. *Methods Enzymol.* **2005**, *402*, 148-185.

(99) Wenk, M. R. *Nat. Rev. Drug Discov.* **2005**, *4*, 594-610.

(100) Wilm, M.; Mann, M. *Anal. Chem.* **1996**, *68*, 1-8.

(101) Wishart, D. S.; Jewison, T.; Guo, A. C.; Wilson, M.; Knox, C.; Liu, Y.; Djoumbou, Y.; Mandal, R.; Aziat, F.; Dong, E.; Bouatra, S.; Sinelnikov, I.; Arndt, D.; Xia, J.; Liu, P.; Yallou, F.; Bjorndahl, T.; Perez-Pineiro, R.; Eisner, R.; Allen, F.; Neveu, V.; Greiner, R.; Scalbert, A. *Nucleic Acids Res.* **2013**, *41*, D801-807.

(102) Wu, Y.; Jiang, X.; Zhang, S.; Dai, X.; Liu, Y.; Tan, H.; Gao, L.; Xia, T. *J. Chromatogr. B* **2016**, *1017-1018*, 10-17.

(103) Wu, Y. M.; Li, L. *Anal. Chem.* **2012**, *84*, 10723-10731.

(104) Wu, Y. M.; Li, L. *Anal. Chem.* **2013**, *85*, 5755-5763.

(105) Xia, J.; Broadhurst, D. I.; Wilson, M.; Wishart, D. S. *Metabolomics* **2013**, *9*, 280-299.

(106) Xu, X.; Gao, B.; Guan, Q.; Zhang, D.; Ye, X.; Zhou, L.; Tong, G.; Li, H.; Zhang, L.; Tian, J.; Huang, J. *J. Pharm. Biomed. Anal.* **2016**, *129*, 34-42.

(107) Yamashita, M.; Fenn, J. B. *J. Phys. Chem.* **1984**, *88*, 4451-4459.

(108) Yan, Z.; Yan, R. *Anal. Chim. Acta* **2015**, *894*, 65-75.

(109) Yin, P. Y.; Xu, G. W. *J. Chromatogr. A* **2015**, *1374*, 1-13.

(110) Yuan, W.; Anderson, K. W.; Li, S. W.; Edwards, J. L. *Anal. Chem.* **2012**, *84*, 2892-2899.

(111) Yuan, W.; Zhang, J. X.; Li, S. W.; Edwards, J. L. *J. Proteome Res.* **2011**, *10*, 5242-5250.

(112) Zerbinati, C.; Galli, F.; Regolanti, R.; Poli, G.; Iuliano, L. *Clin. Chim. Acta* **2015**, *446*, 156-162.

(113) Zhou, R.; Huan, T.; Li, L. *Anal. Chim. Acta* **2015**, *881*, 107-116.

(114) Zhou, R.; Li, L. *J Proteomics* **2015**, *118*, 130-139.

(115) Zhou, R.; Tseng, C. L.; Huan, T.; Li, L. *Anal. Chem.* **2014**, *86*, 4675-4679.

Appendix

Chapter 2 Nanoflow LC-MS for High-Performance Chemical Isotope Labeling Quantitative Metabolomics

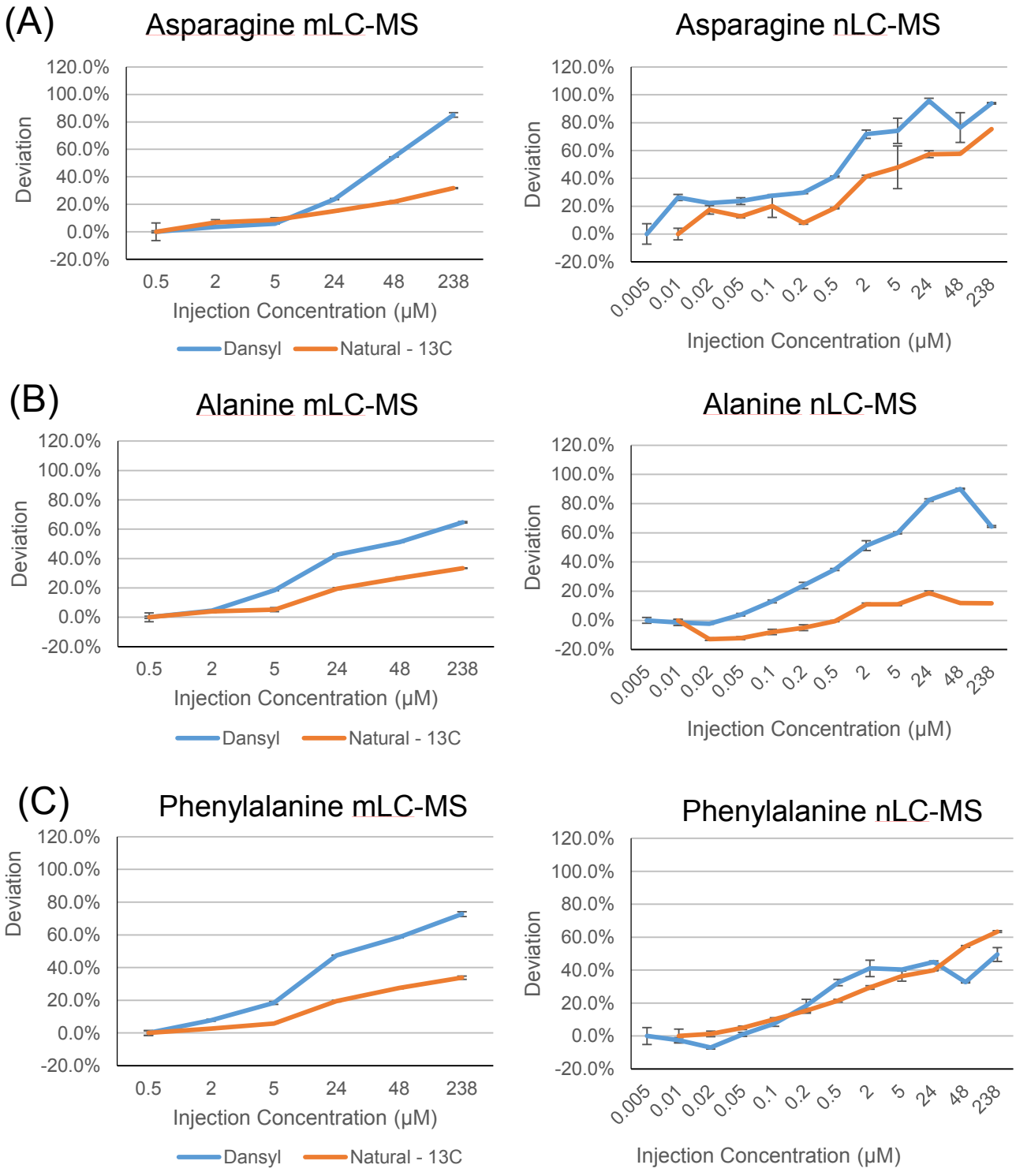

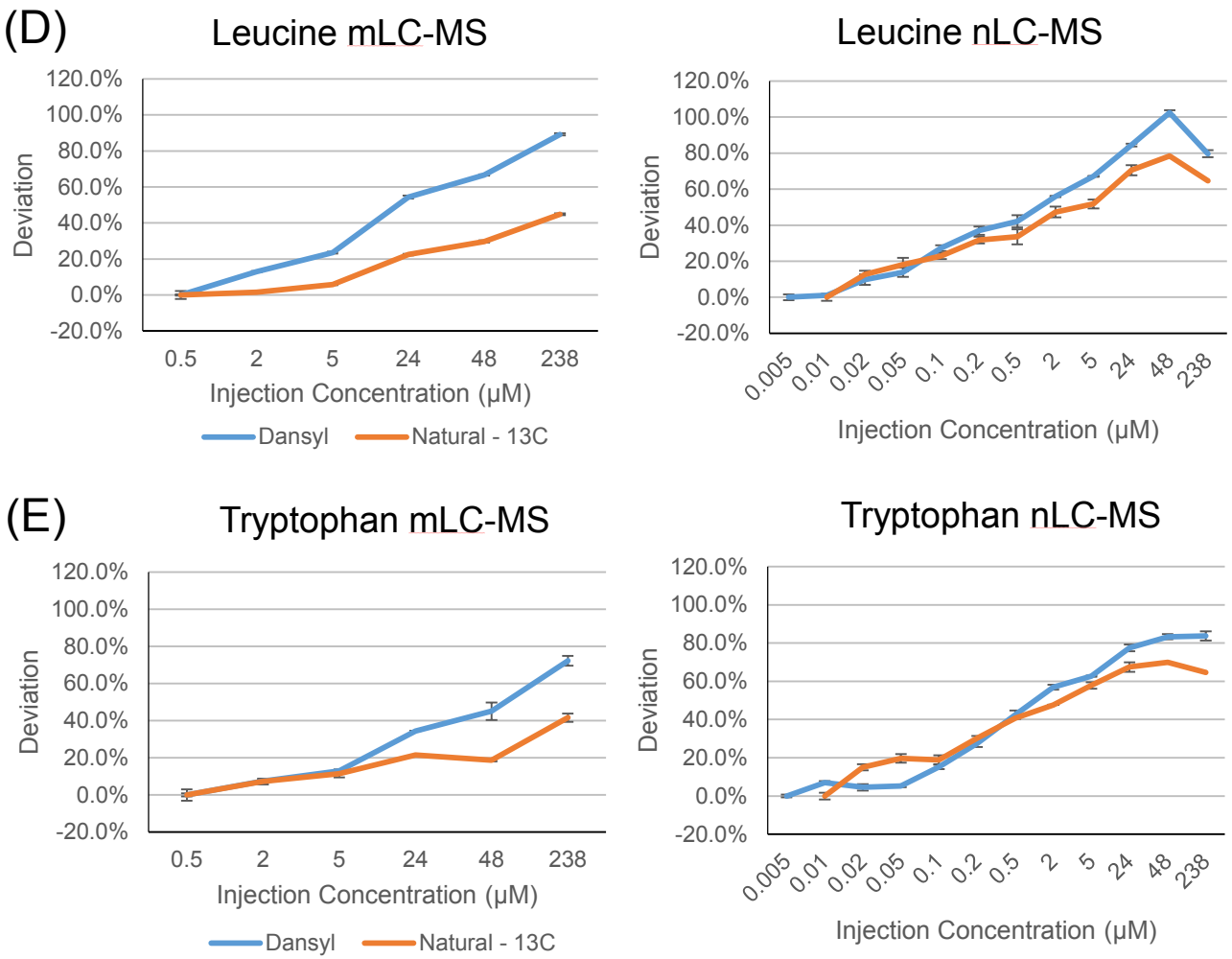

Appendix Figure A2.1. Effect of detector saturation on the calculated peak pair ratio in mLC-MS and nLC-MS. Derivation from the expected 1:2 ratio is plotted as a function of the solution concentration of 1:2 mixture of ^{12}C-dansyl amino acid and ^{13}C-dansyl amino acid.

Chapter 3 UHPLC Combined with Ultra-High Resolution QTOF-MS for Rapid Lipidomic Profiling of Serum for Discovery of Lipid Biomarkers of Parkinson's Disease

Appendix Table A3.1 406 lipids identified by MS/MS matching to Lipid Blast and MS Dial libraries.

RT (min)	Precursor m/z	Rank	Library	Delta (m/z)	Rev-Dot	Lipid
1.16	518.3220	1	MSDial	<0.01	958.6	lysoPC 20:2; [M+H]+; PC(20:2(11Z,14Z)/0:0)
1.25	370.2948	1	MSDial	<0.01	983.6	PC 31:0; [M+H]+; PC(10:0/21:0)
1.32	526.2927	1	MSDial	<0.01	999.3	PC 30:1; [M+H]+; PC(10:0/20:1(11E))
1.65	544.3396	1	LipidBlast-pos	0.0007	847.0	lysoPE 18:0; [M+H]+; PE(18:0/0:0)
1.66	568.3396	1	LipidBlast-pos	0.0007	842.0	lysoPE 20:0; [M+Na]+; PE(20:0/0:0)
1.68	520.3393	1	LipidBlast-pos	0.0010	810.0	lysoPC 20:4; [M+H]+; PC(20:4(5E,8E,11E,14E)/0:0)
1.72	494.3238	1	LipidBlast-pos	0.0009	854.0	lysoPC 18:0; [M+H]+; PC(18:0/0:0)
1.85	496.3400	1	LipidBlast-pos	0.0003	809.0	lysoPC 17:0; [M+H]+; PC(17:0/0:0)
1.86	546.3554	1	LipidBlast-pos	0.0006	839.0	lysoPC 24:0; [M+H]+; PC(24:0/0:0)
1.88	482.3241	1	LipidBlast-pos	0.0005	841.0	lysoPC 16:1; [M+H]+; PC(16:1(7Z)/0:0)
1.90	634.4523	1	CustomPC+Hpos.msp	-0.0075	672.0	PC 31:1; [M+H]+; GPCho(5:0/26:1(5Z))
2.04	522.3556	1	LipidBlast-pos	0.0004	874.0	lysoPC 20:3; [M+H]+; PC(20:3(5Z,8Z,11Z)/0:0)
2.10	544.3375	1	LipidBlast-pos	0.0004	953.0	plasmenyl-PE 34:1; [M+H]+; PE(P-16:0/18:1(11E))
2.14	510.3551	1	LipidBlast-pos	0.0008	852.0	lysoPC 18:0; [M+H]+; PC(O-18:0/0:0)
2.26	518.3214	1	LipidBlast-pos	0.0009	995.0	lysoPC 17:1; [M+H]+; PC(17:1(9Z)/0:0)
2.34	532.3373	1	LipidBlast-pos	0.0006	672.0	N-(docosanoyl)-sphing-4-enine; [M+H]+; Cer(d18:1(4E)/22:0)
2.41	524.3714	1	LipidBlast-pos	0.0002	893.0	lysoPC 18:1; [M+H]+; PC(18:1(11E)/0:0)
2.42	546.3530	1	LipidBlast-pos	0.0005	995.0	lysoPC 20:0; [M+H]+; PC(20:0/0:0)
2.44	482.3242	1	LipidBlast-pos	0.0004	961.0	N-(15Z-tetracosenoyl)-sphing-4-enine; [M+H]+; Cer(d18:1(4E)/24:1(15Z))

2.60	647.5114	1	MSDial	<0.01	961.5	SM 33:1; [M]+; SM(d14:1(4E)/19:0)
2.68	673.5275	1	MSDial	<0.01	969.3	SM 34:1; [M]+; SM(d14:0/20:1(11Z))
2.76	752.5212	1	MSDial	<0.01	870.4	PC 35:2; [M+H]+; PC(16:2/19:0)
3.03	854.5687	1	MSDial	<0.01	949.2	PC 42:8; [M+H]+; PC(16:5/26:3)
3.03	661.5275	1	MSDial	<0.01	901.5	SM 33:2; [M]+; SM(d14:2(4E,6E)/19:0)
3.11	778.5376	1	MSDial	<0.01	962.5	PC 37:2; [M+H]+; PC(18:2(2E,4E)/19:0)
3.11	687.5428	1	MSDial	<0.01	846.3	SM 34:3; [M]+; SM(d14:2(4E,6E)/20:1(11Z))
3.21	766.5376	1	MSDial	<0.01	903.0	PC 36:2; [M+H]+; PC(18:1(11E)/18:1(11E))
3.21	804.5530	1	MSDial	<0.01	963.7	PC 40:4; [M+H]+; PC(18:0/22:4(7Z,10Z,13Z,16Z))
3.24	728.5225	1	MSDial	<0.01	963.4	PC 33:2; [M+H]+; PC(15:0/18:2(2E,4E))
3.24	699.5436	1	MSDial	<0.01	950.5	SM 35:2; [M]+; SM(d14:2(4E,6E)/21:0)
3.40	830.5684	1	MSDial	<0.01	964.7	PC 42:10; [M+H]+; PC(16:5/26:5)
3.50	697.5253	1	MSDial	<0.01	953.0	SM 35:4; [M]+; SM(d17:2(4E,8E)/18:2(9Z,12Z))
3.60	704.5227	1	MSDial	<0.01	966.6	PC 31:1; [M+H]+; PC(13:0/18:1(4E))
3.60	792.5539	1	MSDial	<0.01	965.5	PC 38:3; [M+H]+; PC(18:2(2E,4E)/20:1(11E))
3.60	701.5599	1	MSDial	<0.01	973.5	SM 35:1; [M]+; SM(d14:1(4E)/21:0)
3.65	754.5377	1	MSDial	<0.01	968.1	PC 35:1; [M+H]+; PC(11:0/24:1(15Z))
3.71	730.5385	1	MSDial	<0.01	969.9	PC 33:2; [M+H]+; PC(11:0/22:2(13Z,16Z))
3.81	780.5546	1	MSDial	<0.01	973.0	PC 36:6; [M+H]+; PC(16:5/20:1)
3.81	802.5356	1	MSDial	<0.01	965.4	PC 40:5; [M+H]+; PC(18:0/22:5(4Z,7Z,10Z,13Z,16Z))
3.81	727.5751	1	MSDial	<0.01	972.1	SM 38:3; [M]+; SM(d14:2(4E,6E)/24:1(15Z))
3.99	806.5695	1	MSDial	<0.01	970.0	PC 38:7; [M+H]+; PC(16:5/22:2)
4.02	756.5536	1	MSDial	<0.01	971.3	PC 34:5; [M+H]+; PC(16:5/18:0)
4.02	768.5535	1	MSDial	<0.01	966.1	PC 36:2; [M+H]+; PC(18:0/18:2(2E,4E))

4.02	782.5694	1	MSDial	<0.01	973.5	PC 36:5; [M+H]+; PC(16:5/20:0)
4.06	738.5076	1	MSDial	<0.01	979.2	PE 39:5; [M+H]+; PE(22:5(7Z,10Z,13Z,16Z,19Z)/17:0)
4.12	718.5377	1	MSDial	<0.01	958.5	PC 32:1; [M+H]+; PC(16:0/16:1(9Z))
4.12	689.5596	1	MSDial	<0.01	973.2	SM 34:2; [M]+; SM(d14:1(4E)/20:1(11Z))
4.13	778.5369	1	MSDial	<0.01	913.4	PC 37:4; [M+H]+; PC(13:0/24:4(5Z,8Z,11Z,14Z))
4.22	806.5704	1	MSDial	<0.01	968.6	PC 38:7; [M+H]+; PC(16:2/22:5)
4.30	828.5507	1	MSDial	<0.01	964.1	PC 42:7; [M+H]+; PC(24:4(5Z,8Z,11Z,14Z)/18:3(9Z,12Z,15Z))
4.30	715.5746	1	MSDial	<0.01	965.1	SM 36:2; [M]+; SM(d14:1(4E)/22:1(13Z))
4.39	744.5535	1	MSDial	<0.01	967.6	PC 34:1; [M+H]+; PC(16:0/18:1(11E))
4.39	794.5689	1	MSDial	<0.01	964.3	PC 38:3; [M+H]+; PC(18:0/20:3(5Z,8Z,11Z))
4.39	832.5846	1	MSDial	<0.01	968.0	PC 40:9; [M+H]+; PC(18:3(6Z,9Z,12Z)/22:6(4Z,7Z,10Z,13Z,16Z,19Z))
4.39	764.5221	1	MSDial	<0.01	985.9	plasmenyl-PC 34:0; [M+H]+; PC(P-16:0/18:0)
4.50	770.5692	1	MSDial	<0.01	965.1	PC 36:1; [M+H]+; PC(18:0/18:1(11E))
4.50	854.5660	1	MSDial	<0.01	991.0	PC 42:9; [M+H]+; PC(22:5(4Z,7Z,10Z,13Z,16Z)/20:4(5E,8E,11E,14E))
4.51	647.5107	1	custom-SM+Hpos	0.0021	933.0	SM 32:1; [M]+; SM(d14:0/18:1(9Z))
4.60	804.5507	1	MSDial	<0.01	967.3	PC 39:6; [M+H]+; PC(16:4/23:2)
4.60	766.5742	1	MSDial	<0.01	970.5	plasmenyl-PC 38:3; [M+H]+; PC(P-18:0/20:3(5Z,8Z,11Z))
4.60	744.5548	1	MSDial	<0.01	969.9	PC 34:2; [M+H]+; PC(16:0/18:2(2E,4E))
4.78	808.5854	1	MSDial	<0.01	974.6	PC 38:6; [M+H]+; PC(18:1(11E)/20:5(5Z,8Z,11Z,14Z,17Z))
4.78	790.5744	1	MSDial	<0.01	970.6	plasmenyl-PC 40:3; [M+H]+; PC(P-20:0/20:3(8Z,11Z,14Z))
4.78	703.5754	1	MSDial	<0.01	973.6	SM 34:4; [M]+; SM(d16:2(4E,6E)/18:2(9Z,12Z))
4.78	725.5560	1	MSDial	<0.01	970.3	SM 39:0; [M]+; SM(d14:0/25:0)
4.83	752.5204	1	CustomPC+Hpos.msp	0.0026	672.0	PC 35:2; [M+H]+; GPCho(17:0/18:2(2E,4E))

4.89	820.5857	1	MSDial	<0.01	961.3	PC 40:6; [M+H]+; PC(16:4/24:2)
4.89	830.5669	1	MSDial	<0.01	947.5	PC 42:10; [M+H]+; PC(22:5(4Z,7Z,10Z,13Z,16Z)/20:5(5Z,8Z,11Z,14Z,17Z))
4.89	740.5229	1	MSDial	<0.01	985.0	PE 38:6; [M+H]+; PE(16:4/22:2)
4.99	834.6006	1	MSDial	<0.01	965.6	PC 40:7; [M+H]+; PC(16:5/24:2)
4.99	729.5909	1	MSDial	<0.01	973.4	SM 37:1; [M]+; SM(d14:1(4E)/23:0)
5.02	706.5381	1	MSDial	<0.01	911.6	PC 31:0; [M+H]+; PC(15:0/16:0)
5.02	808.5851	1	MSDial	<0.01	968.5	PC 38:6; [M+H]+; PC(16:4/22:2)
5.09	732.5549	1	MSDial	<0.01	970.0	PC 32:3; [M+H]+; PC(16:3/16:0)
5.09	758.5705	1	MSDial	<0.01	974.8	PC 34:4; [M+H]+; PC(17:2(9Z,12Z)/17:2(9Z,12Z))
5.16	792.5903	1	MSDial	<0.01	971.0	plasmenyl-PC 40:2; [M+H]+; PC(P-20:0/20:2(11Z,14Z))
5.23	716.5228	1	MSDial	<0.01	980.4	PE 36:3; [M+H]+; PE(18:0/18:3(6Z,9Z,12Z))
5.23	755.6057	1	MSDial	<0.01	973.4	SM 40:3; [M]+; SM(d14:2(4E,6E)/26:1(17Z))
5.30	854.5677	1	CustomPC+Hpos.msp	0.0022	672.0	PC 42:7; [M+H]+; GPCho(18:3(6Z,9Z,12Z)/24:4(5Z,8Z,11Z,14Z))
5.30	818.6060	1	MSDial	<0.01	971.5	plasmenyl-PC 42:5; [M+H]+; PC(P-20:0/22:5(4Z,7Z,10Z,13Z,16Z))
5.32	728.5212	1	CustomPC+Hpos.msp	0.0018	672.0	PC 33:2; [M+H]+; GPCho(7:0/26:2(5E,9Z))
5.35	826.5333	1	CustomPC+Hpos.msp	0.0054	810.0	PC 40:4; [M+H]+; GPCho(20:2(11Z,14Z)/20:2(11Z,14Z))
5.39	784.5861	1	MSDial	<0.01	973.2	PC 36:5; [M+H]+; PC(16:0/20:5(5Z,8Z,11Z,14Z,17Z))
5.39	806.5673	1	MSDial	<0.01	967.6	PC 38:8; [M+H]+; PC(16:5/22:3)
5.45	687.5422	1	custom-SM+Hpos	0.0020	933.0	SM 34:2; [M]+; SM(d16:1(4E)/18:1(9Z))
5.49	720.5545	1	MSDial	<0.01	959.1	PC 32:0; [M+H]+; PC(16:0/16:0)
5.49	796.5857	1	MSDial	<0.01	966.6	PC 38:2; [M+H]+; PC(18:2(2E,4E)/20:0)
5.51	800.5178	1	CustomPC+Hpos.msp	0.0052	672.0	PC 39:7; [M+H]+; GPCho(17:1(9Z)/22:6(4Z,7Z,10Z,13Z,16Z,19Z))

5.57	780.5527	1	MSDial	<0.01	912.2	plasmenyl-PC 34:1; [M+H]+; PC(P-16:0/18:1(11E))
5.59	746.5696	1	MSDial	<0.01	968.7	PC 34:0; [M+H]+; PC(17:0/17:0)
5.59	717.5907	1	MSDial	<0.01	972.4	SM 36:1; [M]+; SM(d14:0/22:1(13Z))
5.63	766.5367	1	CustomPC+Hpos.msp	0.0020	672.0	PC 36:1; [M+H]+; GPCho(14:1(9Z)/22:0)
5.70	834.6011	1	MSDial	<0.01	974.5	PC 40:8; [M+H]+; PC(16:5/24:3)
5.70	856.5825	1	MSDial	<0.01	986.7	PE 36:1; [M+H]+; PE(18:0/18:1(9Z))
5.70	768.5905	1	MSDial	<0.01	973.0	plasmenyl-PC 38:2; [M+H]+; PC(P-20:0/18:2(2E,4E))
5.70	750.5432	1	MSDial	<0.01	756.5	SM 30:1; [M]+; SM(d14:0/16:1(9Z))
5.79	772.5853	1	MSDial	<0.01	969.7	PC 35:5; [M+H]+; PC(16:5/19:0)
5.79	860.6149	1	MSDial	<0.01	926.4	PE 34:2; [M+H]+; PE(16:0/18:2(2E,4E))
5.79	742.5748	1	MSDial	<0.01	972.6	plasmenyl-PC 35:2; [M+H]+; PC(P-18:0/17:2(9Z,12Z))
5.79	794.6062	1	MSDial	<0.01	973.6	plasmenyl-PC 40:2; [M+H]+; PC(P-18:0/22:2(13Z,16Z))
5.84	742.5392	1	MSDial	<0.01	985.1	PE 37:1; [M+H]+; PE(18:1(17Z)/19:0)
5.90	820.6210	1	MSDial	<0.01	970.0	plasmenyl-PC 42:2; [M+H]+; PC(P-16:0/26:2(5E,9Z))
5.91	852.5491	1	CustomPC+Hpos.msp	0.0053	713.0	PC 42:8; [M+H]+; GPCho(18:4(6Z,9Z,12Z,15Z)/24:4(5Z,8Z,11Z,14Z))
5.91	632.5254	1	MSDial	<0.01	756.9	lanosteryl palmitoleate; [M+NH4]+
5.91	682.5410	1	MSDial	<0.01	660.0	lysoPC 16:0; [M+H]+; PC(P-16:0/0:0)
5.98	675.5419	1	custom-SM+Hpos	0.0023	939.0	SM 33:0; [M]+; SM(d15:0/18:0)
6.01	776.5182	1	CustomPC+Hpos.msp	0.0048	759.0	PC 37:5; [M+H]+; GPCho(15:0/22:5(4Z,7Z,10Z,13Z,16Z))
6.05	834.6015	1	MSDial	<0.01	973.7	PC 38:5; [M+H]+; PC(16:4/22:1)
6.10	832.5817	1	MSDial	<0.01	962.4	PC 40:8; [M+H]+; PC(20:4(5E,8E,11E,14E)/20:4(5E,8E,11E,14E))
6.10	744.5900	1	MSDial	<0.01	972.7	plasmenyl-PC 35:1; [M+H]+; PC(P-20:0/15:1(9Z))
6.10	726.5428	1	MSDial	<0.01	671.0	plasmenyl-PE 38:2; [M+H]+; PE(P-16:0/22:2(13Z,16Z))

6.21	734.5696	1	MSDial	<0.01	970.9	PC 32:2; [M+H]+; PC(16:1(7Z)/16:1(7Z))
6.21	810.6012	1	MSDial	<0.01	974.7	PC 38:5; [M+H]+; PC(18:1(11E)/20:4(5Z,8Z,11Z,14Z))
6.21	836.6161	1	MSDial	<0.01	971.1	PC 40:6; [M+H]+; PC(18:0/22:6(4Z,7Z,10Z,13Z,16Z,19Z))
6.28	760.5859	1	MSDial	<0.01	974.8	PC 34:3; [M+H]+; PC(18:2(9Z,11Z)/16:1(7Z))
6.28	756.5894	1	MSDial	<0.01	973.1	plasmenyl-PC 36:2; [M+H]+; PC(P-16:0/20:2(11Z,14Z))
6.30	701.5592	1	custom-SM+Hpos	0.0005	939.0	SM 35:1; [M]+; SM(d15:1(4E)/20:0)
6.36	731.6068	1	MSDial	<0.01	973.4	SM 36:4; [M]+; SM(d18:2(4E,14Z)/18:2(9Z,12Z))
6.36	730.5370	1	CustomPC+Hpos.msp	0.0017	743.0	PC 33:1; [M+H]+; GPCho(7:0/26:1(5Z))
6.47	802.5338	1	CustomPC+Hpos.msp	0.0049	731.0	PC 39:6; [M+H]+; GPCho(17:0/22:6(4Z,7Z,10Z,13Z,16Z,19Z))
6.49	780.5535	1	CustomPC+Hpos.msp	0.0009	698.0	PC 36:6; [M+H]+; GPCho(18:3(6Z,9Z,12Z)/18:3(6Z,9Z,12Z))
6.52	783.6374	1	MSDial	<0.01	973.4	SM 44:4; [M]+; SM(d20:0/24:4(5Z,8Z,11Z,14Z))
6.53	582.5094	1	MSDial	<0.01	944.1	DG 36:5; [M+NH4]+; DG(18:2/18:3/0:0)
6.62	786.6016	1	MSDial	<0.01	974.8	PC 36:4; [M+H]+; PC(16:4/20:0)
6.65	818.5678	1	CustomPC+Hpos.msp	0.0021	672.0	PC 40:3; [M+H]+; GPCho(14:1(9Z)/26:2(5E,9Z))
6.67	538.5202	1	MSDial	<0.01	918.0	Cer 40:1; [M+H]+; Cer(d17:1(4E)/23:0)
6.69	756.5535	1	CustomPC+Hpos.msp	0.0008	686.0	PC 35:0; [M+H]+; GPCho(9:0/26:0)
6.71	808.5822	1	MSDial	<0.01	958.9	PC 38:6; [M+H]+; PC(16:5/22:1)
6.71	820.6207	1	MSDial	<0.01	967.8	plasmenyl-PC 42:4; [M+H]+; PC(P-18:0/24:4(5Z,8Z,11Z,14Z))
6.73	846.6360	1	MSDial	<0.01	959.5	plasmenyl-PE 33:0; [M+H]+; PE(P-20:0/13:0)
6.77	768.5528	1	CustomPC+Hpos.msp	0.0015	706.0	PC 36:1; [M+H]+; GPCho(10:0/26:1(5Z))
6.84	764.5214	1	CustomPC+Hpos.msp	0.0017	672.0	PC 36:1; [M+H]+; GPCho(18:0/18:1(11E))
6.93	812.6176	1	MSDial	<0.01	974.5	PC 38:4; [M+H]+; PC(14:0/24:4(5Z,8Z,11Z,14Z))
6.93	718.5751	1	MSDial	<0.01	969.8	plasmenyl-PC 34:2; [M+H]+; PC(P-16:0/18:2(2E,4E))
6.93	689.5587	1	custom-SM+Hpos	0.0011	933.0	SM 34:0; [M]+; SM(d14:0/20:0)

7.03	744.5902	1	MSDial	<0.01	696.9	plasmenyl-PE 38:5; [M+H]+; PE(P-16:0/22:5(4Z,7Z,10Z,13Z,16Z))
7.03	738.5046	1	CustomPC+Hpos.msp	0.0028	672.0	PC 34:1; [M+H]+; GPCho(8:0/26:1(5Z))
7.13	774.6006	1	MSDial	<0.01	967.1	PC 35:3; [M+H]+; PC(15:0/20:3(5Z,8Z,11Z))
7.13	745.6214	1	MSDial	<0.01	970.0	SM 39:1; [M]+; SM(d14:1(4E)/25:0)
7.14	677.5577	1	custom-SM+Hpos	0.0020	933.0	SM 32:2; [M]+; SM(d14:1(4E)/18:1(9Z))
7.23	796.6221	1	MSDial	<0.01	973.2	plasmenyl-PC 38:6; [M+H]+; PC(P-16:0/22:6(4Z,7Z,10Z,13Z,16Z,19Z))
7.33	838.6324	1	MSDial	<0.01	968.5	PC 40:6; [M+H]+; PC(16:5/24:1)
7.33	770.6062	1	MSDial	<0.01	971.7	plasmenyl-PC 38:1; [M+H]+; PC(P-16:0/22:1(13Z))
7.33	798.6288	1	MSDial	<0.01	960.3	plasmenyl-PC 38:4; [M+H]+; PC(P-16:0/22:4(7Z,10Z,13Z,16Z))
7.33	822.6375	1	MSDial	<0.01	970.3	plasmenyl-PC 40:6; [M+H]+; PC(P-18:0/22:6(4Z,7Z,10Z,13Z,16Z,19Z))
7.42	786.6016	1	MSDial	<0.01	972.1	PC 36:4; [M+H]+; PC(18:2(2E,4E)/18:2(2E,4E))
7.43	800.6165	1	MSDial	<0.01	958.6	PC 37:5; [M+H]+; PC(16:5/21:0)
7.43	746.6062	1	MSDial	<0.01	972.4	plasmenyl-PC 34:3; [M+H]+; PC(P-16:0/18:3(6Z,9Z,12Z))
7.43	848.6527	1	MSDial	<0.01	965.3	plasmenyl-PC 44:4; [M+H]+; PC(P-20:0/24:4(5Z,8Z,11Z,14Z))
7.48	715.5737	1	custom-SM+Hpos	0.0017	933.0	SM 36:2; [M]+; SM(d18:1(4E)/18:1(9Z))
7.59	756.5526	1	CustomPC+Hpos.msp	0.0017	672.0	PC 34:4; [M+H]+; GPCho(17:2(9Z,12Z)/17:2(9Z,12Z))
7.63	772.6215	1	MSDial	<0.01	970.6	plasmenyl-PC 36:4; [M+H]+; PC(P-16:0/20:4(5E,8E,11E,14E))
7.68	703.5723	1	custom-SM+Hpos	0.0031	933.0	SM 35:0; [M]+; SM(d15:0/20:0)
7.70	744.5544	1	MSDial	<0.01	986.3	PE 36:5; [M+H]+; PE(16:5/20:0)
7.73	762.6011	1	MSDial	<0.01	969.1	PC 34:2; [M+H]+; PC(16:0/18:2(6Z,9Z))
7.83	788.6171	1	MSDial	<0.01	973.1	PC 36:3; [M+H]+; PC(18:1(11E)/18:2(2E,4E))
7.83	810.5983	1	MSDial	<0.01	960.2	PC 38:5; [M+H]+; PC(18:1(11E)/20:4(5E,8E,11E,14E))
7.90	770.5673	1	CustomPC+Hpos.msp	0.0027	672.0	PC 35:5; [M+H]+; GPCho(13:0/22:5(4Z,7Z,10Z,13Z,16Z))
7.93	722.5105	1	LipidBlast-pos	0.0020	856.0	plasmenyl-PE 38:5; [M+H]+; PE(P-18:0/20:5(5Z,8Z,11Z,14Z,17Z))

8.01	814.6321	1	MSDial	<0.01	965.1	PC 38:3; [M+Na]+; PC(18:2(2E,4E)/20:1(11E))
8.04	812.6169	1	MSDial	<0.01	970.1	PC 38:4; [M+H]+; PC(18:0/20:4(5E,8E,11E,14E))
8.11	811.6694	1	MSDial	<0.01	973.5	SM 44:6; [M]+; SM(d20:2(4E,8E)/24:4(5Z,8Z,11Z,14Z))
8.21	833.6506	1	MSDial	<0.01	955.5	TG 44:2; [M+NH4]+; TG(12:0/14:1/18:1)
8.32	774.6022	1	MSDial	<0.01	970.0	PC 35:4; [M+H]+; PC(11:0/24:4(5Z,8Z,11Z,14Z))
8.36	820.5838	1	CustomPC+Hpos.msp	0.0018	672.0	PC 40:2; [M+H]+; GPCho(20:1(11E)/20:1(11E))
8.47	691.5737	1	custom-SM+Hpos	0.0016	933.0	SM 33:2; [M]+; SM(d15:1(4E)/18:1(9Z))
8.57	758.5684	1	CustomPC+Hpos.msp	0.0015	743.0	PC 34:3; [M+H]+; GPCho(16:1(7Z)/18:2(2E,4E))
8.70	729.5906	1	custom-SM+Hpos	0.0004	939.0	SM 38:1; [M]+; SM(d14:0/24:1(15Z))
8.71	773.6537	1	MSDial	<0.01	973.0	SM 42:3; [M]+; SM(d16:2(4E,6E)/26:1(17Z))
8.81	824.6530	1	MSDial	<0.01	970.2	plasmenyl-PC 40:5; [M+H]+; PC(P-20:0/20:5(5Z,8Z,11Z,14Z,17Z))
8.81	850.6688	1	MSDial	<0.01	971.0	plasmenyl-PC 44:2; [M+H]+; PC(P-18:0/26:2(5E,9Z))
8.84	748.5278	1	LipidBlast-pos	0.0003	854.0	plasmenyl-PE 40:6; [M+H]+; PE(P-18:0/22:6(4Z,7Z,10Z,13Z,16Z,19Z))
8.95	766.5372	1	LipidBlast-pos	0.0015	997.0	plasmenyl-PC 18:0; [M+Na]+; PC(P-16:0/2:0)
9.09	780.5504	1	CustomPC+Hpos.msp	0.0039	756.0	PC 37:2; [M+H]+; GPCho(11:0/26:2(5E,9Z))
9.20	704.5612	1	MSDial	<0.01	786.8	plasmenyl-PE 37:2; [M+H]+; PE(P-20:0/17:2(9Z,12Z))
9.21	826.6696	1	MSDial	<0.01	942.2	plasmenyl-PC 40:5; [M+H]+; PC(P-18:0/22:5(7Z,10Z,13Z,16Z,19Z))
9.34	758.6072	1	MSDial	<0.01	950.4	plasmenyl-PC 36:1; [M+H]+; PC(P-16:0/20:1(11E))
9.47	717.5900	1	custom-SM+Hpos	0.0010	933.0	SM 36:1; [M]+; SM(d14:1(4E)/22:0)
9.54	566.5514	1	MSDial	<0.01	873.6	Cer 40:1; [M+H]+; Cer(d18:1(4E)/22:0)
9.67	742.5372	1	LipidBlast-pos	0.0015	997.0	PE 38:4; [M+H]+; GPEtn(18:0/20:4(5E,8E,11E,14E))
9.67	835.6665	1	MSDial	<0.01	985.1	TG 44:1; [M+NH4]+; TG(14:0/16:1/14:0)
9.81	810.6006	1	CustomPC+Hpos.msp	0.0007	698.0	PC 38:5; [M+H]+; GPCho(14:1(9Z)/24:4(5Z,8Z,11Z,14Z))
9.83	724.5276	1	LipidBlast-pos	0.0005	898.0	plasmenyl-PE 38:4; [M+H]+; PE(P-18:0/20:4(5E,8E,11E,14E))

9.84	746.5695	1	CustomPC+Hpos.msp	0.0004	672.0	PC 33:5; [M+H]+; GPCho(11:0/22:5(4Z,7Z,10Z,13Z,16Z))
9.87	822.5999	1	CustomPC+Hpos.msp	0.0013	672.0	PC 40:10; [M+H]+; GPCho(20:5(5Z,8Z,11Z,14Z,17Z)/20:5(5Z,8Z,11Z,14Z,17Z))
9.95	849.6810	1	MSDial	<0.01	835.5	TG 48:4; [M+NH4]+; TG(16:0/16:2/16:2)
10.00	772.5845	1	CustomPC+Hpos.msp	0.0012	694.0	PC 35:4; [M+H]+; GPCho(11:0/24:4(5Z,8Z,11Z,14Z))
10.08	731.6047	1	custom-SM+Hpos	0.0020	933.0	SM 38:0; [M]+; SM(d14:0/24:0)
10.26	878.7000	1	MSDial	<0.01	971.0	plasmenyl-PE 36:3; [M+H]+; PE(P-16:0/20:3(8Z,11Z,14Z))
10.30	746.5710	1	MSDial	<0.01	987.2	PE 36:4; [M+H]+; PE(16:2/20:2)
10.40	784.5844	1	CustomPC+Hpos.msp	0.0012	672.0	PC 36:4; [M+H]+; GPCho(18:2(2E,4E)/18:2(2E,4E))
10.62	640.5865	1	MSDial	<0.01	997.0	DG 40:8; [M+NH4]+; DG(22:6/18:2/0:0)
10.63	700.5268	1	LipidBlast-pos	0.0013	857.0	plasmenyl-PE 36:4; [M+H]+; PE(P-16:0/20:4(5E,8E,11E,14E))
10.66	750.5424	1	LipidBlast-pos	0.0014	897.0	plasmenyl-PE 40:4; [M+H]+; PE(P-20:0/20:4(5E,8E,11E,14E))
10.82	622.6133	1	MSDial	<0.01	926.2	Cer 42:1; [M+H]+; Cer(d18:1(4E)/24:0)
10.82	648.6287	1	MSDial	<0.01	936.2	DG 32:0; [M+NH4]+; DG(16:0/16:0/0:0)
10.92	837.6822	1	MSDial	<0.01	996.1	SM 45:5; [M]+; SM(d21:1(4E)/24:4(5Z,8Z,11Z,14Z))
10.93	810.5997	1	CustomPC+Hpos.msp	0.0016	706.0	PC 38:4; [M+Na]+; GPCho(18:0/20:4(5E,8E,11E,14E))
10.99	832.5807	1	LipidBlast-pos	0.0025	833.0	PC 38:5; [M+H]+; GPCho(18:0/20:5(5Z,8Z,11Z,14Z,17Z))
11.24	719.6039	1	custom-SM+Hpos	0.0027	933.0	SM 36:0; [M]+; SM(d14:0/22:0)
11.29	786.5995	1	CustomPC+Hpos.msp	0.0017	752.0	PC 36:3; [M+H]+; GPCho(18:1(11E)/18:2(2E,4E))
11.39	624.5581	1	MSDial	<0.01	970.1	DG 40:1; [M+NH4]+; DG(14:0/26:1/0:0)
11.41	768.5532	1	LipidBlast-pos	0.0012	992.0	PE 40:7; [M+H]+; GPEtn(18:1(11E)/22:6(4Z,7Z,10Z,13Z,16Z,19Z))
11.43	757.6214	1	custom-SM+Hpos	0.0010	933.0	SM 39:1; [M]+; SM(d15:0/24:1(15Z))
11.48	608.5248	1	LipidBlast-pos	0.0003	994.0	DG 36:0; [M+NH4]+; DG(18:0/18:0/0:0)
11.51	753.5868	1	custom-SM+Hpos	0.0043	946.0	SM 39:2; [M]+; SM(d15:1(4E)/24:1(15Z))

11.51	636.6290	1	MSDial	<0.01	892.6	Cer 43:1; [M+H]+; Cer(d19:1(4E)/24:0)
11.57	718.5369	1	LipidBlast-pos	0.0018	997.0	PE 36:2; [M+H]+; GPEtn(10:0/26:2(5E,9Z))
11.60	776.5572	1	LipidBlast-pos	0.0022	860.0	SM 32:0; [M]+; SM(d14:0/18:0)
11.63	634.5396	1	LipidBlast-pos	0.0012	964.0	DG 38:6; [M+NH4]+; DG(18:2/20:4/0:0)
11.67	848.6145	1	CustomPC+Hpos.msp	0.0024	672.0	PC 42:5; [M+H]+; GPCho(18:1(11E)/24:4(5Z,8Z,11Z,14Z))
11.74	810.5986	1	CustomPC+Hpos.msp	0.0026	688.0	PC 38:5; [M+H]+; GPCho(16:0/22:5(4Z,7Z,10Z,13Z,16Z))
11.92	809.6519	1	custom-SM+Hpos	0.0017	942.0	SM 43:2; [M]+; SM(d17:1(4E)/26:1(17Z))
12.05	650.6450	1	MSDial	<0.01	963.8	Cer 43:2; [M+H]+; Cer(d19:1(4E)/24:1(15Z))
12.15	846.6351	1	LipidBlast-pos	0.0001	958.0	plasmenyl-PE 34:2; [M+H]+; PE(P-16:0/18:2(2E,4E))
12.30	744.5527	1	LipidBlast-pos	0.0017	998.0	PE 36:4; [M+H]+; GPEtn(12:0/24:4(5Z,8Z,11Z,14Z))
12.34	664.6601	1	MSDial	<0.01	970.8	DG 32:2; [M+NH4]+; DG(14:1/18:1/0:0)
12.65	752.5580	1	LipidBlast-pos	0.0013	885.0	plasmenyl-PE 40:4; [M+H]+; PE(P-18:0/22:4(7Z,10Z,13Z,16Z))
12.67	733.6207	1	custom-SM+Hpos	0.0017	933.0	SM 37:1; [M]+; SM(d15:1(4E)/22:0)
12.83	774.6391	1	MSDial	<0.01	971.3	plasmenyl-PC 36:3; [M+H]+; PC(P-16:0/20:3(5Z,8Z,11Z))
12.83	796.6207	1	MSDial	<0.01	971.8	plasmenyl-PC 38:5; [M+H]+; PC(P-16:0/22:5(4Z,7Z,10Z,13Z,16Z))
12.89	882.7344	1	MSDial	<0.01	748.3	plasmenyl-PE 34:0; [M+H]+; PE(P-18:0/16:0)
12.90	586.5416	1	MSDial	<0.01	871.5	DG 36:1; [M+NH4]+; DG(18:1/18:0/0:0)
12.96	767.6017	1	custom-SM+Hpos	0.0050	948.0	SM 40:2; [M]+; SM(d14:1(4E)/26:1(17Z))
13.03	745.6211	1	custom-SM+Hpos	0.0013	933.0	SM 38:2; [M]+; SM(d14:1(4E)/24:1(15Z))
13.03	942.7543	1	MSDial	<0.01	695.4	TG 58:9; [M+NH4]+; TG(16:1/20:2/22:6)
13.07	702.5428	1	LipidBlast-pos	0.0010	814.0	plasmenyl-PE 36:2; [M+H]+; PE(P-18:0/18:2(2E,4E))
13.14	764.6760	1	MSDial	<0.01	851.0	TG 50:12; [M+NH4]+; TG(16:2/16:5/18:5)
13.29	816.7086	1	MSDial	<0.01	895.2	TG 50:3; [M+NH4]+; TG(16:0/16:1/18:2)
13.29	728.5576	1	LipidBlast-pos	0.0018	771.0	plasmenyl-PE 38:3; [M+H]+; PE(P-18:0/20:3(5Z,8Z,11Z))

13.31	660.5552	1	LipidBlast-pos	0.0012	710.0	lysoPC 14:0; [M+H]+; PC(14:0/0:0)
13.48	842.7231	1	MSDial	<0.01	919.6	TG 52:6; [M+NH4]+; TG(16:2/18:1/18:3)
13.48	918.7549	1	MSDial	<0.01	845.9	TG 58:6; [M+NH4]+; TG(18:1/18:1/22:4)
13.54	868.7389	1	MSDial	<0.01	743.5	TG 53:3; [M+NH4]+; TG(16:2/18:0/19:1)
13.54	944.7703	1	MSDial	<0.01	941.9	TG 58:8; [M+NH4]+; TG(18:1/18:1/22:6)
13.60	584.5241	1	LipidBlast-pos	0.0010	947.0	DG 32:1; [M+NH4]+; DG(14:0/18:1/0:0)
13.65	800.6556	1	MSDial	<0.01	950.4	plasmenyl-PC 38:3; [M+H]+; PC(P-20:0/18:3(9Z,12Z,15Z))
13.65	826.6699	1	MSDial	<0.01	966.1	plasmenyl-PC 40:4; [M+H]+; PC(P-16:0/24:4(5Z,8Z,11Z,14Z))
13.67	864.6459	1	CustomPC+Hpos.msp	0.0023	672.0	PC 42:9; [M+H]+; GPCho(20:3(5Z,8Z,11Z)/22:6(4Z,7Z,10Z,13Z,16Z,19Z))
13.73	610.5400	1	LipidBlast-pos	0.0007	885.0	DG 34:2; [M+NH4]+; DG(16:1/18:1/0:0)
13.83	862.7852	1	MSDial	<0.01	692.2	TG 53:12; [M+NH4]+; TG(16:3/16:4/21:5)
13.90	762.6003	1	CustomPC+Hpos.msp	0.0010	743.0	PC 34:2; [M+H]+; GPCho(17:1(9Z)/17:1(9Z))
13.99	636.5552	1	LipidBlast-pos	0.0012	991.0	DG 38:5; [M+NH4]+; DG(18:1/20:4/0:0)
14.06	759.6356	1	custom-SM+Hpos	0.0024	933.0	SM 39:0; [M]+; SM(d15:0/24:0)
14.06	775.6702	1	MSDial	<0.01	966.2	SM 41:0; [M]+; SM(d15:0/26:0)
14.11	785.6523	1	custom-SM+Hpos	0.0013	935.0	SM 41:2; [M]+; SM(d15:1(4E)/26:1(17Z))
14.13	754.5730	1	LipidBlast-pos	0.0021	837.0	plasmenyl-PE 38:6; [M+H]+; PE(P-16:0/22:6(4Z,7Z,10Z,13Z,16Z,19Z))
14.24	922.7861	1	MSDial	<0.01	999.4	TG 58:11; [M+NH4]+; TG(18:3/20:4/20:4)
14.26	814.6309	1	CustomPC+Hpos.msp	0.0017	692.0	PC 38:4; [M+H]+; GPCho(14:0/24:4(5Z,8Z,11Z,14Z))
14.28	781.6184	1	custom-SM+Hpos	0.0040	942.0	SM 41:4; [M]+; SM(d17:0/24:4(5Z,8Z,11Z,14Z))
14.45	846.7553	1	MSDial	<0.01	999.4	TG 51:2; [M+NH4]+; TG(17:0/17:0/17:2)
14.46	746.5684	1	LipidBlast-pos	0.0015	997.0	PE 36:3; [M+H]+; GPEtn(14:1(9Z)/22:2(13Z,16Z))
14.55	948.8018	1	MSDial	<0.01	996.2	TG 60:12; [M+NH4]+; TG(16:0/22:6/22:6)

14.75	912.8013	1	MSDial	<0.01	689.9	TG 56:4; [M+NH4]+; TG(18:1/18:1/20:2)
14.85	840.6451	1	CustomPC+Hpos.msp	0.0031	672.0	PC 40:5; [M+H]+; GPCho(18:0/22:5(4Z,7Z,10Z,13Z,16Z))
14.86	918.8492	1	MSDial	<0.01	995.5	TG 55:5; [M+NH4]+; TG(17:1/18:1/20:3)
14.88	780.5884	1	LipidBlast-pos	0.0023	823.0	SM 30:1; [M]+; SM(d14:1(4E)/16:0)
14.99	776.6156	1	CustomPC+Hpos.msp	0.0014	672.0	PC 35:2; [M+H]+; GPCho(9:0/26:2(5E,9Z))
15.29	773.6528	1	custom-SM+Hpos	0.0009	933.0	SM 40:0; [M]+; SM(d14:0/26:0)
15.37	928.8328	1	MSDial	<0.01	990.2	TG 56:9; [M+NH4]+; TG(16:1/18:2/22:6)
15.53	787.6680	1	custom-SM+Hpos	0.0013	933.0	SM 41:1; [M]+; SM(d15:0/26:1(17Z))
15.54	761.6526	1	custom-SM+Hpos	0.0010	933.0	SM 38:4; [M]+; SM(d14:0/24:4(5Z,8Z,11Z,14Z))
15.55	780.5900	1	LipidBlast-pos	0.0007	856.0	SM 31:1; [M]+; SM(d15:1(4E)/16:0)
15.69	795.6342	1	custom-SM+Hpos	0.0038	917.0	SM 42:2; [M]+; SM(d16:1(4E)/26:1(17Z))
15.78	904.8333	1	MSDial	<0.01	998.2	TG 55:3; [M+NH4]+; TG(16:2/19:1/20:0)
15.84	608.5997	1	MSDial	<0.01	902.8	Cer 41:1; [M+H]+; Cer(d17:1(4E)/24:0)
15.88	730.5735	1	LipidBlast-pos	0.0015	817.0	plasmenyl-PE 36:5; [M+H]+; PE(P-16:0/20:5(5Z,8Z,11Z,14Z,17Z))
15.92	813.6827	1	custom-SM+Hpos	0.0022	933.0	SM 42:5; [M]+; SM(d18:1(4E)/24:4(5Z,8Z,11Z,14Z))
16.12	612.5562	1	LipidBlast-pos	0.0002	943.0	DG 34:2; [M+NH4]+; DG(16:0/18:2/0:0)
16.14	788.6152	1	CustomPC+Hpos.msp	0.0018	672.0	PC 36:2; [M+H]+; GPCho(18:1(11E)/18:1(11E))
16.39	638.5718	1	LipidBlast-pos	0.0002	879.0	DG 36:4; [M+NH4]+; DG(18:2/18:2/0:0)
17.03	775.6671	1	custom-SM+Hpos	0.0023	933.0	SM 39:4; [M]+; SM(d15:0/24:4(5Z,8Z,11Z,14Z))
17.21	771.6370	1	custom-SM+Hpos	0.0010	933.0	SM 40:1; [M]+; SM(d14:0/26:1(17Z))
17.47	842.6606	1	CustomPC+Hpos.msp	0.0032	743.0	PC 40:5; [M+H]+; GPCho(16:1(7Z)/24:4(5Z,8Z,11Z,14Z))
17.63	854.7019	1	MSDial	<0.01	950.4	plasmenyl-PC 42:6; [M+H]+; PC(P-20:0/22:6(4Z,7Z,10Z,13Z,16Z,19Z))
17.74	827.6991	1	custom-SM+Hpos	0.0015	933.0	SM 43:5; [M]+; SM(d19:1(4E)/24:4(5Z,8Z,11Z,14Z))
17.76	622.6149	1	MSDial	<0.01	902.8	Cer 41:1; [M+H]+; Cer(d18:1(4E)/23:0)

17.89	801.6837	1	custom-SM+Hpos	0.0013	945.0	SM 42:1; [M]+; SM(d16:0/26:1(17Z))
17.98	823.6638	1	custom-SM+Hpos	0.0055	930.0	TG 40:0; [M+NH4]+; TG(12:0/12:0/16:0)
18.04	803.7013	1	MSDial	<0.01	950.5	SM 44:5; [M]+; SM(d20:1(4E)/24:4(5Z,8Z,11Z,14Z))
18.27	789.6827	1	custom-SM+Hpos	0.0023	933.0	SM 40:4; [M]+; SM(d16:0/24:4(5Z,8Z,11Z,14Z))
18.42	900.6794	1	LipidBlast-pos	0.0028	729.0	plasmenyl-PE 36:1; [M+H]+; PE(P-18:0/18:1(11E))
18.86	662.6466	1	MSDial	<0.01	796.9	DG 35:2; [M+NH4]+; DG(17:1/18:1/0:0)
19.05	640.5859	1	LipidBlast-pos	0.0017	955.0	DG 36:3; [M+NH4]+; DG(18:1/18:2/0:0)
19.29	648.6284	1	Cer-d-Hpos	0.0012	999.0	N-(tetracosanoyl)-sphinganine; [M+H]+; Cer(d18:0/24:0)
19.41	622.6127	1	Cer-d-Hpos	0.0013	999.0	PC 25:1; [M+H]+; GPCho(3:0/22:1(13Z))
19.48	636.6301	1	MSDial	<0.01	913.5	Cer 42:2; [M+H]+; Cer(d18:1(4E)/24:1(15Z))
19.49	841.7146	1	custom-SM+Hpos	0.0017	933.0	TG 42:1; [M+NH4]+; TG(12:0/12:0/18:1)
20.23	829.7148	1	custom-SM+Hpos	0.0015	933.0	SM 43:4; [M]+; SM(d19:0/24:4(5Z,8Z,11Z,14Z))
20.92	642.6024	1	LipidBlast-pos	0.0009	905.0	DG 36:2; [M+NH4]+; DG(18:1/18:1/0:0)
21.21	650.6440	1	Cer-d-Hpos	0.0012	999.0	PC 30:1; [M+H]+; GPCho(4:0/26:1(5Z))
22.23	652.6603	1	Cer-d-Hpos	0.0005	953.0	PC 31:0; [M+H]+; GPCho(8:0/23:0)
22.98	866.7238	1	LipidBlast-pos	-0.0004	907.0	TG 53:2; [M+NH4]+; TG(17:0/18:1/18:1)
23.02	892.7374	1	LipidBlast-pos	0.0016	922.0	TG 55:3; [M+NH4]+; TG(18:1/18:2/19:0)
23.15	712.6448	1	LipidBlast-pos	0.0004	952.0	TG 44:1; [M+NH4]+; TG(12:0/16:1/16:0)
23.24	738.6596	1	LipidBlast-pos	0.0012	953.0	TG 46:0; [M+NH4]+; TG(14:0/16:0/16:0)
23.32	764.6752	1	LipidBlast-pos	0.0012	918.0	TG 46:2; [M+NH4]+; TG(12:0/18:1/16:1)
23.33	942.7538	1	LipidBlast-pos	0.0008	781.0	TG 58:4; [M+NH4]+; TG(18:1/18:2/22:1)
23.35	790.6918	1	LipidBlast-pos	0.0003	945.0	TG 48:2; [M+NH4]+; TG(14:0/16:1/18:1)
23.59	918.7545	1	LipidBlast-pos	0.0001	877.0	TG 58:10; [M+NH4]+; TG(18:2/20:4/20:4)

23.68	842.7219	1	LipidBlast-pos	0.0014	993.0	TG 51:1; [M+NH4]+; TG(17:0/17:0/17:1)
23.70	968.7703	1	LipidBlast-pos	0.0000	751.0	Cer 34:1; [M+H]+; Cer(d18:1(4E)/16:0)
23.75	892.7383	1	LipidBlast-pos	0.0006	674.0	TG 55:2; [M+NH4]+; TG(18:0/18:2/19:0)
23.78	868.7372	1	LipidBlast-pos	0.0017	995.0	TG 53:1; [M+NH4]+; TG(17:0/18:0/18:1)
23.91	894.7538	1	LipidBlast-pos	0.0008	991.0	TG 55:2; [M+NH4]+; TG(16:1/18:1/21:0)
23.94	944.7693	1	LipidBlast-pos	0.0009	978.0	TG 58:2; [M+NH4]+; TG(18:1/18:1/22:0)
24.09	994.7852	1	LipidBlast-pos	0.0007	674.0	Cer 39:1; [M+H]+; Cer(d16:1(4E)/23:0)
24.37	766.6913	1	LipidBlast-pos	0.0007	961.0	TG 46:1; [M+NH4]+; TG(14:0/16:0/16:1)
24.42	740.6760	1	LipidBlast-pos	0.0004	959.0	TG 44:2; [M+NH4]+; TG(12:0/16:1/16:1)
24.43	920.7697	1	LipidBlast-pos	0.0006	978.0	TG 57:8; [M+NH4]+; TG(17:0/18:2/22:6)
24.44	792.7065	1	LipidBlast-pos	0.0012	984.0	TG 48:1; [M+NH4]+; TG(14:0/16:0/18:1)
24.54	818.7233	1	LipidBlast-pos	0.0001	977.0	TG 49:2; [M+NH4]+; TG(16:0/16:1/17:1)
24.58	844.7386	1	LipidBlast-pos	0.0004	999.0	TG 51:1; [M+NH4]+; TG(16:0/17:0/18:1)
24.65	970.7847	1	LipidBlast-pos	0.0012	674.0	TG 62:13; [M+NH4]+; TG(18:1/22:6/22:6)
24.89	968.7702	1	MSDial	<0.01	692.2	TG 60:7; [M+NH4]+; TG(18:0/20:3/22:4)
24.92	688.6028	1	CE+NH4pos	0.0004	849.0	20:5 Cholesteryl ester; [M+NH4]+
24.93	870.7542	1	LipidBlast-pos	0.0005	992.0	TG 52:6; [M+NH4]+; TG(16:1/18:2/18:3)
24.94	896.7696	1	LipidBlast-pos	0.0007	995.0	TG 54:7; [M+NH4]+; TG(18:2/18:2/18:3)
24.96	946.7849	1	LipidBlast-pos	0.0010	994.0	TG 60:12; [M+NH4]+; TG(18:1/20:5/22:6)
25.13	832.7377	1	LipidBlast-pos	0.0012	984.0	TG 50:2; [M+NH4]+; TG(16:0/16:1/18:1)
25.17	922.7836	1	LipidBlast-pos	0.0023	991.0	TG 56:9; [M+NH4]+; TG(16:0/18:3/22:6)
25.18	858.7529	1	LipidBlast-pos	0.0017	886.0	TG 52:1; [M+NH4]+; TG(16:0/18:0/18:1)
25.24	766.6926	1	MSDial	<0.01	704.2	TG 49:1; [M+NH4]+; TG(16:0/16:1/17:0)
25.29	714.6184	1	CE+NH4pos	0.0005	846.0	22:6 Cholesteryl ester; [M+NH4]+

25.34	884.7691	1	LipidBlast-pos	0.0011	999.0	TG 54:2; [M+NH4]+; TG(16:0/18:0/20:2)
25.45	794.7219	1	LipidBlast-pos	0.0015	979.0	TG 48:0; [M+NH4]+; TG(16:0/16:0/16:0)
25.48	820.7385	1	LipidBlast-pos	0.0004	980.0	TG 49:1; [M+NH4]+; TG(16:0/16:0/17:1)
25.50	846.7538	1	LipidBlast-pos	0.0008	994.0	TG 51:0; [M+NH4]+; TG(16:0/17:0/18:0)
25.51	664.6023	1	CE+NH4pos	0.0010	894.0	18:3 Cholesteryl ester; [M+NH4]+
25.67	878.8151	1	LipidBlast-pos	0.0021	687.0	TG 52:4; [M+NH4]+; TG(16:0/18:1/18:3)
25.69	898.7853	1	LipidBlast-pos	0.0006	998.0	TG 54:7; [M+NH4]+; TG(16:0/16:1/22:6)
25.78	896.7709	1	MSDial	<0.01	999.2	TG 55:4; [M+NH4]+; TG(16:2/19:2/20:0)
25.78	890.8149	1	LipidBlast-pos	0.0023	790.0	TG 53:4; [M+NH4]+; TG(17:1/18:1/18:2)
25.83	690.6177	1	CE+NH4pos	0.0012	860.0	20:4 Cholesteryl ester; [M+NH4]+
25.87	872.7701	1	LipidBlast-pos	0.0001	997.0	TG 52:5; [M+NH4]+; TG(16:1/18:2/18:2)
25.95	834.7538	1	LipidBlast-pos	0.0008	993.0	TG 50:1; [M+NH4]+; TG(16:0/16:0/18:1)
26.03	716.6331	1	CE+NH4pos	0.0014	850.0	22:5 Cholesteryl ester; [M+NH4]+
26.03	860.7690	1	LipidBlast-pos	0.0013	974.0	TG 52:0; [M+NH4]+; TG(16:0/18:0/18:0)
26.11	924.8009	1	LipidBlast-pos	0.0006	998.0	TG 56:7; [M+NH4]+; TG(18:1/18:2/20:4)
26.12	886.7852	1	LipidBlast-pos	0.0007	997.0	TG 54:1; [M+NH4]+; TG(18:0/18:0/18:1)
26.12	922.7858	1	MSDial	<0.01	849.6	TG 58:10; [M+NH4]+; TG(18:2/18:2/22:6)
26.17	904.8315	1	LipidBlast-pos	0.0013	739.0	TG 54:3; [M+NH4]+; TG(18:1/18:1/18:1)
26.18	950.8156	1	LipidBlast-pos	0.0016	999.0	TG 58:9; [M+NH4]+; TG(18:1/20:4/20:4)
26.34	822.7543	1	LipidBlast-pos	0.0003	977.0	TG 49:0; [M+NH4]+; TG(16:0/16:0/17:0)
26.36	848.7681	1	LipidBlast-pos	0.0021	977.0	TG 50:5; [M+NH4]+; TG(16:1/16:1/18:3)
26.37	912.8003	1	LipidBlast-pos	0.0012	768.0	TG 55:6; [M+NH4]+; TG(17:2/18:0/20:4)
26.38	796.7381	1	LipidBlast-pos	0.0009	930.0	TG 46:3; [M+NH4]+; TG(14:1/16:1/16:1)

26.45	874.7862	1	LipidBlast-pos	-0.0003	968.0	TG 52:5; [M+NH4]+; TG(16:0/18:2/18:3)
26.47	910.7849	1	MSDial	<0.01	821.5	TG 56:7; [M+NH4]+; TG(16:0/18:1/22:6)
26.48	666.6187	1	CE+NH4pos	0.0002	880.0	18:2 Cholesteryl ester; [M+NH4]+
26.49	900.8011	1	LipidBlast-pos	0.0004	994.0	TG 54:6; [M+NH4]+; TG(18:1/18:2/18:3)
26.51	640.6028	1	CE+NH4pos	0.0004	869.0	16:1 Cholesteryl ester; [M+NH4]+
26.62	906.8468	1	LipidBlast-pos	0.0016	747.0	TG 54:3; [M+NH4]+; TG(18:0/18:1/18:2)
26.68	692.6336	1	CE+NH4pos	0.0009	877.0	20:3 Cholesteryl ester; [M+NH4]+
26.88	862.7858	1	LipidBlast-pos	0.0001	935.0	TG 51:4; [M+NH4]+; TG(16:1/17:1/18:2)
26.88	888.8012	1	LipidBlast-pos	0.0003	978.0	TG 54:1; [M+NH4]+; TG(16:0/18:0/20:1)
26.89	926.8168	1	LipidBlast-pos	0.0003	998.0	TG 56:6; [M+NH4]+; TG(16:0/18:1/22:5)
26.98	952.8319	1	LipidBlast-pos	0.0009	972.0	TG 58:7; [M+NH4]+; TG(18:1/18:1/22:5)
27.00	906.8472	1	LipidBlast-pos	0.0012	728.0	TG 54:2; [M+NH4]+; TG(18:0/18:0/18:2)
27.02	718.6498	1	CE+NH4pos	0.0004	652.0	22:4 Cholesteryl ester; [M+NH4]+
27.13	654.6183	1	CE+NH4pos	0.0006	809.0	17:1 Cholesteryl ester; [M+NH4]+
27.14	914.8162	1	LipidBlast-pos	0.0009	929.0	TG 55:6; [M+NH4]+; TG(16:0/17:0/22:6)
27.23	876.8013	1	LipidBlast-pos	0.0002	991.0	TG 52:4; [M+NH4]+; TG(16:0/18:2/18:2)
27.23	850.7855	1	LipidBlast-pos	0.0004	990.0	TG 50:4; [M+NH4]+; TG(16:1/16:1/18:2)
27.24	902.8165	1	LipidBlast-pos	0.0007	989.0	TG 54:6; [M+NH4]+; TG(16:0/18:1/20:5)
27.28	836.7701	1	MSDial	<0.01	849.5	TG 50:5; [M+NH4]+; TG(16:1/16:2/18:2)
27.28	824.7691	1	LipidBlast-pos	0.0011	913.0	TG 48:3; [M+NH4]+; TG(14:1/16:1/18:1)
27.35	888.8016	1	MSDial	<0.01	998.2	TG 55:2; [M+NH4]+; TG(18:1/18:1/19:0)
27.57	694.6484	1	CE+NH4pos	0.0018	790.0	20:2 Cholesteryl ester; [M+NH4]+
27.58	668.6326	1	CE+NH4pos	0.0019	887.0	18:1 Cholesteryl ester; [M+NH4]+

27.68	864.8008	1	LipidBlast-pos	0.0007	966.0	TG 51:2; [M+NH4]+; TG(17:0/17:1/17:1)
27.76	838.7845	1	LipidBlast-pos	0.0013	950.0	TG 49:3; [M+NH4]+; TG(16:1/16:1/17:1)
27.87	916.8316	1	LipidBlast-pos	0.0012	903.0	TG 55:5; [M+NH4]+; TG(17:0/18:1/20:4)
27.88	928.8320	1	LipidBlast-pos	0.0008	987.0	TG 56:5; [M+NH4]+; TG(16:0/18:1/22:4)
27.98	954.8469	1	LipidBlast-pos	0.0016	735.0	TG 58:7; [M+NH4]+; TG(18:0/18:2/22:5)
28.08	930.8469	1	LipidBlast-pos	0.0015	981.0	TG 56:4; [M+NH4]+; TG(18:0/18:1/20:3)
28.11	852.7997	1	LipidBlast-pos	0.0018	949.0	TG 50:3; [M+NH4]+; TG(16:1/16:1/18:1)
28.28	956.8618	1	LipidBlast-pos	0.0023	909.0	TG 58:6; [M+NH4]+; TG(18:3/18:3/22:0)
28.48	866.8160	1	LipidBlast-pos	0.0012	967.0	TG 51:2; [M+NH4]+; TG(16:0/17:1/18:1)
28.69	696.6646	1	CE+NH4pos	0.0013	652.0	20:1 Cholesteryl ester; [M+NH4]+
28.76	932.8627	1	LipidBlast-pos	0.0014	948.0	TG 56:3; [M+NH4]+; TG(18:0/18:2/20:1)
28.91	958.8788	1	LipidBlast-pos	0.0009	961.0	TG 58:6; [M+NH4]+; TG(18:0/18:1/22:5)
28.92	880.8314	1	LipidBlast-pos	0.0014	952.0	TG 52:3; [M+NH4]+; TG(16:0/18:1/18:2)
29.37	960.8940	1	LipidBlast-pos	0.0014	937.0	TG 58:5; [M+NH4]+; TG(18:0/20:1/20:4)
29.38	934.8785	1	LipidBlast-pos	0.0013	963.0	TG 56:2; [M+NH4]+; TG(18:0/18:0/20:2)

Appendix Table A3.2 Cholesterol species identified by matching and manual interpretation using 369.352 m/z.

RT (min)	Precursor m/z	Rank	Library	Delta (m/z)	Rev-Dot	Lipid
4.76	369.3520		Manual Interpretation			Cholestreol
20.90	672.6299		Manual Interpretation			Cholestreol Species
22.20	646.6539		Manual Interpretation			Cholestreol Species
24.50	994.7898		Manual Interpretation			Cholestreol Species
24.92	688.6028	1	CE+NH4pos	0.0004	849	20:5 Cholesteryl ester; [M+NH4]+
25.00	679.7465		Manual Interpretation			Cholestreol Species
25.00	662.5892		Manual Interpretation			Cholestreol Species
25.29	714.6184	1	CE+NH4pos	0.0005	846	22:6 Cholesteryl ester; [M+NH4]+
25.40	818.7259		Manual Interpretation			Cholestreol Species
25.50	683.6033		Manual Interpretation			Cholestreol Species
25.50	770.7081		Manual Interpretation			Cholestreol Species
25.51	664.6023	1	CE+NH4pos	0.0010	894	18:3 Cholesteryl ester; [M+NH4]+
25.83	690.6177	1	CE+NH4pos	0.0012	860	20:4 Cholesteryl ester; [M+NH4]+
26.03	716.6331	1	CE+NH4pos	0.0014	850	22:5 Cholesteryl ester; [M+NH4]+
26.10	948.8036		Manual Interpretation			Cholestreol Species
26.10	922.7888		Manual Interpretation			Cholestreol Species
26.48	666.6187	1	CE+NH4pos	0.0002	880	18:2 Cholesteryl ester; [M+NH4]+
26.50	1041.9384		Manual Interpretation			Cholestreol Species
26.51	640.6028	1	CE+NH4pos	0.0004	869	16:1 Cholesteryl ester; [M+NH4]+
26.68	692.6336	1	CE+NH4pos	0.0009	877	20:3 Cholesteryl ester; [M+NH4]+
26.80	991.9210		Manual Interpretation			Cholestreol Species

26.90	1017.9367		Manual Interpretation			Cholestreol Species
27.00	662.7199		Manual Interpretation	0.0022		CE(18:4)
27.00	892.8358		Manual Interpretation			Cholestreol Species
27.02	718.6498	1	CE+NH4pos	0.0004	652	22:4 Cholesteryl ester; [M+NH4]+
27.13	654.6183	1	CE+NH4pos	0.0006	809	17:1 Cholesteryl ester; [M+NH4]+
27.57	694.6484	1	CE+NH4pos	0.0018	790	20:2 Cholesteryl ester; [M+NH4]+
27.58	668.6326	1	CE+NH4pos	0.0019	887	18:1 Cholesteryl ester; [M+NH4]+
27.70	1019.9510		Manual Interpretation			Cholestreol Species
27.80	737.6974		Manual Interpretation			Cholestreol Species
27.80	663.4554		Manual Interpretation			Cholestreol Species
28.00	682.6492		Manual Interpretation			Cholestreol Species
28.40	670.6518		Manual Interpretation	0.0022		CE(18:0)
28.40	866.8200		Manual Interpretation			Cholestreol Species
28.69	696.6646	1	CE+NH4pos	0.0013	652	20:1 Cholesteryl ester; [M+NH4]+

Appendix Table A3.3 Lipids identified by accurate mass and MS/MS matching to Lipid Maps, HMDB, MyCompoundID, Lipid Blast and MS Dial libraries of the upregulated and down regulated features in Figure. 3.4A

				Bold = Definitive ID
RT(min)	**Mass (m/z)**	**FC**	**P-Value**	**Compound Name**
1.02	596.335	0.668	4.44E-04	FA(31:3(OH4,Ke2,Ep2,cyclo))
13.10	892.738	0.664	2.23E-02	**TG 55:3; [M+NH4]+; TG(18:1/18:2/19:0)**
3.16	792.493	0.663	7.20E-05	SQDG(31:3)
9.44	827.7	0.662	3.89E-06	**SM 43:5; [M]+; SM(d19:1(4E)/24:4(5Z,8Z,11Z,14Z))**
9.64	837.68	0.658	8.67E-08	PA(P-47:3)
2.57	610.467	0.652	2.02E-02	Stigmastanol
11.55	638.644	0.652	3.21E-09	Cer(d41:0)
1.08	548.336	0.646	2.92E-04	FA(27:0(OH4,Ke2,Ep2))
13.02	866.722	0.633	2.95E-02	PG(O-42:0)
10.37	841.715	0.631	1.55E-08	**TG 42:1; [M+NH4]+; TG(12:0/12:0/18:1)**
9.49	801.684	0.625	2.96E-07	**SM 42:1; [M]+; SM(d16:0/26:1(17Z))**
6.60	733.621	0.625	4.83E-09	**SM 37:1; [M]+; SM(d15:1(4E)/22:0)**
1.17	316.32	0.623	9.74E-04	FA(19:0)
1.05	572.335	0.611	1.34E-03	FA(29:1(OH4,Ke2,Ep2,cyclo))
11.90	699.595	0.605	3.86E-04	DG(42:5)
9.44	865.654	0.602	3.26E-07	3-O-Sulfogalactosylceramide (d18:1/22:0)
0.83	185.129	0.599	1.66E-08	HMDB61384
1.28	650.439	0.595	6.55E-07	LPG(27:3)
8.92	775.667	0.595	3.85E-10	CerP(d44:1)
10.89	829.715	0.574	2.84E-07	**SM 43:4; [M]+; SM(d19:0/24:4(5Z,8Z,11Z,14Z))**

8.16	787.668	0.568	8.13E-08	**SM 41:1; [M]+; SM(d15:0/26:1(17Z))**
9.63	815.699	0.563	7.13E-10	CerP(d47:2)
11.90	786.699	0.554	1.18E-05	DG(47:5)
8.18	761.652	0.549	2.46E-12	CerP(d43:1)
1.65	754.625	0.530	1.37E-03	DG(45:7)
10.38	803.698	0.520	3.15E-11	CerP(d46:1)
9.68	789.683	0.513	3.70E-12	**SM 40:4; [M]+; SM(d16:0/24:4(5Z,8Z,11Z,14Z))**
1.85	595.649	0.488	1.92E-02	No Match
1.04	288.29	0.485	1.34E-06	FA(17:0)
1.49	282.279	0.436	4.56E-02	HMDB37543
6.04	685.435	1.50	3.56E-06	LPI(24:0)
1.93	609.665	1.52	3.19E-03	#N/A
13.43	911.864	1.53	1.15E-02	WE(64:9)
1.95	784.672	1.53	4.67E-02	HexCer(d40:1)
0.99	294.206	1.53	2.46E-03	FA(17:3(Ep,cyclo))
3.67	884.605	1.54	6.60E-06	PG(18:0/22:5(4Z,7Z,10Z,13Z,16Z))
5.62	370.404	1.54	3.19E-04	Tetracosanoic acid
0.88	430.204	1.54	8.23E-03	FA(20:1(OH3,Ke2,Ep2,cyclo))
3.73	412.426	1.57	2.78E-03	#N/A
0.99	221.117	1.57	1.42E-03	FA(13:3(Ep,cyclo))
6.08	663.702	1.58	7.00E-05	WE(45:0)
3.91	864.621	1.59	9.17E-10	SHexCer(d40:1)
2.27	751.359	1.59	8.51E-06	#N/A
1.00	214.123	1.60	9.54E-07	HMDB59631

0.84	433.353	1.61	1.11E-04	FA(24:0(OH4))
1.98	684.428	1.61	1.32E-05	LPS(30:5)
1.70	392.376	1.62	4.78E-07	#N/A
1.29	591.245	1.62	3.08E-08	N-Acetyl-D-glucosayldiphosphodolichol
13.91	413.266	1.62	2.03E-09	FA(26:5(Ep2,cyclo))
1.03	228.138	1.66	2.78E-05	HMDB32561
1.32	298.217	1.70	1.11E-08	17a-Ethynylestradiol
6.04	1032.849	1.72	3.12E-05	TG(16:0/18:0/20:4(5Z,8Z,11Z,14Z))[iso6]
0.89	547.457	1.81	2.87E-04	WE(38:9)
1.69	764.667	1.82	9.22E-04	CerP(d18:1/24:0)
0.82	212.118	1.85	8.17E-03	HMDB15398
4.14	854.566	1.87	9.52E-07	**PC 42:9; [M+H]+; PC(22:5(4Z,7Z,10Z,13Z,16Z)/20:4(5E,8E,11E,14E))**
2.53	651.712	1.88	1.09E-03	#N/A
6.05	721.506	2.07	3.88E-06	PG(32:1)
0.90	561.473	2.88	1.46E-04	#N/A

Appendix Table A3.4 Lipids identified by accurate mass and MS/MS matching to Lipid Maps, HMDB, MyCompoundID, Lipid Blast and MS Dial libraries of the upregulated and down regulated features in Figure. 3.4B.

				Bold = Definitive ID
RT (min)	**M/Z**	**FC**	**P-Value**	**Name**
12.60	887.687	0.666	4.28E-02	PS(O-43:3)
7.90	848.652	0.665	1.43E-06	PC(O-42:6)
8.09	772.621	0.662	2.78E-03	CerP(t44:2)
1.08	548.336	0.662	2.52E-02	FA(27:0(OH4,Ke2,Ep2))
14.32	678.618	0.658	1.51E-02	WE(46:8)
4.04	790.574	0.656	7.47E-04	PC(P-38:6)
0.99	195.102	0.655	2.21E-02	FA(11:2(Ep,cyclo))
10.49	870.693	0.653	2.22E-03	PA(47:3)
4.37	778.573	0.651	2.29E-03	PA(P-42:6)
2.07	583.613	0.649	4.46E-03	Ceramide (d18:1/20:0)
2.06	385.416	0.645	9.63E-03	Docosanamide
13.58	925.724	0.635	4.64E-03	PI-Cer(d43:0)
0.89	520.349	0.628	1.12E-02	**lysoPC 20:4; [M+H]+; PC(20:4(5E,8E,11E,14E)/0:0)**
6.98	772.621	0.620	3.65E-06	CerP(t44:2)
3.89	740.558	0.619	3.26E-03	LPC(34:4)
12.72	942.753	0.611	2.36E-02	PG(O-48:4)
1.53	424.282	0.608	4.92E-03	S1P(t20:1)
2.55	878.568	0.597	4.43E-02	PI(36:3)
1.05	572.335	0.587	4.51E-03	FA(29:1(OH4,Ke2,Ep2,cyclo))
14.61	704.633	0.587	4.40E-02	WE(48:9)
2.75	639.675	0.581	6.08E-03	N-Lignoceroylsphingosine
5.46	726.542	0.566	6.91E-03	PA(O-38:5)
14.61	383.367	0.565	3.03E-02	#N/A
0.95	304.3	0.559	1.19E-02	5b-Pregnanediol
2.88	300.326	0.484	1.04E-02	HMDB01958
14.09	651.676	0.461	4.18E-03	Ceramide (d18:1/24:0)
15.16	707.738	0.404	2.25E-03	#N/A
10.15	645.542	1.50	7.51E-05	DG(14:0/18:0/0:0)
15.55	948.895	1.51	5.94E-04	HMDB47054
11.27	620.633	1.51	5.18E-05	DG(34:1)
8.66	612.556	1.51	1.70E-04	#N/A
9.98	645.542	1.51	1.53E-05	DG(14:0/18:0/0:0)
10.60	719.738	1.52	1.29E-04	PA(O-35:1)
15.32	836.769	1.52	3.56E-02	**SM 43:5; [M]+; SM(d19:1(4E)/24:4(5Z,8Z,11Z,14Z))**
6.08	663.702	1.52	6.72E-04	WE(42:1)

14.62	827.709	1.52	1.64E-04	TG(48:4)
8.47	612.556	1.52	6.04E-05	#N/A
15.00	967.843	1.52	2.28E-08	**TG 54:3; [M+NH4]+; TG(18:0/18:1/18:2)**
13.48	842.722	1.53	4.29E-02	TG(49:1)
13.94	612.571	1.53	7.38E-05	**DG 34:2; [M+NH4]+; DG(16:1/18:1/0:0)**
14.13	904.831	1.53	2.20E-04	**TG 53:4; [M+NH4]+; TG(17:1/18:1/18:2)**
12.73	636.665	1.53	5.13E-05	WE(41:1)
8.47	577.519	1.54	7.72E-05	DG(P-33:2)
14.64	523.472	1.54	1.05E-03	LPC(18:2)
14.25	896.769	1.54	3.01E-02	**TG 52:4; [M+NH4]+; TG(16:0/18:1/18:3)**
15.33	934.878	1.54	2.88E-03	TG(54:2)
14.77	918.847	1.55	4.18E-04	TG(54:3)
2.01	401.341	1.55	1.26E-02	3-Hydroxydodecanoic acid
13.03	816.707	1.55	3.61E-02	N-Acetylneuraminic acid
1.03	228.138	1.56	7.50E-04	HMDB32561
2.27	451.376	1.56	7.48E-04	Tetracosahexaenoic acid
0.79	467.302	1.56	4.28E-02	FA(28:0(Ep2,cyclo))
0.81	144.102	1.56	4.41E-02	HMDB04827
15.42	928.832	1.56	2.50E-03	TG(54:3)
3.28	726.504	1.56	1.19E-03	#N/A
14.09	773.662	1.58	1.42E-02	TG(44:1)
14.66	848.930	1.58	3.16E-02	TG(50:4)
13.54	813.636	1.58	1.26E-02	HMDB42100
3.70	692.522	1.58	1.28E-03	DG(38:4)
7.20	610.540	1.58	9.95E-04	WE(40:1)
1.29	355.284	1.58	1.27E-02	FA(16:0(OH4,Ep2))
15.34	864.801	1.59	4.88E-05	HMDB11698
6.44	813.303	1.59	2.70E-02	TG(47:2)
11.85	634.649	1.59	8.66E-06	WE(41:2)
1.46	331.284	1.59	2.28E-05	HMDB33527
14.63	892.832	1.61	1.20E-04	TG(52:1)
15.34	869.755	1.61	3.44E-06	**TG 51:2; [M+NH4]+; TG(17:0/17:1/17:1)**
15.55	945.858	1.61	1.39E-03	**TG 54:3; [M+NH4]+; TG(18:1/18:1/18:1)**
14.18	887.780	1.62	6.89E-05	TG(52:2)
14.42	839.709	1.62	1.02E-07	TG(49:1)
0.96	450.308	1.62	7.65E-05	Docosatrienoic acid
14.89	841.724	1.62	2.49E-05	TG(49:1)
11.75	608.633	1.62	4.06E-06	DG(34:3)
6.15	746.568	1.64	2.23E-04	PA(37:5)
10.60	632.633	1.64	8.67E-05	DG(36:3)

3.19	700.488	1.64	3.54E-02	#N/A
13.20	592.675	1.64	1.86E-04	DG(34:3)
5.57	547.472	1.65	9.12E-06	FA(31:6(OH,Ke2,Ep2,cyclo))
1.49	339.289	1.65	3.04E-03	FA(19:0(OH2))
13.89	902.816	1.66	9.44E-05	PA(O-50:0)
14.14	820.739	1.66	1.36E-04	**SM 42:5; [M]+; SM(d18:1(4E)/24:4(5Z,8Z,11Z,14Z))**
14.63	906.846	1.67	9.70E-05	TG(53:1)
14.40	813.692	1.67	2.29E-04	TG(47:0)
13.89	832.738	1.67	2.00E-04	TG(48:3)
14.42	834.754	1.68	1.29E-05	**TG 49:0; [M+NH4]+; TG(16:0/16:0/17:0)**
6.05	721.506	1.68	7.07E-04	PA(35:4)
12.27	622.649	1.69	1.21E-06	CE(14:1)
14.50	872.770	1.69	1.65E-03	**TG 51:2; [M+NH4]+; TG(17:0/17:1/17:1)**
13.49	787.620	1.69	1.28E-02	TG(45:1)
1.49	357.300	1.70	6.84E-03	FA(21:0(Ep2))
1.55	553.602	1.70	4.47E-04	HMDB31169
3.42	752.519	1.70	2.38E-05	TG(42:2)
13.59	888.801	1.71	2.00E-04	TG(52:2)
14.10	799.678	1.71	6.22E-04	**TG 48:0; [M+NH4]+; TG(16:0/16:0/16:0)**
2.57	610.467	1.71	1.12E-02	#N/A
2.28	630.530	1.71	3.54E-04	DG(34:0)
13.59	818.723	1.71	1.95E-04	PA(44:2)
13.59	902.816	1.71	9.54E-05	PA(O-50:0)
0.88	675.531	1.73	1.02E-04	DG(38:4)
14.41	904.832	1.73	2.25E-05	TG(53:1)
2.21	812.703	1.74	3.56E-04	TG(47:3)
14.62	866.817	1.75	2.61E-03	TG(51:2)
13.83	862.748	1.75	1.93E-03	#N/A
14.63	796.738	1.77	3.74E-03	TG(46:3)
4.80	720.553	1.78	4.46E-04	PA(34:1)
10.06	614.571	1.78	5.72E-05	**DG 34:2; [M+NH4]+; DG(16:1/18:1/0:0)**
1.93	609.665	1.78	1.12E-03	#N/A
14.89	563.503	1.80	2.29E-08	#N/A
14.12	521.456	1.81	1.54E-05	FA(25:2(OH4,Ke2,Ep2,cyclo))
14.64	822.755	1.81	6.41E-05	TG(48:5)
12.89	795.646	1.81	2.28E-03	PA(42:1)
8.33	591.495	1.81	1.30E-06	DG(32:0)
11.85	721.753	1.82	1.55E-07	TG(40:0)
0.81	365.157	1.82	2.89E-03	FA(21:0(OH2,cyclo))
8.33	551.503	1.82	8.65E-06	MG(32:4)

16.31	986.910	1.84	4.33E-02	TG(55:2)
6.04	1032.849	1.84	1.55E-05	**TG 56:5; [M+NH4]+; TG(16:0/18:1/22:4)**
14.89	836.770	1.84	3.33E-06	TG(49:2)
6.88	549.487	1.85	4.95E-06	DG(30:2)
1.95	784.672	1.86	1.74E-02	**SM 42:3; [M]+; SM(d16:2(4E,6E)/26:1(17Z))**
7.08	589.480	1.86	6.01E-06	DG(32:1)
8.55	591.495	1.86	5.60E-06	DG(32:0)
0.81	349.183	1.88	2.03E-03	HMDB61835
6.72	523.472	1.90	1.82E-04	LPC(18:2)
10.46	537.444	1.90	3.92E-02	DG(P-30:1)
14.65	849.473	1.91	4.04E-03	#N/A
14.89	860.769	1.91	1.41E-06	TG(50:1)
14.18	846.914	1.91	7.50E-04	TG(51:5)
13.26	804.706	1.91	2.18E-04	TG(48:6)
10.06	619.526	1.92	2.03E-06	DG(34:1)
7.08	584.524	1.94	2.38E-05	DG(O-34:3)
13.95	844.738	1.98	4.61E-03	**TG 49:3; [M+NH4]+; TG(16:1/16:1/17:1)**
13.83	876.800	1.99	5.51E-05	**TG 51:2; [M+NH4]+; TG(16:0/17:1/18:1)**
14.85	834.753	1.99	1.53E-03	**TG 49:1; [M+NH4]+; TG(16:0/16:0/17:1)**
14.65	849.049	2.00	6.31E-04	#N/A
2.53	651.712	2.00	1.49E-03	WE(42:2)
0.81	344.228	2.01	6.91E-03	FA(21:0(Ep,cyclo))
12.33	736.644	2.05	4.00E-03	PA(36:1)
13.66	868.738	2.06	6.33E-03	TG(51:2)
5.77	582.509	2.07	3.79E-08	FA(33:6(OH2,Ke2,Ep2,cyclo))
14.18	847.032	2.08	2.79E-04	**TG 42:1; [M+NH4]+; TG(12:0/12:0/18:1)**
6.96	558.509	2.11	2.31E-04	DG(P-32:1)
14.18	847.456	2.12	1.33E-03	**TG 51:1; [M+NH4]+; TG(17:0/17:0/17:1)**
8.55	586.540	2.13	5.25E-05	DG(32:1)
14.38	782.722	2.23	2.58E-04	**SM 40:1; [M]+; SM(d14:0/26:1(17Z))**
15.32	862.785	2.24	5.51E-06	#N/A
12.84	785.604	2.24	4.20E-03	TG(45:2)
13.54	797.662	2.24	1.27E-04	**TG 48:1; [M+NH4]+; TG(14:0/16:0/18:1)**
14.89	906.847	2.24	4.92E-06	HMDB46156
13.85	806.722	2.30	5.65E-05	HMDB10411
0.81	476.306	2.30	2.84E-02	FA(23:2(OH3,Ke2,Ep2,cyclo))
15.12	850.945	2.32	2.21E-03	#N/A
0.81	393.210	2.33	2.12E-03	#N/A
14.11	864.801	2.37	5.00E-04	HMDB11698
14.11	878.815	2.38	5.72E-04	HexCer(d45:2)

6.88	584.524	2.39	8.63E-08	DG(O-34:3)
14.40	878.816	2.42	2.18E-05	HMDB44130
12.53	814.691	2.43	9.82E-05	DG(49:6)
12.89	790.691	2.47	2.43E-03	HMDB42989
14.39	808.738	2.49	2.58E-05	HexCer(d40:3)
13.44	778.691	2.51	4.49E-04	TG(44:0)
0.80	437.236	2.55	2.50E-03	#N/A
0.81	453.210	2.58	1.23E-03	HexSph(t16:1)
0.81	388.254	2.59	4.46E-03	FA(19:2(OH,Ke2,Ep2,cyclo))
13.49	771.646	2.60	1.22E-03	TG(44:2)
14.11	794.723	2.61	3.35E-04	PA(42:2)
0.80	569.314	2.61	4.56E-03	DG(30:0)
13.56	876.800	2.62	4.64E-04	**TG 51:2; [M+NH4]+; TG(16:0/17:1/18:1)**
13.81	850.784	2.67	4.41E-04	HMDB13568
0.81	432.280	2.67	3.04E-03	CAR(15:1)
13.55	792.707	2.68	5.23E-04	DG(47:6)
0.81	497.236	2.71	2.76E-03	HMDB15090
0.80	481.262	2.76	3.85E-03	FA(26:0(OH,Ke2,Ep2,cyclo))
13.50	850.784	2.83	1.57E-03	HMDB13568
13.55	862.785	2.86	4.71E-04	#N/A
15.12	851.062	3.05	3.75E-04	SQDG(37:8)
0.81	520.333	3.06	4.33E-03	FA(29:6(Ke2,Ep2,cyclo))
14.14	861.764	3.08	1.07E-06	TG(50:1)
0.80	525.288	3.20	4.11E-03	DG(P-30:1)
12.84	769.631	3.44	3.46E-03	TG(43:0)
13.81	780.707	3.47	1.46E-04	HexCer(d38:3)
13.80	754.691	3.62	7.14E-04	**TG 46:0; [M+NH4]+; TG(14:0/16:0/16:0)**
14.10	768.707	3.72	1.05E-03	PA(39:6)
14.10	838.785	3.88	1.10E-03	**TG 50:1; [M+NH4]+; TG(16:0/16:0/18:1)**
13.50	766.691	4.01	1.33E-03	PA(38:2)
13.50	836.769	4.10	8.49E-04	**SM 43:5; [M]+; SM(d19:1(4E)/24:4(5Z,8Z,11Z,14Z))**
12.85	764.675	4.69	5.83E-03	**TG 44:2; [M+NH4]+; TG(12:0/16:1/16:1)**
13.48	810.753	6.35	3.92E-03	HexCer(d40:2)
13.48	740.676	6.77	4.48E-03	#N/A
12.76	738.660	7.95	1.49E-02	PS(P-31:1)
12.73	712.644	12.17	3.66E-02	WE(45:0)